The intracellular lectin vesicular integral-membrane protein (VIP36) as a potential sorting receptor for the glycoproteins dipeptidyl peptidase IV and sucrase-isomaltase in the early secretory pathway

Von der Naturwissenschaftlichen Fakultät
der Gottfried Wilhelm Leibniz Universität Hannover
zur Erlangung des Grades
Doktorin der Naturwissenschaften
Dr. rer. nat.
genehmigte Dissertation
von

Dipl.-Biol. Miriam Wessels
geboren am 14.11.1981 in Hannover

2011

Referent: Prof. Dr. Hassan Y. Naim
Korreferentin: Prof. Dr. Rita Gerardy-Schahn
Tag der Promotion: 28.02.2011

Für Gerrit

Zusammenfassung

Die korrekte Faltung und Sortierung ist sehr wichtig für Proteine um ihren Zielort zu erreichen und die physiologische Funktion auszuüben. Entlang des sekretorischen Weges spielen mehrere Faktoren eine Rolle um dieses in der Zelle umzusetzen. Zum einen ist die Glykosylierung von Proteinen an der Zielfindung beteiligt. Um die Glykoproteine richtig sortieren zu können bedarf es spezieller Proteine, die Zuckerstrukturen erkennen können und diese binden. Intrazelluläre Lektine bewerkstelligen dies und sind dabei in die Sortierung, dem Transport und der Qualitätskontrolle von neu synthetisierten Glykoproteinen involviert. Darüber hinaus wurde in den letzten Jahren die Bedeutung von speziellen Membran-Mikrodomänen (Lipid rafts oder Detergenz Resistente Membranen (DRMs)) entdeckt. Die Assoziation mit diesen Mikrodomänen ist ebenfalls ein wichtiger Faktor für die Sortierung und Funktion von vielen Proteinen. Wenn Proteine aufgrund von Defekten in der Sortierungsmaschinerie falsch sortiert werden, kann sich dies in verschiedenen Krankheiten äußern. Fortschritte in der Aufklärung von neu charakterisierten Lektinen, sowie deren Zusammenspiel mit anderen Lektinen und Glykoproteinen entlang des sekretorischen Weges in speziellen Membran-Mikrodomänen, erweitern unser Verständnis über die Sortierungsmaschinerie und können Aufschluss über Pathomechanismen in diesem Bereich der Zelle geben.

Ziel dieser Studie war die Charakterisierung des Proteins Vesicular integral-membrane protein (VIP36) und deren Rolle in der Sortierung und dem Transport von Glykoproteinen. VIP36 ist ein intrazelluläres Lektin welches 1994 erstmals aus CHAPS DRMs isoliert wurde. Dieses Protein wurde in verschiedenen zellulären Kompartimenten, wie dem Endoplasmatischen Retikulum (ER), ER-Golgi Intermediär Kompartiment (ERGIC) und Golgi-Apparat gefunden. Auch ein Erreichen der Zellmembran konnte in einigen Studien gezeigt werden. VIP36 bindet hauptsächlich Glykoproteine, die in ihrer mannosereichen Form vorliegen, und wird als Lektin in Sortierungsprozessen und der Qualitätskontrolle nach dem ER vermutet. In dieser Arbeit wurden neue Interaktionspartner von VIP36 gesucht und die Bindungseigenschaften sowie die zelluläre Lokalisation untersucht.

Mit dem Einsatz von konfokaler Lasermikroskopie und Immunopräzipitations-Experimenten war es mir möglich die beiden Raft-assoziierten Glykoproteine Dipeptidylpeptidase IV (DPPIV) und Saccharase-Isomaltase (SI) als neue Interaktionspartner von VIP36 zu identifizieren. Keine Interaktion konnte mit den Proteinen Aminopeptidase N (APN) und Laktase-Phlorizin Hydrolase (LPH) gefunden werden, welche ebenfalls Glykoproteine sind

aber keine Assoziation mit Rafts in späteren zellulären Kompartimenten aufweisen. Die Interaktion von VIP36 mit DPPIV und SI ist abhängig von deren Glykosylierung, da Glykosylierungsinhibitoren die Bindung von VIP36 schwächen. Dies spricht für die Rolle als Beförderungsgut der beiden Proteine von VIP36. Darüber hinaus konnte ich in Pulse-Chase Experimenten zeigen, dass VIP36 sowohl mannosereich glykosylierte als auch komplex glykosylierte Proteinformen von DPPIV und SI bindet und somit im ER und im Golgi-Apparat aktiv ist. Die Verbindung von VIP36 und den beförderten Proteinen löst sich im Trans-Golgi-Netzwerk, da keine Interaktion an der Zelloberfläche beobachtet werden konnte. Somit konnte gezeigt werden, dass VIP36 an Sortierungsereignissen in frühen Kompartimenten wie dem ER und ERGIC, sowie später entlang des sekretorischen Weges (Golgi-Apparat, Trans-Golgi-Netzwerk) eine Rolle spielt.

Mit der Isolierung von verschiedenen DRMs konnte gezeigt werden, dass VIP36 mit Tween 20 DRMs assoziiert ist. Diese DRMs stellen frühe Sortierungsplattformen für apikale Proteine wie DPPIV und SI dar, in der VIP36 als Sortierungsrezeptor involviert sein könnte. Eine Assoziation mit DRMs, die in Membranen des Golgi-Apparates vorherrschen, konnte nicht beobachtet werden. Diese Verteilung änderte sich allerdings, wenn die Glykosylierung im Golgi-Apparat gehemmt wurde. Unter diesen Bedingungen wird VIP36 in Lubrol WX DRMs rekrutiert. Dies könnte aufgrund der Bindung zu DPPIV erfolgen, welches von VIP36 zurück in frühere Kompartimente entlang des sekretorischen Weges transportiert werden könnte, um eine korrekte Glykosylierung zu erreichen. Dies macht VIP36 zu einem potenziellen Kandidaten für die Post-ER Qualitätskontrolle.

Zusammenfassend konnten die Daten zeigen, dass VIP36 ein multifunktionales Lektin ist, welches eine Rolle in der Sortierung von Glykoproteinen sowie der Post-ER Qualitätskontrolle spielt.

Schlagwörter: Vesicular intergal-membrane protein (VIP36), intrazelluläre Lektine, sekretorischer Weg, Glykoproteintransport, Detergenz Resistente Membranen (DRMs)

Abstract

Proteins need to be correctly folded and transported to their targets in the cell to fulfil their physiological functions. Along the secretory pathway there are different processes which are involved in the sorting machinery. One important feature for reaching the final destination is the glycosylation of proteins. For the recognition of glycoproteins special proteins exist, namely intracellular lectins, which are involved in sorting, trafficking and quality control of newly synthesized glycoproteins. Another feature which became important in the last years is the association with special membrane microdomains called lipid rafts or detergent resistant membranes (DRMs). Association with lipid rafts was shown to be crucial for the right sorting and function of many proteins. Different diseases can be caused by missorted proteins which are based on defects in the sorting machinery.

The aim of this study was the characterization of the biochemical role of vesicular integral-membrane protein (VIP36) in glycoprotein trafficking and sorting. VIP36 is an intracellular lectin which was first isolated from CHAPS DRMs in 1994. It was found to be localized in different cellular compartments (e.g. endoplasmic reticulum (ER), ER-Golgi intermediate compartment (ERGIC), and Golgi-apparatus) and at the cell surface, binding mainly to high-mannose glycosylated proteins. Furthermore it is proposed to play a role in sorting events and post-ER quality control. In this study, I was searching for new interaction partners of VIP36 and investigated binding properties as well as cellular localization of this particular protein.

By using confocal laser microscopy and immunoprecipitation experiments, I was able to identify the two raft-associated glycoproteins dipeptidyl peptidase IV (DPPIV) and sucrase-isomaltase (SI) as interaction partners for VIP36. No interaction with the proteins aminopeptidase N (APN) and lactase-phlorizin hydrolase (LPH), which are not associated with DRMs of later cellular compartments, could be observed. The interaction of VIP36 with DPPIV and SI was found to be glycosylation-dependent since treatment with glycosylation-inhibitors impairs the binding of VIP36. This makes these proteins potential cargo for this lectin. Moreover, it could be shown that VIP36 binds to its cargo in early as well as in late compartments along the secretory pathway, which was obtained by pulse chase experiments showing an association of VIP36 with SI and DPPIV, when mannose-rich and complex glycosylated. VIP36 and its cargo separate at the stage of the trans-Golgi network (TGN) since no association could be observed when the two glycoproteins were supposed to reach the cell surface. Therefore, VIP36 might play a role in sorting events in early compartments (e.g. ER, ERGIC) and also later along the secretory pathway (e.g. Golgi-apparatus, TGN).

ABSTRACT

DRM extraction experiments revealed an association of VIP36 with Tween 20 DRMs, which are proposed to play a role in early polarized sorting. This indicates an involvement of VIP36 in early polarized sorting of DPPIV and SI. No association with DRMs of Golgi membranes could be observed. However, when glycosylation in the Golgi was inhibited VIP36 was recruited in Lubrol WX DRMs possibly because of binding to DPPIV, relocating it back to earlier compartments for an additional round of glycosylation. This makes VIP36 a promising candidate for post-ER quality control.

Taken together, VIP36 is a multifunctional intracellular lectin which plays a role in sorting of glycoproteins along the secretory pathway and possibly in post-ER quality control.

Keywords: Vesicular integral-membrane protein (VIP36), intracellular lectins, secretory pathway, transport of glycoproteins, detergent resistant membranes (DRMs)

Table of contents

Abbreviations

°C	degree Celsius
µg	microgram
µl	microlitre
A	alanine
Ab	antibody
APN	aminopeptidase N
Asn	asparagine
BiP	immunoglobulin-binding protein
cDNA	complementary deoxyribonucleic acid
CHO	Chinese hamster ovary
CMP	cytosine monophosphate
CNX	calnexin
COP	coat protein
CRD	carbohydrate recognition domain
CRT	calreticulin
D	aspartic acid
DMEM	Dulbecco's modified eagle's medium
dMM	1-Deoxymannojirimycin
dNM	1-Deoxynojirimycin
DPPIV	dipeptidyl peptidase IV
DRMs	detergent resistant membranes
E	glutamic acid
EDEM	ER-degradation enhancing α-mannosidase like protein
e.g.	for example
ER	endoplasmic reticulum
ERAD	ER-associated degradation
ERGIC	ER-Golgi intermediate compartment
ERGIC-53	ERGIC 53 kDa protein
et al.	et alii
F	diphenylalanine
FCS	fetal calf serum

Fig.	figure
g	gravitation
g	gram
GalNAc	N-acetylgalactosamine
GDP	guanine diphosphate
GFP	green fluorescence protein
Glc	glucose
GlcNAc	N-acetylglucosamine
GlcNAc-T	N-acetylglucosaminyltransferase
Golgi	Golgi apparatus
GPI	glycosylphosphatidylinositol
h	hour
IF	immunofluorescence
IP	immunoprecipitation
K	dilysine
kb	kilo base
kDa	kilo Dalton
L	leucine
l_d	lipid-disordered
Lec1	CHO-Lec1
Lec2	CHO-Lec2
l_o	lipid-ordered
LPH	lactase-phlorizin hydrolase
mAb	monoclonal Antibody
Man	mannose
MDCK	Mardin-Darby canine kidney
MEM	minimum essential medium
mg	milligram
min	minute
ml	millilitre
mm	millimeter
mM	millimolar
N	asparagine
nm	nanometer

OS9	osteosalcoma-9 protein
PAGE	polyacrylamide gel electrophoresis
PBS	phosphate buffered saline
R	arginine
rb	rabbit
rpm	rounds per minute
SDS	sodium dodecyl sulfate
Ser	serine
SI	sucrase-isomaltase
TGN	trans-Golgi network
Thr	threonine
TLC	thin layer chromatography
U	unit
UDP	uracil diphosphate
VIP36	vesicular integral-membrane protein
VIPL	VIP36-like protein
WB	Western blot
Y	tyrosine

Scientific Presentations

Parts of this work have been already communicated:

Posters

Transportverhalten hochglykosylierter Membranproteine in glykosylierungsdefekten CHO-Lec Zellen

M. Wessels, M. Alfalah, H.Y. Naim

18. Symposium der DVG-Fachgruppe Physiologie und Biochemie in Leipzig, 09.–11.03.2008

Transport of Membrane Glycoproteins in Glycosylation-defective Mutant Chinese Hamster Ovary Cell Lines

M. Wessels, M. Alfalah, H.Y. Naim

7th Congress of the European Life Scientist Organization (ELSO) in Nice, 30.08.–02.09.2008

Vesicular integral-membrane protein (VIP36) as a potential sorting receptor in the early secretory pathway

M. Wessels and H.Y. Naim

1st International Symposium for PhD Students on Protein Trafficking in health and disease in Hamburg, 26.–28.05.2010

Oral

The interaction of the intracellular lectin vesicular integral-membrane protein (VIP36) with dipeptidyl peptidase IV (DPPIV) along the secretory pathway in CHO-Lec cells

M. Wessels and H.Y. Naim

20th Joint Glycobiology Meeting in Cologne, 08.–10.11.2009

The interaction of vesicular integral-membrane protein (VIP36) with dipeptidyl peptidase IV (DPPIV) along the secretory pathway

M. Wessels and H.Y. Naim

19. Symposium der DVG-Fachgruppe Physiologie und Biochemie in Hannover, 14.–16.02.2010

Vesicular integral-membrane protein (VIP36) as a potential sorting receptor along the secretory pathway

M. Wessels and H.Y. Naim

Seminars in Biochemistry and Virology in Hannover, 28.04.2010

Membrane topology of the small intestine in health and disease

M. Wessels and H.Y. Naim

Klausurtagung SFB 621 in Soltau, 11.–12.06.2010

Figures

1. Introduction

Proteins need to be correctly sorted and transported to their targets in the cell to fulfil their physiological functions. Several diseases are caused by the missorting or malfunction of proteins including the gastrointestinal tract disorders congenital sucrase-isomaltase deficiency, cystic fibrosis, glucose-galactose malabsorbtion, and congenital lactase deficiency (Naim et al. 1988a, Riordan et al. 1989, Turk et al. 1991, Kuokkanen et al. 2006).

Along the secretory pathway there are many different processes which play a role for protein trafficking and sorting. One important feature is the glycosylation of proteins. The glycosylation process is present in the cytosol, the endoplasmic reticulum (ER) and the Golgi apparatus (Golgi). It plays a crucial role as a sorting signal and is required for the proper folding of glycoproteins. Defects in glycosylation of a certain protein can cause missorting, loss of function and could be associated with the pathogenesis of different diseases.

During the glycosylation process, proteins are transported and controlled by other proteins. Several of these events are exerted by intracellular lectins, such as calnexin (CNX), calreticulin (CRT), and mannose-6-phosphate receptors. It is known that these lectins are essential for the quality control and exit of the ER or transport to other cellular compartments (e.g. lysosomes). When lectins are not able to bind certain glycoproteins, this can also cause diseases like bleeding disorder (Nichols et al. 1998) or even embryonic or perinatal lethality, as was shown for the absence of CNX or CRT in mice (reviewed in Anelli & Sitia 2008).

Another feature which becomes important in the last three decades is the association of proteins with lipid rafts or detergent resistant membranes (DRMs) in biological membranes. Many proteins need this association for finding interaction partners, sorting and signalling. It is known that lipid rafts play a regulatory role in diseases of the central nervous system, metabolic disorders as well as bacterial and viral infections.

Taken these three subjects together, this study will focus on the potential intracellular lectin vesicular integral-membrane protein (VIP36) and its association with glycoproteins and DRMs along the secretory pathway. This protein was extracted from CHAPS DRMs and binds to glycoproteins mainly on the mannose-rich D1-arm. Therefore it might play an important role as a sorting receptor in the early secretory pathway.

Advances in enlighten the contribution of new characterized intracellular lectins and their interplay with other lectins and glycoproteins along the secretory pathway in special membrane domains support our understanding of the sorting machinery in the cell. This might

help to enhance our understanding of pathomechanisms which are associated with a defect in sorting and trafficking of glycoproteins.

1.1 Protein glycosylation

Protein glycosylation plays an important role in numerous cellular functions like development (Haltiwanger & Lowe 2004), wound repair (Lackie & Adam 2006), innate immunity (Marth & Grewal 2008) and of course quality control and transport of proteins along the secretory pathway (Ellgaard & Helenius 2003, Helenius & Aebi 2004, Hebert & Molinari 2007, Lederkremer 2009). There are two distinct types of glycosylation which can be found solely or in parallel on proteins, namely the N- and O-glycosylation.

1.1.1 N-glycosylation

One of the most common protein modifications is the N-glycosylation (Apweiler et al. 1999). In the SWISS-PROT protein sequence data bank, two thirds of all proteins registered have at least one potential N-glycosylation site.

The N-glycosylation needs three cellular compartments: the endoplasmic reticulum (ER), Golgi apparatus (Golgi) and cytosol. In the cytosol the mannose donor GDP-mannose is synthesized from fructose 6-phosphate. N-glycan assembly starts on the cytoplasmic side of the ER were glycans are initially synthesized on a lipid-like molecule termed dolichol phosphate. First, N-acetylglucosamine (GlcNAc) is transferred to dolichol phosphate from UDP-GlcNAc, catalyzed by GlcNAc-1 phosphotransferase. Then a second GlcNAc is transferred on dolichol phosphate, followed by stepwise addition of five mannose residues from GDP-mannose. This glycan is further processed after flipping in the luminal side, a mechanism which is not fully understood (reviewed in Jaeken & Matthijs 2007). Hereby, the dolichol phosphate is translocated across the ER membrane into the lumen of the ER, mediated by a flippase. In the lumen, the glycan, linked to dolichol phosphate, is extended by the addition of four mannose residues, and three glucoses. The mannose and glucose donors are linked to dolichol phosphate and are also build in the cytoplasm. Therefore, they must also be flipped across the membrane.

Membrane and secretory proteins which originate from membrane-bound ribosomes are simultaneously translated and translocated into the ER lumen. Here, the newly synthesized

proteins immediately become glycosylated by "en bloc" transfer of the $Glc_3Man_9GlcNAc_2$ glycan on the side chain of asparagine residues in Asn-X-Ser/Thr motifs by the oligosaccharyl-transferase (Kornfeld and Kornfeld 1985, Alberts et al. 2004). In the amino acid motif, X represents any amino acid except proline (Khalkhall & Marshall 1975). After transfer to the protein, the glycans were further processed in the ER and Golgi.

The further processing starts with removal of the outer glucose which is located on the D1-arm of the glycan, by α-glucosidase I in the ER, followed by the action of α-glucosidase II, trimming the next glucose. At this state of glycosylation, the monoglucosylated proteins bind to CNX or CRT (Vassilakos et al. 1998). While the proteins bind to CNX/CRT they begin to fold and are interacting with chaperones which promote its folding (e.g. ERp57). Removal of the terminal glucose by α-glucosidase II releases the glycoprotein from the binding of CNX/CRT. If the protein is correctly folded it exits the ER on its way to the Golgi. Before leaving the ER, many glycoproteins are trimmed by ER α-mannosidase I, which specifically removes the terminal α-1,2 mannose from the D1-arm (Herscovics 2001). Incorrect folded proteins without terminal glucose are re-glucosylated by the enzyme UDP-glucose glycoprotein glucosyltransferase and subsequently get into an additional folding cycle by binding to CNX/CRT. In many cases many rounds of deglucosylation and reglucosylation are necessary until the protein reaches its native folding. Otherwise when the protein is misfolded it is targeted for degradation via the ER-associated degradation pathway (ERAD, Soldà et al. 2007).

When correctly folded proteins reach the Golgi the trimming continues, resulting into a transformation from the mannose-rich to a complex glycosylated form. First, additional mannose residues are removed by the action of α-mannosidase I a, b and c in the cis-Golgi, resulting into a $Man_5GlcNAc_2$ glycan. GlcNAc is then added to the glycan by N-acetylglucosaminyltransferase I (GlcNAc-TI). In the medial-Golgi, two mannose residues are removed by α-mannosidase II. This step is only initiated when GlcNAc-TI has been active previously. Additionally a second GlcNAc is transferred to the glycan by a GlcNAc-T. There is also a core modification in this cellular compartment by the addition of fucose, linked to the GlcNAc which is adjacent to Asn. When proteins reach the trans-Golgi there is no further trimming but an addition of galactose and sialic acid. The addition of the negatively charged sialic acid by the CMP-sialic acid transporter is the last step of N-glycosylation and proteins exit the Golgi to their final destination (reviewed in Varki et al. 2009). An overview of the whole process is shown in figure 1.1.

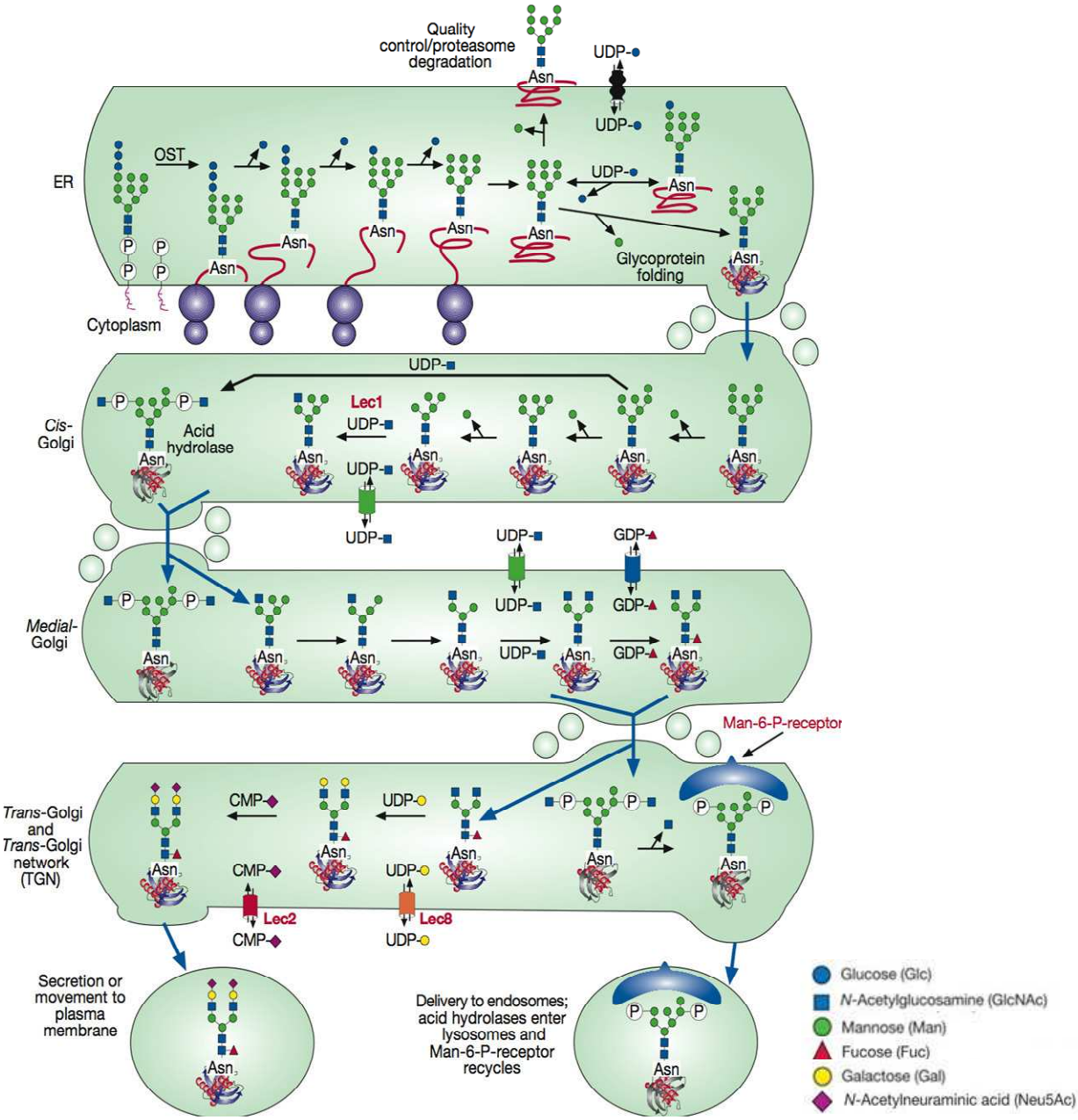

Figure 1.1 Processing and maturation of an N-glycan. Dolichol phosphate transferred the $Glc_3Man_9GlcNAc_2$ glycan to newly synthesized proteins. The glucosidases I and II in the ER remove the three glucose residues, and ER mannosidase removes one mannose residue. Additional mannose residues are removed in the cis-Golgi until $Man_5GlcNAc_2Asn$ is generated. The action of GlcNAc-TI in the medial-Golgi initiates the first branch of an N-glycan. Alpha-mannosidase II removes two outer mannoses. GlcNAc-TII translocates GlcNAc to the branches. The resulting N-glycan is extended by the addition of fucose, galactose, and sialic acid to generate a complex N-glycan. Complex N-glycans can have more sugars than shown in this figure, including additional residues attached to the core, additional branches, branches extended with poly-*N*-acetyllactosamine units, and different "capping" structures. Also shown is the special case of lysosomal hydrolases that acquire a GlcNAc-1-P at C-6 of mannose residues on oligomannose N-glycans in the cis-Golgi and the defects of the CHO-Lec cells Lec1, Lec2, and Lec8 (modified from Kornfeld & Kornfeld 1985).

Typical N-linked oligosaccharides always contain mannose as well as N-acetylglucosamine and they have several branches, each terminates with a negatively charged sialic acid residue (Lodish et al. 2000). However, the population of sugars attached to glycoproteins depends on cell type and physiological status of the cell. Therefore, N-glycans can be very diverse. The number of branches can vary as well as the length by addition of tandem repeats consisting of GlcNAc and galactose. The final elongation by sialic acid plays an important role since this carbohydrate is necessary for many processes, like stabilizing the conformation of proteins including enzymes, protecting molecules from attack by proteases, and modulating processes involved in signalling, growth, and differentiation (reviewed in Varki et al. 2009). Since sialic acid acts as a "mask" for the underlying saccharides, it also prevents binding by intracellular lectins that recognize these glycans, regulating cellular processes (reviewed in Varki et al. 2009). Not all glycans are trimmed to the complex-type but some remain in the mannose-rich state. There are also four other N-glycan linkages known, however, the GlcNAc to Asn is the most common.

1.1.2 O-glycosylation

The O-glycosylation is initiated by the covalent α-linkage of N-acetylgalactosamine (GalNAc) residue from UDP-GalNAc to the hydroxyl group of serine or threonine by an O-glycosidic bond, catalyzed by a polypeptide N-acetylgalactosaminyltransferase (Lodish et al. 2000). This type of glycosylation, which takes place in the Golgi, has no defined amino acid sequences for attachment of glycans in comparison to the N-glycosylation. However, there are certain amino acids which increases the GalNAc addition (e.g. proline), and others which may interfere this linkage (e.g. charged amino acids). The role of proline may be to expose Ser or Tre in a β–turn conformation, leading to more efficient O-glycosylation (reviewed in Varki et al. 2009).

The O-linked glycans consists of short side chains of about 1 to 4 sugar residues (in some cases up to 10 residues, Alberts et al. 2004), including galactose, N-acetylgalactosamine, fucose or sialic acid (Lodish et al. 2000). In contrast to the initial reactions of N-glycosylation, no lipid-linked intermediates are involved, and no glycosidases appear to be involved in the processing of O-linked glycans. The sugars which are attached to the protein depend on the cell type. Figure 1.2 shows an overview of the most common O-glycosylation. As mentioned before, it is initiated by the addition of GalNAc to a Ser or Thr of the protein by an α-linkage. The next sugar residue is galactose, followed by sialic acid, which are both

attached to GalNAc. In an additional step, fucose is transported to the glycan and binds to galactose wire α-1,2 linkage (Voet et al. 2002).

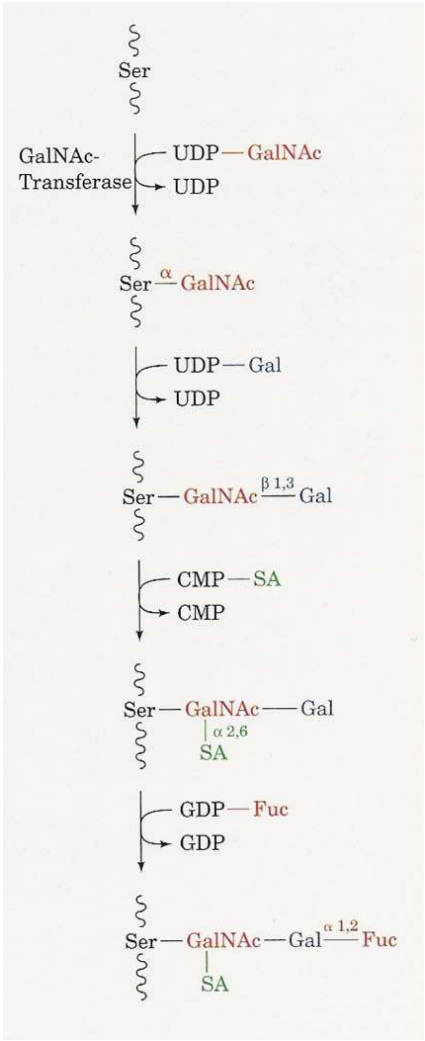

Figure 1.2 Model of O-glycosylation. The O-glycosylation is initiated by the transfer of N-acetylgalactosamine (GalNAc) to serine (Ser) catalyzed by the GalNAc-transferase. Sequentially galactose (Gal) and sialic acid (SA) are added to GalNAc wire β-1,3 and α-2,6 linkages, respectively. Fucose (Fuc) is then linked to Gal by α1,2 linkage (taken from Voet et al. 2002).

1.1.3 Defects in glycosylation

The N- as well as the O-glycosylation are important for many proteins for their proper folding, sorting and their correct function. For example, O-glycosylation of mucous glycoproteins is essential for their ability to hydrate and protect the underlying epithelium in respiratory, gastrointestinal and genitourinary tracts. It is also known that mucins (O-glycosylated proteins) can trap bacteria via specific receptors (reviewed in Varki et al. 2009).

In born errors in the glycosylation process in man are termed congenital disorders of glycosylation. To date more than 28 congenital disorders of glycosylation are known (reviewed in Jaeken & Matthijs 2007). The first patients were reported in 1980. The disorders reach from mild to severe diseases, with multisystem or mono-organic disorders. Genetic glycosylation disorders cause a wide range of phenotypes, with examples from all specialities. Many well known diseases such as Walker-Warburg syndrome and muscle-eye-brain disease are caused by a glycosylation defect (reviewed in Jaeken & Matthijs 2007). Some of these disorders cause death early after birth, e.g. loss of galactose and sialic acid residues on glycoproteins (Lübbehusen et al. 2010). The absence of GlcNAc-TI in mice results into death during embryonic development (Ioffe & Stanley 1994), and also the elimination of sialic acid production causes embryonic lethality (reviewed in Varki et al. 2009). Mutations, concerning sialic acid transport have also been found to be involved in degenerative diseases such as atherosclerosis and diabetes, as well as neurological disorders such as Alzheimer`s disease (reviewed in Varki et al. 2009).

For the investigation of glycosylation-defects or glycoprotein function and trafficking, different models can be used, such as protein mutants, cell mutants, and glycosylation-inhibitors.

Protein mutations were generated in the past, to delete or add glycosylation sites. Herewith one could determine whether single glycosylation sites in the protein play a special role or if all of them are important for function and trafficking. Several groups could show in the past, that deletion of N- and/or O-glycosylation sites resulted in missorting of apical glycoproteins to the basolateral surface, whereas addition of N-glycosylation sites targeted the proteins to the apical cell surface (Scheiffele et al. 1995, Yeaman et al. 1997, Gut et al. 1998, Benting et al. 1999, Jacob et al. 2000, Pang et al. 2004).

Glycosylation-defective cell lines are also a common tool to investigate glycoprotein function. Mutants with a glycosylation defect become resistant to cytotoxic lectins by reducing the expression of single sugars or a group of sugars on cell surface glycans. The most common cell models are Chinese hamster ovary (CHO)-Lec cells which were established by Stanley et al. in 1975. There are many loss-of-function as well as gain-of-function mutants available. Glycosylation mutants help to define the genes which encode for the affected transferases or glycosidases. They also provide an insight into the functions of glycosylation in cells and tissues and provide a model for human born errors in metabolism and disease. The restriction in this case is the restriction to the cell type and organism from which it was isolated (reviewed in Varki et al. 2009).

The usage of glycosylation-inhibitors is common in research of glycoproteins, since many are known and commercially available. They are mostly small molecules which are taken up readily by a variety of cell types. They can also be absorbed through the gut, which provides an opportunity for investigation of whole organisms and to design drugs for the treatment of human glycosylation-diseases and -disorders. Tunicamycin, for example, is an inhibitor of dolichol phosphate-GlcNAc assembly, and thereby prevents N-glycosylation. 1-deoxynoijrimycin (dNM) retains the three glucose residues on the N-linked glycan and usually loses one or two mannose residues as the protein pass through the ER and medial-Golgi. By the use of 1-deoxymannoijrimycin (dMM), the action of α-mannosidase I in the cis-Golgi can be blocked, resulting in a $Man_8GlcNAc_2$ glycan on mature proteins. Many studies were carried out with these glycosylation-inhibitors to investigate several glycoprotein functions (Gut et al. 1998, Huet et al. 1998, Naim et al. 1999, Alfalah et al. 2002, Vagin et al. 2004, Delacour et al. 2005).

1.1.4 Glycoproteins

Dipeptidyl peptidase IV (DPPIV)

Dipeptidyl peptidase IV (DPPIV/ CD26) is a type II transmembrane glycoprotein. This multifunctional protein belongs to the family of serine proteases and cleaves N-terminal dipeptides from polypeptides with proline or alanine next to last position (Havre et al. 2008). It is widely expressed on the surface of epithelial, endothelial, and lymphoid cells (De Abbott et al. 1994, De Meester et al. 1999). However, a soluble form can also be found in the plasma (Iwaki-Egawa et al. 1998). The human DPPIV consists of 766 amino acids (Darmoul et al. 1992, Misumi et al. 1992). However, the molecular mass of DPPIV depends on the species, tissue, and its stage of glycosylation and range between 100 kDa and 150 kDa (Ikehara et al. 1994). The molecular mass for the mannose-rich ($DPPIV_h$) and the mature form ($DPPIV_c$) in Caco-2 cells are 100 kDa and 124 kDa (Matter & Hauri 1991), in CHO cells 100 kDa and 110 kDa (Hong et al. 1989), respectively. DPPIV is transported to the apical membrane on two distinct pathways, either directly from the trans-Golgi network (TGN) or through the transcytotic pathway across the basolateral membrane (Le Bivic et al. 1990, Matter et al. 1990, Low et al. 1991). The transmembrane form of DPPIV exists as a homodimer (Jascur et al. 1991). This dimerization is essential for its enzymatic activity (De Meester et al. 1992).

In human cells, it has nine potential N-glycosylation sites (Misumi et al. 1992) and is also highly O-glycosylated at the Ser/Thr-rich stalk domain (Matter & Hauri 1991). In CHO cells, eight N-glycosyl chains are acquired (Hong et al. 1989). The N- and O-glycosylation is important for DPPIV to reach the apical surface, since inhibition of glycosylation results in transport to the basolateral membrane (Fan et al. 1997, Huet et al. 1998, Naim et al. 1999). DPPIV is associated with lipid rafts and this association is important for its proper sorting (Alfalah et al. 2002, Alfalah et al. 2005). Stechly et al. (2009) found that the lectin galectin-4 is involved in sorting of DPPIV into Triton X-100 rafts and apical delivery.

Sucrase-isomaltase (SI)

Sucrase-isomaltase (SI) (EC 3.2.1.48-10) is a type II transmembrane glycoprotein (Blobel 1980) which consists of 5 functional domains including the two subunits sucrase and isomaltase (Fig. 1.3). It belongs to the family of intestinal disaccharidases or hydrolases and is located at the apical membrane in the microvilli of enterocytes and Caco-2 cells. Its cDNA encodes for a sequence of 1827 amino acids and it is synthesized in the ER as a common precursor protein (pro-SI) (Hunziker et al. 1986, Naim et al. 1988b). On the way through the ER and Golgi this precursor is modified and provides five O-glycosylation sites as well as eight N-glycosylation sites on each subunit. Seven of the N-glycosylation sites of sucrase are complex glycosylated whereas the eights site remains in the mannose-rich form (Naim et al. 1988b). After these modifications, pro-SI is transported directly to the apical cell surface (Le Bivic et al. 1990, Matter et al. 1990). For the correct sorting of SI, the O-glycosylation as well as its association with lipid rafts is required (Alfalah et al. 1999, Jacob et al. 2003).

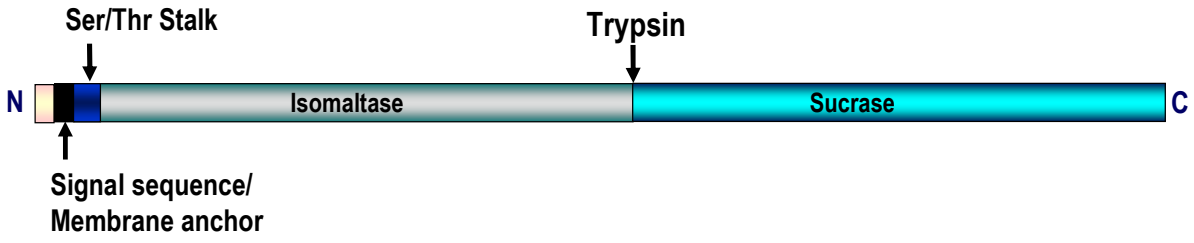

Figure 1.3 Model of sucrase-isomaltase. Sucrase-isomaltase consists of five subunits. The N-terminal domain is directed into the lumen of the cell. The signal sequence, which functions also as a membrane anchor, is followed by the Ser/Thr rich stalk domain. The two subunits isomaltase and sucrase are directed together with the stalk domain into the lumen of the gastrointestinal tract.

When pro-SI reaches the plasma membrane it is proteolytically cleaved by pancreatic trypsin to isomaltase with a size of 145 kDa and sucrase with a size of 130 kDa (Hauri et al. 1985, Naim et al. 1988b), however the two subunits remain connected (Hunziker et al. 1986). The sucrase subunit cleaves sucrose at position α-1,2 to glucose and fructose, whereas isomaltase cleaves isomaltose at position α-1,6 and produces also glucose. The monosaccharide glucose can then be absorbed by the cells.

1.2 Lectins

Lectins are defined as proteins that significantly recognize and bind to glycans without catalyzing a modification of the glycan. The first lectin was discovered by Stillmark in 1888. He found out that seed extracts of the plant *Ricinus communis* contain a toxin that can agglutinate erythrocytes (reviewed in Varki et al. 2009) and termed it due to its function agglutinate. This protein family was later renamed in lectins from the Latin word *legere*, meaning to select, and become important members of the general class of glycan-binding proteins.

Lectins can be found in plants, animals and bacteria. They recognize specific terminal sugar residues on glycans linked to proteins or lipids with a specific binding site, namely the carbohydrate recognition domain (CRD). There are different classes of lectins known (e.g. R-type, L-type), characterized by its origin or properties of CRD. L-type lectins, for example, were first extracted from the seeds of legominous plants. However, this class of lectins has also representatives in mammalian cells (reviewed in Varki et al. 2009).

Many L-type lectins are well defined and used as tools for analytical and biomedical procedures due to their variety of carbohydrate-binding specificities. Their structure consists of two antiparallel pleated sheets and a CRD (Sharon & Lis 1990). This CRD forms two cavities, one containing Ca^{2+} or Mn^{2+} ions, the other containing the monosaccharide. In between these two cavities, an aspartate and an asparagine are located, which side chains bind Ca^{2+} ions and provide hydrogen bonds to the monosaccharide (Sharon & Lis 1990, Shaanan et al. 1991)

In plants, lectins help to find symbiotic partners or defend against bacteria. In mammalian cells many intracellular lectins are involved in quality control, sorting and transport of glycoproteins and glycolipids.

1.2.1 Mammalian intracellular lectins along the secretory pathway

It is hypothesized that the glycans which are attached to glycoproteins represent "cellular addresses", which mediate progression through the secretory pathway and define their final destinations (Helenius & Aebi 2001). This predicts the existence of compartment-specific receptors that recognize and bind different oligosaccharides. Such receptors have been identified as intracellular lectins.

Intracellular lectins play important roles in transport and sorting along the secretory pathway: Calnexin (CNX) and calreticulin (CRT) act as molecular chaperones (Ou et al. 1993, Nauseef et al. 1995, Ware et al. 1995), ERGIC 53 kDa protein (ERGIC-53) functions as a transport cargo receptor (Appenzeller et al. 1999), VIP36-like protein (VIPL) is proposed to play a role in protection of folded high mannose-type glycoproteins (Kamiya et al. 2008), and mannose-6-phosphate receptor recognizes the marker for lysosomal enzymes (Dahms et al. 1989).

These receptors share a general domain organization. They consist of a luminal (exoplasmic) domain which contains one or multiple carbohydrate recognition domains (CRD), a single transmembrane domain, and a short cytoplasmic domain with sorting signals that can interact with cytosolic coat components and mediates sorting within the secretory pathway.

Calnexin (CNX) and calreticulin (CRT)

CNX and CRT are ER-resident proteins. CNX is an 88 kDa type I transmembrane protein, which mainly interacts with N-glycans close to the ER membrane, whereas CRT is a soluble protein of 55 kDa that binds proteins present in the lumen or to those that have large lumenally oriented domains. Both are L-type lectins and require one glucose and three mannose residues on the D1-arm to recognize and bind to glycoproteins (Ware et al. 1995, Spiro et al. 1996, Vassilakos et al. 1998). Their binding activity is sensitive to changes in Ca^{2+} concentration. The structure of CNX consists of two main components: a globular lectin domain and an extended arm-like domain, the so called P-domain (Schrag et al. 2001). The lectin domain mainly consists of a β-sandwich formed by two curved β-sheets, similar to legominous plant lectins, and a calcium binding site that stabilizes the protein (Brockmeier & Williams 2006). The P-domain interacts with the thiol-oxidoreductase ERp57 which is involved in folding of glycoproteins (Frickel et al. 2002, Kozlov et al. 2006). The lectin and

P-domain are also preserved in CRT and are similar to that of CNX; additionally it has a KDEL ER-retention signal at the C-terminus (Peterson & Helenius 1999, Kozlov et al. 2010). The structure of CRT is most similar (33 % sequence identity of lectin domain) to CNX, but shares also similarities to Emp47p (a homolog of ERGIC-53 in yeast), ERGIC-53 and VIP36, which are all recognizing the D1-arm for carbohydrate binding (Kozlov et al. 2010).

ERGIC-53

ERGIC-53 is a type I transmembrane protein which is associated with the ER-Golgi intermediate compartment (ERGIC, Hauri & Schweizer 1992) and recycles between the ER and ERGIC (Lippincott-Schwartz et al. 1990). Its cytoplasmic carboxyl terminus contains the ER-retention signal KKFF, where the dilysine part is recognized by COPI coatomer complex. This enables the coated vesicles to be recycled from the Golgi back to the ER (Itin et al. 1995b). On the other hand, the diphenylalanine direct COPII coated vesicles to ER exit sites by binding to the COPII coatomer (Kappeler et al. 1997). ERGIC-53 is a mannose specific, calcium dependent lectin which is homologue to leguminous plant lectins (Arar et al. 1995, Itin et al. 1996), belonging to the family of L-type lectins with a long half-life of approximately 30 h (Neve et al. 2003). It is known that this protein forms homodimers or homohexamers which is not necessary for interacting with cargo but to exit the ER (Appenzeller et al. 1999). ERGIC-53 binds high-mannose type oligosaccharides (at the D1-arm) with a broad specificity at pH 7.4 but not at slightly lower pH (Kamiya et al. 2005) and requires the amino acids A120, D121 and N156 for carbohydrate binding (Itin et al. 1996). It is known that this lectin acts as a cargo receptor for a limited set of glycoproteins including cathepsin C (Vollenweider et al. 1998), cathepsin Z (Appenzeller et al. 1999), blood coagulation factors V and VIII (Nichols et al. 1998, Moussalli et al. 1999), α-1-antitrypsin (Nyfeler et al. 2008), and immunoglobulin M (Cortini & Sitia 2010). Dysfunctional ERGIC-53 leads into a bleeding disorder caused by a deficiency of coagulation factors V and VIII (Nichols et al. 1998).

VIPL

VIPL is an ER-resident protein (Nufer et al. 2003, Neve et al. 2003). It was first identified in 2003 and named VIPL since it has 68 % similarity to VIP36 (Nufer et al. 2003). This type I transmembrane protein has a predicted size of 35.6 kDa and contains one N-glycosylation site

which is high mannose-type glycosylated (Neve et al. 2003). It is expressed in many cell types and tissues, having a very short half-life of about 30 min (Neve et al. 2003). The existence of an ER-retrieval signal (RKR) at its cytoplasmic tail leads to its ER localization (Nufer et al. 2003, Neve et al. 2003). The binding of VIPL to glycoproteins is calcium dependent and reaches its maximum at pH 7.4, which refers to the pH in the ER (Yamaguchi et al. 2007). It has binding specificity for the D1-arm of high-mannose N-liked glycans, since glucosylation of the D1-arm inhibits it's binding (Yamaguchi et al. 2007). Overexpression of this lectin results into a striking redistribution of ERGIC-53 to the ER (Nufer et al. 2003). Neve et al. (2003) found that VIPL binds to glycoproteins of different size (35 and 250 kDa) and Yamaguchi et al. (2007) identified porcine thyroglobulin as a binding partner, suggesting that it may be involved in the regulation of export from the ER of a subset of glycoproteins. Another potential function is to prevent degradation of folded proteins by protection from demannosylation and interaction with proteins of the ERAD pathway (Kamiya et al. 2008, Yamamoto 2009), but to date its function is not fully understood.

Other lectins along the secretory pathway

The mannose-6-phosphate receptor operates in the TGN. It recognizes terminal mannose-6-phosphate residues on N-linked carbohydrates of glycoproteins (Fig. 1.1) and sort them into clathrin-coated vesicles destined for endosomes (Kornfeld 1992). The cargo is then released in the endosome and the receptor recycles back to the TGN for an additional round of sorting and transport.

A domain homolog to mannose-6-phosphate receptor was found in the ER protein osteosalcoma 9 (OS-9) (Kimura et al. 1998, Munro 2001). This lectin binds to terminal mannose of the C-arm of high mannose-type glycans and is involved in the ERAD pathway (Hosokawa et al. 2009, Mikami et al. 2010). Together with the lectin XTP3-transactivated gene B protein precursor it is involved in translocation for ubiquitination of misfolded proteins (reviewed in Anelli and Sitia 2008).

Another lectin which is also involved in ERAD is the ER-degradation enhancing α-mannosidase like protein (EDEM, Hosokawa et al. 2001). This protein has binding specificity for high mannose-type glycans, sorting misfolded proteins to the ERAD pathway (Hosokawa et al. 2001, Jacob et al. 2001).

The two Lectins of the galectin family galectin-3 and galectin-4 play also a role in the secretory pathway. They are localized in the late secretory pathway beyond the Golgi and are

required for apical protein sorting of different glycoproteins (Delacour et al. 2005, Delacour et al. 2006, Stechly et al. 2009).

1.2.2 Lectin-interplay in the early secretory pathway

The working model of intracellular lectins in the early secretory pathway so far is shown in figure 1.4.

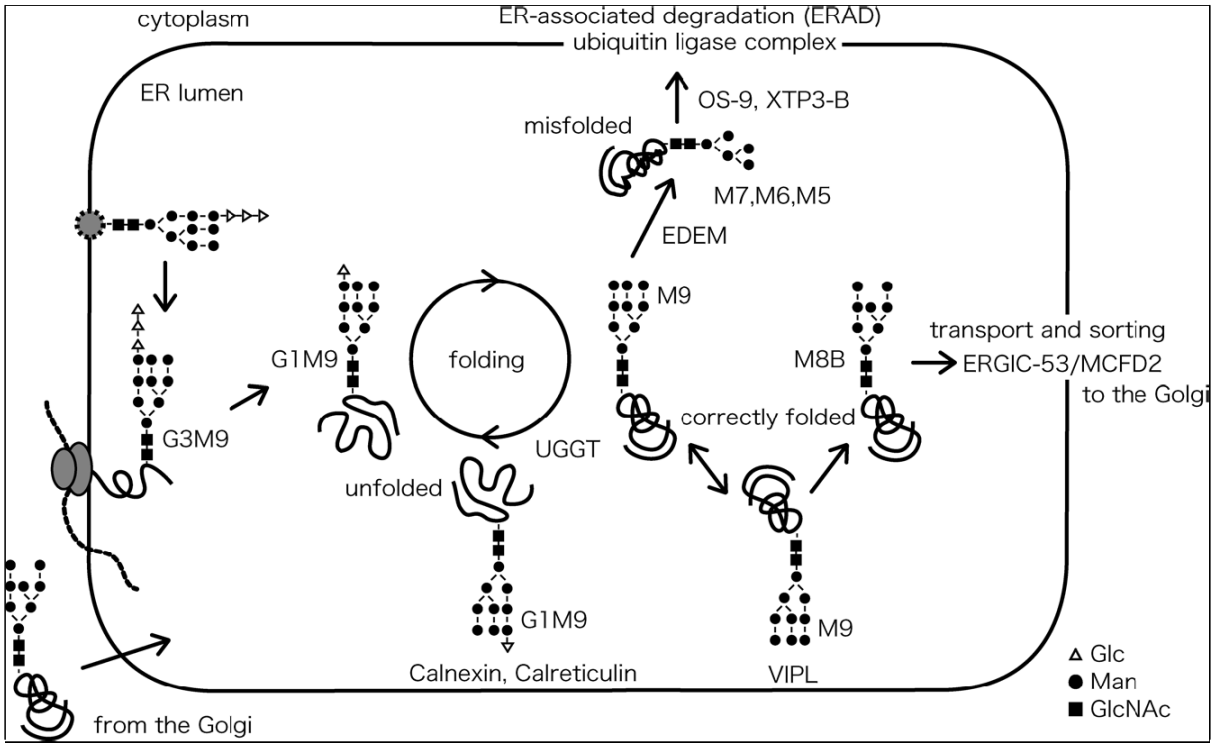

Figure 1.4 Intracellular lectins involved in quality control and transport of glycoproteins in the ER. The quality control pathway is classified into three kinds of reactions: folding of unfolded proteins, ER-associated degradation of misfolded proteins, and transport and sorting of correctly folded proteins. These reactions are regulated by several intracellular lectins, which recognize N-glycans attached to glycoproteins as tags. UGGT: UDP-glucose: glycoprotein glycosyltransferase, EDEM: ER-degradation enhancing α-mannosidase like protein, OS-9: osteosalcoma-9 protein, XTP3-B: XTP3-transactivated gene B protein precursor, ERGIC-53: ER-Golgi intermediate compartment 53 kDa protein, MCFD2: multiple coagulation factor deficiency 2 protein, VIPL: VIP36-like protein (modified from Yamamoto 2009).

CNX and CRT bind to monoglucosylated N-linked glycans on newly synthesised proteins and release them when the terminal glucose is processed. When proteins are not correctly folded, lectins, which are involved in the ER-associated degradation like EDEM and OS-9, bind to

these proteins. In the ERAD process, the misfolded proteins are translocated across the ER-membrane, conjugated with ubiquitin, and targeted to the proteasome for destruction in the cytoplasm.
Correctly sorted proteins are bound by VIPL which prevent the degradation process.
Some of the proteins are then handed to ERGIC-53 which transports them out of the ER in COP II coated vesicles which fuse to the ERGIC which is located near the cis-Golgi (Bannykh et al. 1998, Klumperman et al. 1998, Horstmann et al. 2002). Afterwards, ERGIC-53 recycles back to the ER. The ERGIC plays an important role in the sorting of proteins since it receives anterograde cargo coming from the ER and on the other hand, is involved in retrograde transport of escaped proteins back to the ER (Klumperman et al. 1998, Martinez-Menarguez et al. 1999). Proteins that have reached the ERGIC are further transported in a microtubule-dependent manner to the cis-Golgi (Saraste & Svensson 1991, Presley et al. 1997).
Another lectin which is proposed to play a role in the secretory pathway is vesicular integral-membrane protein (VIP36) which is discussed in the next paragraph.

1.2.3 Vesicular integral-membrane protein (VIP36)

Vesicular integral-membrane protein (VIP36) is an intracellular L-type lectin of 36 kDa, which has homologies to leguminous plant lectins (Fiedler et al. 1994). This type I transmembrane protein consists of 322 amino acids and has a CRD in its luminal part (Fig. 1.5). The CRD exhibits optimal binding affinities for glycoproteins that leave the CNX/CRT cycle in the ER and yet do not undergo trimming of the D1 mannosyl branch in the cis-Golgi (Kamiya et al. 2005). However it can also bind to other high mannose type glycans but with a lower binding affinity (Kamiya et al. 2005). The high specificity for deglucosylated D1 branch is governed by a single aspartate residue in its sugar-binding pocket (Kamiya et al. 2008). It was also reported that VIP36 binds to GalNAc found on O-linked glycans (Fiedler & Simons 1995).
VIP36 contains a c-terminal endocytosis signal (KRFY) similar to that of ERGIC-53 (Itin et al. 1995a). Moreover it shares 46 % similarity of its CRD with ERGIC-53. The human gene encoding for VIP36 is located on chromosome 5 and has a total length of 14.9 kb with 8 exons (Nufer et al. 2003).
It is ubiquitously expressed in epithelial and non-epithelial tissues, having a half-life of approximately 5 h (Neve et al. 2003) and carrying one N-glycosylation site (Fiedler & Simons

1995), which is complex glycosylated (Füllekrug et al. 1999). VIP36 binds mainly to membrane proteins but can also bind secretory proteins and has its maximal binding activity at 37°C and pH 6 (Hara-Kuge et al. 1999) which indicates a localization manly in the cis-Golgi.

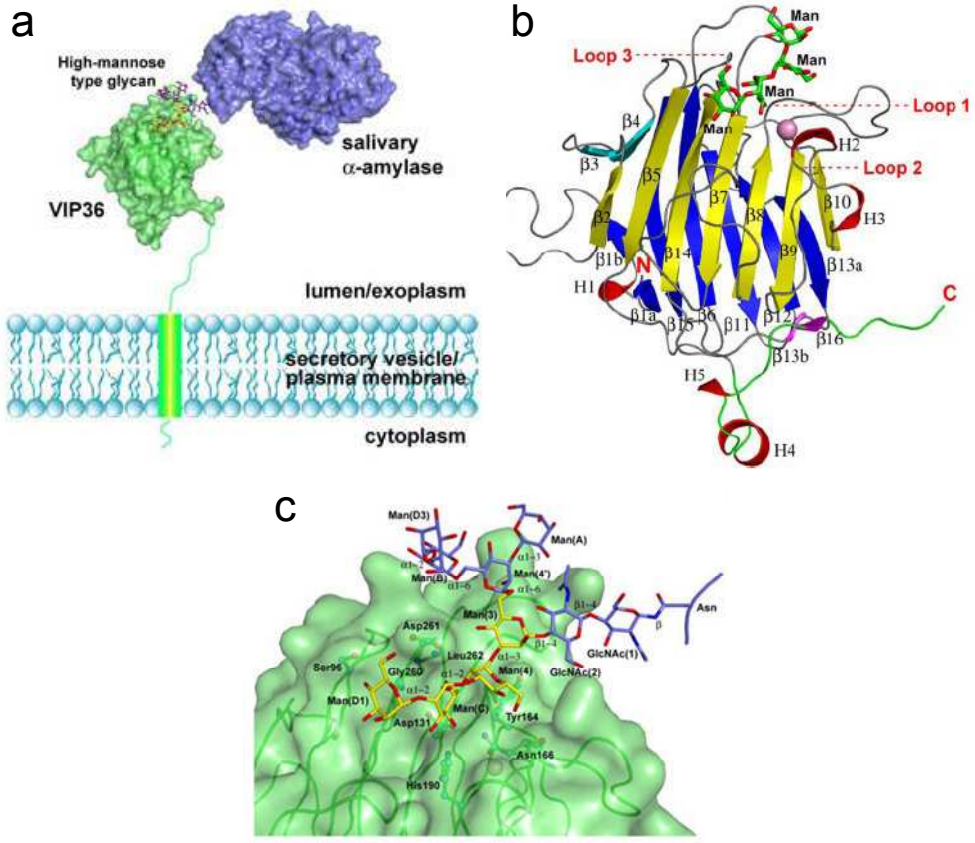

Figure 1.5 Structure of VIP36. a: The type I transmembrane protein VIP36. It consists of a short cytoplasmic domain followed by the transmembrane domain. The luminal/exoplasmic domain carries the CRD and consists of the amino acids 45-322. Here, the model of VIP36 binding to salvary α-amylase carrying $Man_8GlcNAc_2$ in rat secretory vesicles is shown. b: Ribbon model of the overall structure of the luminal/exoplasmic domain of VIP36. The secondary structures are highlighted (concave β-sheets: yellow, convex β-sheets: blue, β-hairpin: cyan, β-sheet between stalk domain and one of the CRD loops: magenta, helices: red). The loops of the CRD and the stalk domain are coloured gray and green, respectively. c: the high mannose-type glycan of VIP36 indicated by a stick model. Modelled D2- and D3-arms and N-linked chitobiose moiety of the high mannose-type glycan are shown in purple, types of glycosidic linkages are indicated (modified from Satoh et al. 2007).

Fiedler et al. (1994) first isolated VIP36 from CHAPS detergent resistant membranes (DRMs) or glycolipid rafts from Mardin-Darby canine kidney (MDCK) cells containing apical marker proteins. They found a localization of this lectin in the Golgi, endosomal and vesicular

structures and to the apical and basolateral cell surface (Fiedler et al. 1994). However, Füllekrug et al. (1999) found that this lectin is also localized to the early secretory pathway, by showing a significant overlap of VIP36 with ERGIC and COPI vesicles and that it is cycling between the ER and Golgi. Further, by modifying the methods of Fiedler et al. (1994) to isolate DRMs, they showed that VIP36 is not associated with DRMs of the Golgi, suggesting that VIP36 is unlikely to play a role in formation of glycolipid rafts (Füllekrug et al. 1999). The cycling of VIP36 leads to the suggestion that VIP36 recognizes glycoproteins that have escaped trimming by cis-Golgi α-mannosidase I and recycle them back for an additional trimming (Hauri et al. 2000). However VIP36 seems to have no ability to distinguish correctly folded from misfolded proteins (Mikami et al. 2010). Dahm et al. (2001) showed that VIP36 traffics with cargo only in the early secretory pathway, separating at the level of the Golgi-apparatus. However, secretory glycoproteins recognized by VIP36 were secreted 2-fold more efficient from the apical membrane than from the basolateral membrane (Hara-Kuge et al. 2002).

VIP36 interacts with the apical secretory glycoprotein clusterin (Hara-Kuge et al. 2002), α-amylase in rat parotid gland cells (Hara-Kuge et al. 2004) and, partial colocalize with ERGIC-53 in transport vesicles (Shimada et al. 2003b). A carbohydrate-independent interaction could be shown between VIP36 and immunoglobulin-binding protein (BiP) over a long period of time in the ER (Nawa et al. 2007). Since VIP36 is Endo H resistant when interacting with BiP, it might be relocated to the ER from the Golgi after complex glycosylation. An interaction with BiP in the early secretory pathway indicates that VIP36 plays a role in early sorting events. Alpha-1-antitrypsin was also found as cargo for VIP36 between the ER and Golgi (Reiterer et al. 2010). This binding was increased when complex N-glycosylation was prevented (Reiterer et al. 2010). Therefore they suggest that VIP36 may function as a post-ER quality control of α-1-antitrypsin.

1.3 Lipid rafts

In the last decades, there were a lot of studies concerning the composition of the membrane bilayer which was first described as a continuous two-dimensional fluid phase, acting as a neutral solvent for membrane proteins in which all molecules diffuse freely (Singer & Nicolson 1972). To date, it is known that lipids are distributed asymmetrically between the outer and inner leaflets of the bilayer (Van Meer 1989). This membrane model leads to a

different organization of membrane components on the lateral axis, leading to a variety of lipid-lipid, lipid-protein, and actin cytoskeleton interactions (Anderson & Jacobson 2002, Edidin 2003, Kwik et al. 2003).

1.3.1 Structure and function of lipid rafts

The membrane bilayer is separated into a lipid-disordered (l_d) and a lipid-ordered (l_o) phase (Brown & London 1998). The l_o-phase is enriched in cholesterol and sphingolipids with their saturated fatty acids, and saturated glycerophospholipids. The structure of their hydrophobic parts allows them to pack more tightly than the linked unsaturated glycerophospholipids. Therefore they establish a more ordered state (Brown & London 1998). These phases are termed lipid rafts (or lipid microdomains, membrane microdomains, DRMs), which have been investigated from several groups in the last two decades (Simons & Van Meer 1988, Brown & Rose 1992, Simons & Ikonen 1997). Pike (2006) defined them as small (10-200 nm), highly dynamic, sterol and sphingolipid-enriched microdomains that compartmentalize cellular processes. Size and composition of lipid rafts varies depending on cell type (Schuck et al. 2003), nutrition conditions (Peretti et al. 2005) and differentiation stage of the cell (Fitzner et al. 2006).

Lipid rafts are dynamic structures. They are dispersed in membranes but can move in it and diffuse laterally to build clusters (Henderson et al. 2004). It has been reported, that they can cluster into larger structures to bring signalling molecules together to initiate intracellular signalling. They might play a role as “reaction vessels”, increasing the chance that two specific proteins of low concentration will meet on the membrane (Nicolau et al. 2006).

Phase separation of lipid rafts has been demonstrated in model membranes and biological membranes; however the length and time scales on which this phase separation occurs are still a matter of debate (Simons & Ikonen 1997, Edidin 2003, Kwik et al. 2003, Kusumi et al. 2004). Moreover, it is still put into question if DRMs, lipid rafts and l_o phases are synonymous, although it was found that they are all dependent on cholesterol and are organized almost by the same principles (reviewed in Lindner & Naim 2009).

Many proteins associate with lipid rafts, like GPI-anchored proteins, transmembrane signalling proteins (e.g. tyrosine kinases), and acylated proteins (e.g. Ser family). Their GPI-anchor or other signals or structural features in their transmembrane domain enable them to associate with lipid rafts. Some proteins require oligomerization or ligand binding for sorting into these microdomains (Holowka & Baird 2001, Paladino et al. 2004). It is also known that

proteins stabilize lipid rafts through their association with the cytoskeleton (Nakada et al. 2003). Several growth factor receptors including epidermal growth factor receptor, insulin receptor, and the nerve growth factor receptor are localized in membrane microdomains. Their signalling functions are significantly modulated by glycolipids (reviewed in Varki et al. 2009). The glycosphingolipids may play a role in the flow of information from the outside to the inside of cells, which is supported by the observation that antibody-induced glycosphingolipid clustering activates lipid raft-associated signalling (reviewed in Varki et al. 2009). Other proteins also need the association for signal transduction like IgE in allergic response and T-cell antigen receptor signalling (Field et al. 1995, Janes et al. 2000). Correct targeting of various apically sorted proteins such as DPPIV or SI is dependent on an association with lipid rafts, whereas basolateral sorted proteins are normally not included (reviewed in Schuck & Simons 2004).

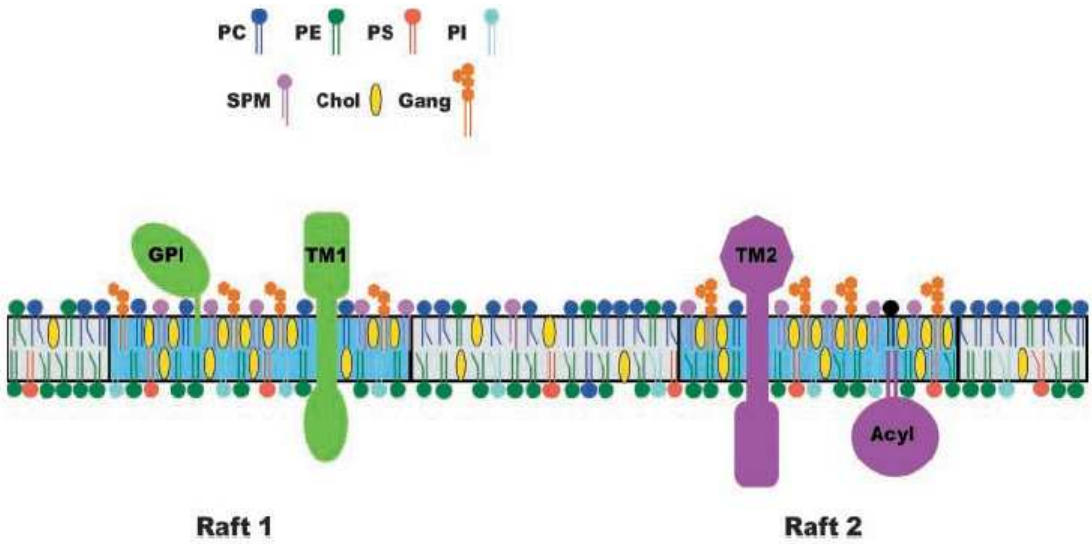

Figure 1.6 Structure of lipid rafts. Lipid rafts (blue bilayer) are specialized membrane domains containing high concentrations of cholesterol, sphingomyelin, and gangliosides. They are also enriched in phospholipids that contain saturated fatty acyl chains (straight lines in lipid tails). This composition results in lateral phase separation and the generation of a lipid ordered (l_o) phase. Bulk plasma membrane (gray) contains less cholesterol, sphingomyelin and gangliosides, and more phospholipids with unsaturated fatty acyl chains. As a result, it is more fluid than lipid rafts. A variety of proteins partition into lipid rafts: glycosylphosphatidylinositol-anchored proteins (GPI), transmembrane proteins (TM), dually acylated proteins (Acyl). As shown in this figure, not all lipid rafts have the identical protein or lipid composition (Raft 1 and Raft 2). PC: phosphatidylcholine, PE: phosphatidyletanolamine, PS: phosphatidylserine, PI: phosphatidylinositol, SPM: sphingomyelin, Chol: cholesterol, Gang: gangliosides (taken from Pike 2003).

Since lipid rafts are involved in intra- and intercellular sorting and signalling, many studies were conducted in focus on diseases, where lipid microdomains play a role. These studies showed that lipid rafts are involved in infectious diseases (e.g. HIV infection, Campbell et al. 2001), prion-related diseases and cancer (reviewed in Simons & Ehehalt 2002).
All these features of lipid rafts make them a very important tool for proteins and lipids in signalling, transport and sorting.

1.3.2 Detergent resistant membranes (DRMs)

The advantage to extract membrane microdomains is their ability to resist extraction with non-ionic detergents (e. g. Triton X-100) at 4°C and floating to lighter fractions on sucrose-density gradients (Brown & Rose 1992, Brown & London 1998). This widely established method to isolate lipid rafts has led to the term Detergent Resistant Membranes (DRMs, Brown & Rose 1992) which encompasses several membrane populations that share the common ability to remain insoluble in various detergents. Most common is the isolation of Triton X-100 DRMs. However, other non-ionic detergents such as CHAPS, Brij, Lubrol WX and Tween 20 are also used to isolate different membrane populations. These detergents have different strength to solubilise DRMs and have different lipid and protein compositions (Drobnik et al. 2002, Schuck et al. 2003, Alfalah et al. 2005). This diversity of lipid and protein composition is also shown in membranes of different cellular compartments, which leads to the theory that the DRMs, isolated by different detergents, originate from different cellular compartments and are not restricted to the plasma membrane. Several studies showed the existence of DRMs in ER membranes, isolating DRMs which contain early biosynthetic forms of proteins (Paladino et al. 2004, Browman et al. 2006, Hein et al. 2009), and identifying them as early sorting platforms (Alfalah et al. 2005).
Delauney et al. (2008) isolated DRMs of the Golgi with different detergents, namely Triton X-100 and Lubrol WX. They found that Lubrol WX DRMs contain more lipids of the inner membrane leaflet, whereas Triton X-100 DRMs represents more the outer membrane leaflet (Delauney et al. 2008). Other studies also showed that these two distinct DRMs exist in the same membrane, by isolating proteins from Lubrol WX DRMs which are soluble in Triton X-100 DRMs (promimin: Roper et al. 2000, prostate-specific membrane antigen: Castelletti et al. 2008).

1.4 Aim of the study

The sorting machinery along the secretory pathway is a complex of many proteins which are responsible for the correct sorting, folding and routing through the cellular compartments. The correct sorting of proteins plays a crucial role for their physiological functions. There are many diseases known such as congenital sucrase-isomaltase deficiency, cystic fibrosis, glucose-galactose malabsorbtion, and congenital lactase deficiency (Naim et al. 1988a, Riordan et al. 1989, Turk et al. 1991, Kuokkanen et al. 2006), which are caused by missorted and misfolded proteins which are dysfunctional. Therefore, it is important to get a better understanding of the sorting machinery along the secretory pathway, where many intracellular lectins are involved.

In the past years many lectins were identified which play a role in ER quality control (e.g. calnexin, calreticulin) or for the transport between cellular compartments (e.g. ERGIC-53, mannose-6-phosphate receptor). But not for all lectins which have been identified in the secretory pathway, their function is fully defined. One of these lectins is VIP36. It has been shown that it is mainly localized in the cis-Golgi but can also be found in the ER, ERGIC or even at the cell surface (Fiedler et al. 1994, Füllekrug et al. 1999). Kamiya et al. (2005) found that VIP36 has high binding affinities for glycoproteins that leave the CNX/CRT cycle in the ER and yet do not undergo trimming of the D1 mannosyl branch in the cis-Golgi, but that it is also able to bind other glycoforms.

The general aim of the study was to characterize the function and localization of the intracellular lectin VIP36.

The following specific aims were investigated:

1. Since only a few glycoproteins have already been identified as cargo for VIP36, I wanted to identify additional interaction partners which might act as cargo for VIP36 in different cell lines. Hara-Kuge et al. found in 1999 and 2002, that VIP36 recognizes more apical than basolateral sorted glycoproteins, which are associated with the cell membrane. Therefore, I focused on apical transmembrane glycoproteins as VIP36 interaction partners.
2. Moreover, I wanted to investigate when interaction of VIP36 and cargo takes place and if different glycoforms of the proteins play a role in this process. For this, pulse chase experiments as well as glycosylation-inhibitors and glycosylation-defective cell lines were used.

3. DRMs or lipid rafts are found to function as a platform for signalling and sorting along the secretory pathway. Therefore, many proteins need the association with DRMs for a proper function and sorting, and further to get in contact with the right interaction partners. Since VIP36 was isolated from CHAPS DRMs, I was wondering if there is an association with other types of DRMs along the secretory pathway. Thus, I wanted to show where VIP36 might localize along the secretory pathway when interacting with cargo and if DRMs might function as a platform for interacting with glycoproteins for this lectin. To investigate the association of VIP36 with DRMs and its cargo at different stages of glycosylation, I used glycosylation-defective cell lines. To proof the hypothesis that obtained differences are not only due to a different lipid composition of DRMs in the defective cell lines, lipid analysis followed by statistical analysis of the different DRMs were conducted.

2. Materials and Methods

2.1 Materials

All solutions, buffers and plastic ware used for cell culture were autoclaved (121°C, 1 bar, 20 min) before usage. Reagents were at least of p. a. quality.

2.1.1 Used chemicals

Acetic acid glacial	Roth, Karlsruhe, Germany
Acetic acid methyl acetate	Roth
Acrylamide, Rotiphorese Gel30	Roth
Ammonium chloride (NH_4Cl)	Fluka, Steinheim, Switzerland
Ammoniumperoxodisulfate (APS)	Merck, Darmstadt, Germany
Bovine serum albumine (BSA)	PAA, Pasching, Austria
Chloroforme	Roth
Coomassie Brilliant Blue	SERVA, Heidelberg, Germany
Copper sulphate ($CuSO_4$ x 5 H_2O)	Merck
1-Deoxymannojirimycin hydrochloride (dMM)	Sigma, Taufkirchen, Germany
1-Deoxynojirimycin hydrochloride (dNM)	Sigma
Diethyl ether	Roth
Dimethylsulfoxide (DMSO)	Fluka
Dithiolthreitol	Sigma
Ethanol	Roth
Ethylendiamintetraacetic acid (EDTA)	Roth
Fetal calf serum (FCS)	Gibco, Eggenstein, Germany
FuGENE® HD Transfection Reagent	Roche, Mannheim, Germany
Geneticin® (G418-Sulphate)	PAA
Glycerol	Sigma
L-glutamine	PAA
Lubrol WX	Merck
2-Mercaptoethanol	Sigma
Methanol	Roth

Mowiol 4-88	Calbiochem, an affiliate of Merck
N-hexane	Roth
N,N,N',N'-Tetramethylethylendiamine (TEMED)	Roth
Paraformaldehyde	Fluka
Peniciline-streptomycine	PAA
Potassium chloride (KCl)	Roth
Potassium dihydrogen phosphate (KH_2PO_4)	Roth
1-Propanol	Roth
Protease inhibitor:	
Antipain, Aprotinin, Leupeptin, Pepstatin, Trypsin inhibitor	Sigma
PMSF	Boeringer Ingelheim, Ingelheim, Germany
Protein assay concentrate	Bio-Rad Laboratories, Munich, Germany
Protein A-Sepharose	Amersham Biosciences GE Healthcare, Freiburg, Germany
Saponin	Sigma
Sodium chloride (NaCl)	Roth
Di-Sodium hydrogen phosphate anhydrous (Na_2HPO_4)	Roth
Sodium hydroxide (NaOH)	Merck
Sodium dodecyl sulphate (SDS)	Roth
Sucofin skim milk powder	TSI GmbH & Co. KG, Zeven, Germany
Sucrose	MP Biomedicals LLC, Ohio, USA
SuperSignal ELISA Femto Maximum Sensitivity Substrate	Perbio Science, Bonn, Germany
Tris-HCL	Roth
Triton X-100	Sigma
Trypsin for cell culture	PAA
Trypsin (from bovine pancreas)	Sigma
Tween 20	Roth
[^{35}S]methionine	Amersham Biosciences GE Healthcare

2.1.2 Used antibodies

Primary antibodies:

Vesicular integral-membrane protein: polyclonal rabbit Ab sc-67131 (H-90), 200µg/ml
WB: 1:330, IP: 1µg
(Santa Cruz Biotechnology, Heidelberg, Germany)

Dipeptidyl peptidase IV: mAb HBB 3/775/42 (Hauri et al. 1985)
WB: 1:2000, IP: 1 µg

Sucrase-isomaltase: mAb HBB 3/705/60 (Hauri et al. 1985)
WB: 1:330, IP: 1µg
mAb HSI2 (Beaulieu et al. 1989)
IP: 1 µg

Lactase-phlorizin hydrolase: mAb mLac 10 (Maiuri et al. 1991)
WB: 1:1000
mAb HBB 1/909 (Hauri et al. 1985)
IP: 1 µg

Aminopeptidase N: mAb HBB 3/153/63
IP: 1 µg (Hauri et al. 1985)

Flotillin-2: mAb sc-28320 (B-6), 200µg/ml
WB: 1:1000
(Santa Cruz Biotechnology)

RhoA: mAb sc-418 (26C4), 200µg/ml
WB: 1:1000
(Santa Cruz Biotechnology)

Secondary Antibodies:

Rabbit IgG-ECL
WB: 1:10 000 (Darko, Hamburg, Germany)

Mouse IgG-ECL
WB: 1:10 000 (Amersham Biosciences, Freiburg, Germany)

Rabbit IgG AlexaFlour568
IF: 1:500
(Molecular Probes, Invitrogen GmbH, Darmstadt, Germany)

2.1.3 Used marker

For the SDS-PAGE the PageRuler™ Prestained Protein Ladder Plus (Fermentas GmbH, St. Leon-Rot, Germany) was used. This marker provide 9 bands of equal intensities in SDS-PAGE and after Western blotting onto a PVDF membrane ranging from 11 kDa to 250 kDa. Therefore, it was used for high percentage (12 %) gels to detect VIP36, rhoA and flotillin-2, as well as for low percentage (6 %) gels to detect high molecular weight proteins (e.g. DPPIV, SI).
For the lipid-analysis a standard mix of twelve different lipid components was used with a concentration of 200 µg / ml per lipid component. Cholesterol ester, triglycerides, oleic acid, cholesterol, monoacylglycerol, galactosyl cerebroside, ethanolamine, cardiolipin, serine, choline, and L-choline were purchased from Sigma (Taufkirchen, Germany); sphingomyelin were obtained from Fluka (Steinheim, Switzerland).

2.1.4 Mammalian cell lines

In this study the following cell lines were used:

Caco-2 cells are derived from human colonic adenocarcinomas and have retained the ability to differentiate in culture (Zweibaum et al. 1991). They express several morphological and biochemical characteristics of small intestinal enterocytes (Giuliano & Wood 1991, Pinto et al. 1983). Similar to enterocytes, they develop an apically brush border membrane, which consists of uniformly organized microvilli. Several glycoproteins of the small intestine are endogenously expressed in Caco-2 cells, like DPPIV, SI and APN (Hauri et al. 1985, Zweibaum et al. 1984).

Chinese hamster ovary (CHO) K1 cells are non-polarizing, fibroblastoid cells. The CHO K1 cell line is a subclone from the original cell line, which was established from *cricetulus griseus* ovary biopsy tissue (Puck et al. 1958).

CHO-Lec cells were first established by Pamela Stanley from lectin-resistant CHO cells (Stanley et al. 1975a). They were isolated for the resistance to the cytotoxity of plant lectins and are characterized by specific defects in their glycosylation. There are several cell lines

available with different glycosylation defects. In this study, the two mutants CHO-Lec1 (Lec1) and CHO-Lec2 (Lec2) were used.

CHO-Lec1 cells are deficient in N-acetylglucosaminyltransferase I (Stanley et al. 1975b) in the cis-Golgi (Fig. 2.1). Therefore, the complex N-glycosylation is not achieved and the $Man_5GlcNAc_2$ glycan is not further processed. However, O-glycosylation is unaffected.
CHO-Lec2 cells lack the CMP-sialic acid transporter (Deutscher et al. 1984), which inhibits the last step of the N-glycosylation (Fig. 2.1). The O-glycosylation is also affected in this cell type.

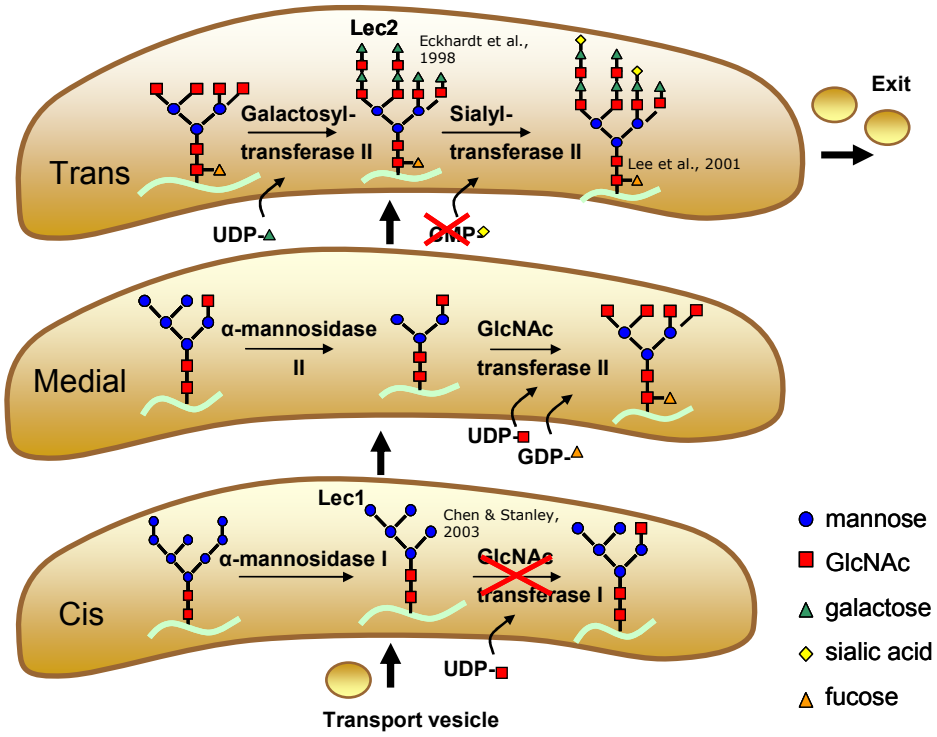

Figure 2.1 N-glycan processing in the Golgi apparatus of CHO K1 and Lec cells. Terminal N-linked glycans are present in the CHO K1 cell line (Lee et al. 2001). The defect in the Lec1 cells occurs in the cis-Golgi due to a defective GlcNAc-transferase I. This leads to the $Man_5GlcNAc_2$ glycan (Chen & Stanley 2003). In the Lec2 mutant, the CMP-sialic acid transporter is lacking, which results into glycans without the terminal sialic acid residues (Eckhardt et al. 1998).

2.2 Methods

2.2.1 Cell culture

Caco-2 cells were cultured in Dulbecco's Modified Eagle Medium (DMEM) high glucose (1g/l) medium (PAA Laboratories, Pasching, Austria). CHO cells, CHO-Lec1 cells and, CHO-Lec2 cells were cultured in RPMI-1640 medium (PAA Laboratories, Pasching, Austria).
Media was supplemented with 10 % fetal calf serum (FCS), 500,000 U / l penicillin and 10 mg / l streptomycin (PAA Laboratories, Pasching, Austria). The cells were developed in tissue culture dishes (Sarstedt, Nümbrecht, Germany) at 37°C, 95 % relative humidity and 5 % carbon dioxide atmosphere.
When cells reach a confluence state, they were passaged. Therefore cells were washed with PBS and then trypsinized. When cells lost their connection to the culture dish, trypsin activity was stopped with culture medium (containing FCS) and cells were centrifuged for 2 min at 850 *g*. After discarding the media containing trypsin they were seeded on new culture dishes.
When cells were used for biosynthetic labelling, they were cultured for 2 to 3 h in methionine-free Minimum Eagle`s Medium (MEM, PAA Laboratories) supplemented with 500,000 U / l penicillin, 10 mg / l streptomycin and, 200 mM L-glutamine.

2.2.2 Establishment of stable cell lines

For the establishment of stable cell lines, expressing DPPIV, CHO K1 cells, Lec1 cells and, Lec2 cells were transfected using FuGENE® HD Transfection Reagent. FuGENE® HD Transfection Reagent is a multi-component reagent which forms a complex with plasmid DNA and transports it into animal or insect cells. According to the producer's protocol plasmid DNA (encoding GFP chimera of DPPIV, pEGFP-N1 vector, Takara Bio Europe/Clontech, Saint Germain en Laye, France) was diluted in serum-free medium to a concentration of 0.02 µg / µl. The transfection reagent was added in a ratio of 4:2 (reagent to DNA) and incubated for 5 min to achieve a complex building. The arised complex was then added to the cells, and incubated for 24 h. The following day, cells were passaged 1:30 as described above.
For selection of the cells, the medium was supplemented with 500 µg / ml Geneticin®. Medium was changed every four days. Thereby, only cells which stably incorporated the

plasmid DNA into their genome, coding for Geneticin®-resistance are able to inactivate the antibiotic and survive. Positive clones were identified by confocal laser microscopy and Western blot analysis.

2.2.3 Immunofluorescence

For the characterization of the stable cell lines and for visualization of the interaction of DPPIV-GFP and VIP36, immunofluorescence was conducted.
CHO K1 and Lec cells, which were stably transfected with DPPIV-GFP, were grown on cover slips (12 mm diameter, Roth). When they reached a confluent state, they were rinsed twice with PBS and then fixed with 4 % paraformaldehyd for 20 min.
For the analysis of the stable cell lines, cells were afterwards mounted with mowiol 4-88.
To study the interaction of DPPIV-GFP and VIP36, cells were further processed according to Leitner et al. (2006). The rbAb sc-67131 (H-90) (1:40) was used as a primary antibody in blocking buffer (0.5 % Saponin in PBS and 1 % BSA) for the detection of VIP36. As a secondary antibody goat anti-rabbit AlexaFlour568 (1:500) was used. After antibody treatment and washing procedures, cells were mounted with mowiol 4-88. As a negative control the same procedure was conducted by using only the secondary antibody.
The following day, cells were visualized in the confocal laser microscope.

2.2.4 Confocal laser microscopy

Cells were prepared as reported previously (see 2.2.3). The fluorescence images were visualized using a Leica TCS SP5 microscope with an x63 oil planapochromat lens (numerical aperture: 1.4). Scans were made using an argon laser for the visualization of DPPIV-GFP (absorbance 476 nm, maximal emission 510 nm).
Dual colour images with GFP and AlexaFluor568 were detected by sequential scans. AlexaFluor568 was visualized by a neon laser (absorbance 576 nm, maximal emission 599 nm).

2.2.5 Western blot analysis

For Western blot analysis of different proteins in Caco-2, CHO K1 and Lec cells, cells were lysed with 1 ml 1 % Triton X-100 in PBS with protease inhibitors and homogenized by trituration with a G21 needle and then maintained on ice for 1.5 h. Cells were then centrifuged for 10 min at 13 000 *g* and cell debris was discarded.

A protein measurement was conducted according to Bradford (1976) using the Bio-Rad Protein Assay concentrate. The samples were processed by SDS-PAGE on 6 % or 12 % polyacrylamid gels (Laemmli 1970), with 50 µg of each sample loaded.

SDS-PAGE was followed by Western blot analysis. Transfer of separated proteins to a Hybond-PVDF membrane (Amersham Biosciences GE Healthcare, Freiburg) was conducted using a tank blot for 1.5 h at 250 mA. After transfer, the membrane was blocked over night in 5 % milk (skim milk powder in PBS) at 4°C. Immunostaining was performed with different primary antibodies for 45 min in 2 % milk (skim milk powder in PBS). After washing in 0.5 % Tween 20 in PBS, anti-mouse or anti-rabbit ECL-peroxidase was used as a secondary antibody and incubated for 35 min. The detection was carried out with SuperSignal ELISA Femto Maximum Sensivity Substrate via chemilumininescence with the supersensitive 16-bit ChemiDoc XRS camera of a Molecular Imager® (Bio-Rad Laboratories, Munich). Further processing of images was performed with Quantity One® (Bio-Rad Laboratories, 1998).

2.2.6 Immunoprecipitation

Immunoprecipitation followed by Western blot analysis was conducted for the protein interaction experiments using Caco-2, CHO K1, and Lec cells.

Cells were lysed as reported before (see 2.2.5). The samples were immunoprecipitated with an antibody directed against DPPIV, SI, APN, and LPH, depending on the experimental procedure, in the presence of protein A-Sepharose (Naim et al. 1991). The immunoisolates were further processed by SDS-PAGE on 12 % polyacrylamid gels (Laemmli 1970) followed by Western blot analysis. Immunostaining was performed with rbAb sc-6713 (H-90) directed against VIP36. For the negative control for immunoprecipitation, samples were precipitated with protein A-Sepharose without any antibody.

2.2.7 DRM extraction

To investigate the association of proteins with DRMs, a discontinuous sucrose-density gradient was used, modifying a protocol reported by Babiychuk and Draeger in 2006.
Cells were washed with PBS and then solubilised in PBS containing 1 % detergent (Lubrol WX, Triton X-100 or Tween 20) and protease inhibitors. After homogenization with a G21 needle, cells were maintained on ice for 2.5 h. Cell lysates were then centrifuged for 10 min at 10 000 *g* and cell debris was discarded. The sample was then diluted to a final concentration of 40 % sucrose (500 µl of the sample and 500 µl of 80 % sucrose) and layered onto an 80 % sucrose cushion. The 1 ml sample was then overlaid with 7 ml of 30 % sucrose followed by 1 ml 5 % sucrose on the top (Fig. 2.2). The discontinuous sucrose-density gradient was then centrifuged for 18 h at 33 000 rpm (Beckman SW 40 Ti rotor) at 4°C. During centrifugation, the DRM-associated proteins float to the upper fractions, also called floating-fractions, of the gradient, whereas the non-associated proteins remain in the lower non-floating-fractions. Nine fractions of 1 ml each were collected from the top and analysed for protein content by Western blotting. The two proteins flotillin-2 and rhoA were used as controls for the DRM-fractions and the non-DRM-fractions, respectively.

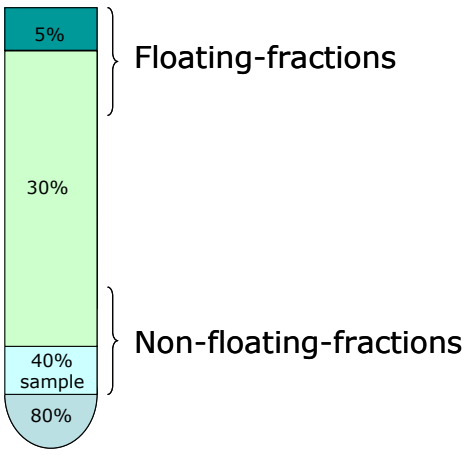

Figure 2.2 Composition of the discontinuous sucrose-density gradient. The 80 % sucrose fraction at the bottom consists of 1 ml, as well as the sample in 40 % sucrose and the 5 % sucrose fraction on the top. The 30 % sucrose fraction consists of 7 ml. Floating fractions were defined as the upper three fractions and non-floating fractions as the lower three fractions above the 80 % sucrose cushion.

2.2.8 Modification of N-glycosylation

To investigate the binding properties of VIP36 to glycoproteins at different stages of glycosylation, Caco-2 cells were treated with the glycosylation-inhibitors 1-deoxymannojirimycin (dMM) or 1-deoxynoijrimycin (dNM). As reported previously, dMM hampers the α-mannosidase I in the cis-Golgi, resulting in $Man_8GlcNAc_2$ N-linked glycans. The inhibition of α-glucosidase I and II is achieved by treatment with dNM. Without the action of the glucosidases, the three glucose residues remain on the N-linked glycan which prevents interaction of glycoproteins with CNX and CRT.

Caco-2 cells that were 6 days post-confluence were treated with dMM (concentration: 100 mM) or dNM (concentration: 100 mM) for 24 h in DMEM high glucose (1g/l) medium. Medium containing dMM or dNM were changed once after 12 h. Cells were lysed as reported before (see 2.2.5). The samples were divided in three parts, one for Western blotting with immunostaining of VIP36 the other two were used for immunoprecipitation of DPPIV (mAb HBB 3/775/42) or SI (mAb HSI2). SDS-PAGE of 12 % gels (Laemmli 1970) was followed by Western blot analysis with immunostaining of VIP36, as reported above.

Another experimental procedure to investigate different glycosylation stages was the use of the Lec cells with the defect in N-acetylglucosaminyltransferase I (Lec1) and CMP-sialic acid transporter (Lec2). The cell lines which were stably transfected with DPPIV-GFP were lysed and further processed like the treated Caco-2 cell samples.

2.2.9 Pulse Chase

Pulse chase experiments were conducted for the investigation of the N-glycan processing and maturation of DPPIV and SI.

Caco-2 cells that were 6 days post-confluence were incubated for 2 h in methionine-free medium and afterwards labelled with 100 μCi [S^{35}]methionine for 30 min. At time points 0, 30, 60, 90, 120 and 240 min cells were lysed with 1 % Triton X-100 in PBS as reported above (see 2.2.5). The samples were divided in two and immunoprecipitated with the mAbs HBB 3/775/42 or HSI2 directed against DPPIV or SI, respectively, in the presence of protein A-Sepharose (Naim et al. 1991). Immunoisolates were separated on 6 % polyacrylamid gels (Laemmli 1970) and dried. The dried gel was incubated with a storage phosphor screen for at least two days. Visualization of protein bands was conducted by the phosphor imaging device Personal Molecular Imager FX® (Bio-Rad Laboratories, Munich, Germany).

2.2.10 Trypsin digestion

For the analysis of the folding properties of SI at different glycosylation stages, Caco-2 cells were treated with the two glycosylation-inhibitors dMM and dNM, which was then followed by a trypsin digestion. As reported above, trypsin cleaves correctly folded SI into the two subunits sucrase and isomaltase.

Caco-2 cells that were 6 days post-confluence were treated with dMM or dNM (concentration: 100 mM) for 3 h concomitant with incubation in methionine-free medium. The medium containing dMM or dNM was changed once after 1.5 h. Afterwards cells were labelled with 100 µCi [S^{35}]methionine for 4 h in the presence of dMM or dNM (concentration: 100 mM), followed by lysis with 1 % Triton X-100 in PBS. The samples were maintained on ice for 2 hours. Afterwards, samples were immunoprecipitated with mAbs HSI2 and HBB 3/705/60 directed against SI in the presence of protein A-Sepharose (Naim et al. 1991). The immunoisolates were then incubated with 500 µg trypsin for 1 h at 37°C. The trypsin-digested samples were further processed by SDS-PAGE on 6 % polyacrylamid gels (Laemmli 1970), dried, and the incubated phosphor screen was analyzed by the phosphor imaging device Personal Molecular Imager FX®.

2.2.11 Co-immunoprecipitation

The co-immunoprecipitation experiment preceded by pulse chase experiment was used to investigate the binding of VIP36 to DPPIV and SI in dependence of N-glycosylation processing and maturation of these proteins.

Caco-2 cells that were 6 days post-confluence were cultured for 2 h in methionine-free medium and then labelled with 100 µCi [S^{35}]methionine for 30 min. At time points 0, 30, 60, 90, 120, and 240 min cells were lysed with 1 % Triton X-100 in PBS as reported before (see 2.2.5). For the following immunoprecipitation samples were divided in two and incubated with the mAbs HBB 3/775/42 or HSI2 directed against DPPIV or SI, respectively, in the presence of protein A-Sepharose (Naim et al. 1991). The immunoisolates were then incubated with 0.5 % SDS in PBS for 1 h at 37°C. With this step, the connection between SI or DPPIV and VIP36 as well as protein A-Sepharose was destroyed. Afterwards, cells were centrifuged and the supernatant was again immunoprecipitated. The rbAb sc-67131 (H-90) against VIP36 was used in the presence of protein A-Sepharose (Naim et al. 1991). Therefore only the VIP36 molecules which bound to either DPPIV or SI are precipitated. Immunoisolates were

further processed by SDS-PAGE on 12 % polyacrylamid gels (Laemmli 1970), dried and the incubated phosphor screen was analyzed by the phosphor imaging device Personal Molecular Imager FX®.

2.2.12 Lipid-analysis of DRMs

To determine if there are significant differences in the lipid composition of the different DRM-types between CHO K1 and the two Lec cell lines, a lipid-analysis was performed.
For the lipid-analysis, CHO K1, Lec1, and Lec2 cells were used. Three confluent culture dishes of each cell line were lysed with 1 % detergent (Triton X-100, Tween 20 or Lubrol WX) in PBS and maintained on ice for 2.5 h. After centrifugation at 10 000 *g* for 10 min cell debris was discarded and the samples were centrifuged for 1.5 h at 100 000 *g* in a Ti 100 rotor (Beckman). During centrifugation, the DRMs are separated from the rest of the cell lysate and can be found as a pellet at the bottom of the centrifuge tube. After centrifugation, the supernatant was discarded. The pellet was washed three times in 1 ml PBS and one time in 1 ml H_2O for 10 min at 1900 *g* to get rid of the remaining detergent. Samples were then diluted in 1 ml PBS and used for the lipid extraction.
The lipid extraction was performed following Bligh and Dyer (1959). For analysis of lipid components, samples were dried at room temperature and then resolved in chloroform / methanol (2:1 volume).
Samples were isolated on thin layer chromatography (TLC) (glass, SI-60, Phenomenex) according to a protocol from the IBM Jena (Quantitative Lipidanalyse biologischer Proben durch hochauflösende Dünnschichtchromatographie). The TLC was processed in a glass chamber. The plate was then dried and stained with copper sulphate solution and developed at 110°C.
Dried TCL plates were analysed using the software “ImageJ 1.41i” and “Microsoft Office Exel 2003”.

All performed experiments were repeated at least three times. One representative figure is shown for every experiment in the results.

2.2.13 Statistical analysis

For the analysis of the lipid composition in the different DRM fractions for the CHO K1 and Lec cells the values of eight samples were used for each cell line per lipid component and DRM extraction.

First, it was tested if the values have a normal distribution. Since this was not confirmed, the Mann-Whitney U test was used.

The Mann-Whitney U test is a method to determine whether two independent variables have equally large values (Mann & Whitney 1947). It is a two tailed, non-parametric analysis, based on the rank of the values of both variables.

In this study, it was used to test for significant difference between the amount of the different lipids in µg for CHO K1 and the two different Lec cells. The working hypothesis was defined as H_0: $Values_{CHO} = Values_{Lec1}$ or $Values_{CHO} = Values_{Lec2}$ for the different lipid components. The hypothesis was rejected if p-value was ≤ 0.05. All statistical analysis were conducted using the program SPSS (version 18, PSAW, IBM Deutschland GmbH, Munich, Germany). The significant threshold was 5 % for all analyses.

3. Results

3.1 Characterization of the stable transfected CHO cell lines

In order to analyze the binding of VIP36 to DPPIV under glycosylation-deficient conditions, Lec1 and Lec2 cells, which both have been shown to exhibit glycosylation defects, were stably transfected with DPPIV-GFP using FuGENE® HD Transfection Reagent. The stable cell lines were used to investigate the interaction of DPPIV with VIP36 when later steps of the N-glycosylation beyond the cis-Golgi were inhibited. The CHO K1 cells without glycosylation defects were used as a control.

A verification of correct expression, intracellular localization and transport competence of DPPIV-GFP was performed by confocal laser microscopy and Western blot analysis.

For the confocal analysis cells were grown on coverslips, fixed and then mounted with mowiol 4-88. Figure 3.1 shows the expression of DPPIV-GFP in the three cell lines in a steady state situation. The images show that the transfection was successful for all three cell lines since there are many cells which could be detected by the argon laser, visualizing DPPIV-GFP, which is shown in green colour. However, the transfection rate is not equal in the cell lines. As shown in Figure 3.1 the transfection rate is higher in the Lec cells, visualized by the stronger signal. DPPIV-GFP is expressed to a great extend at the cell surface and also in intracellular compartments in all three cell lines. The data show that DPPIV-GFP is transported to the cell surface even when the glycosylation is not complete.

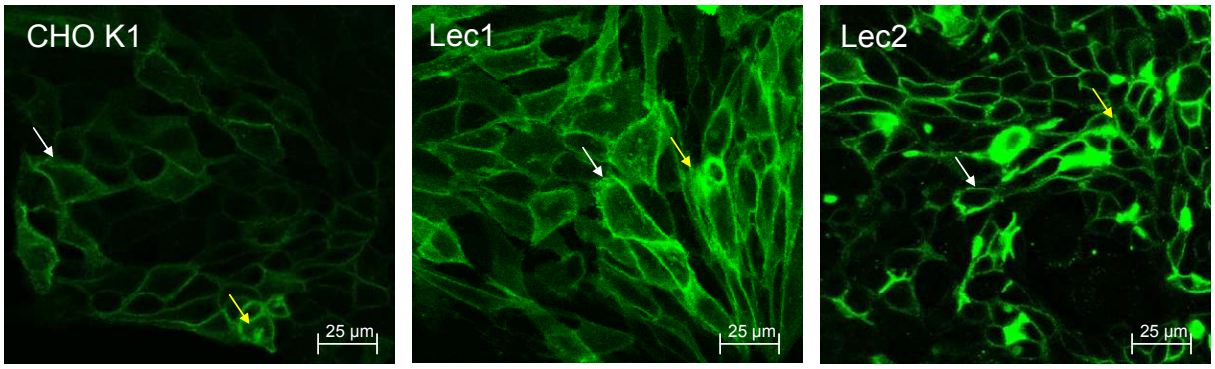

Figure 3.1 Confocal images of the DPPIV-GFP stable cell lines. CHO K1, Lec1, and Lec2 were stably transfected with DPPIV-GFP using FuGENE® HD Transfection Reagent. The left image shows the fixed CHO K1 cells, the image in the middle Lec1 cells and the right image Lec2 cells. The white arrows mark DPPIV-GFP at the cell surface and the arrows in yellow point out intracellularly distributed DPPIV-GFP in the cells.

For the Western blot analysis cells were lysed and 50 µg protein amount, measured by protein assay, were loaded on SDS-PAGE. Immunostaining was conducted using the mAb HBB 3/775/4 directed against DPPIV.

Western blot analysis obtained a protein band corresponding to DPPIV-GFP that can be detected for all three cell lines (Fig. 3.2). However, the size of the protein bands differs in the cell lines. The CHO K1 cell line expresses complex glycosylated DPPIV-GFP with the predicted size of ~137 kDa, consisting of the 110 kDa DPPIV and the 27 kDa GFP (Fig. 3.2, lane 1). The protein band for the Lec1 cell line is lower in comparison to the control band (Fig. 3.2, lane 2). This is a result of the defective glycan processing in the Lec1 mutant, where the N-acetylglucosaminyltransferase I is lacking and therefore the $Man_5GlcNAc_2$ is no further processed (Fig. 3.2, lane 2). The size of the protein band in the Lec2 mutant is only slightly lower in comparison to the control. In this case the lack of CMP-sialic acid transporter leads to the missing sialic acid as a final carbohydrate residue on N-linked glycans in this cell line (Fig. 3.2, lane 3).

The amount of DPPIV also differs between the three cell lines. DPPIV-GFP is expressed to a lesser extend in the control cell line in comparison to the Lec cells, where stronger protein bands are detectable for DPPIV-GFP when loading the same protein amount for every cell line (Fig. 3.2). This finding is in agreement with the confocal data.

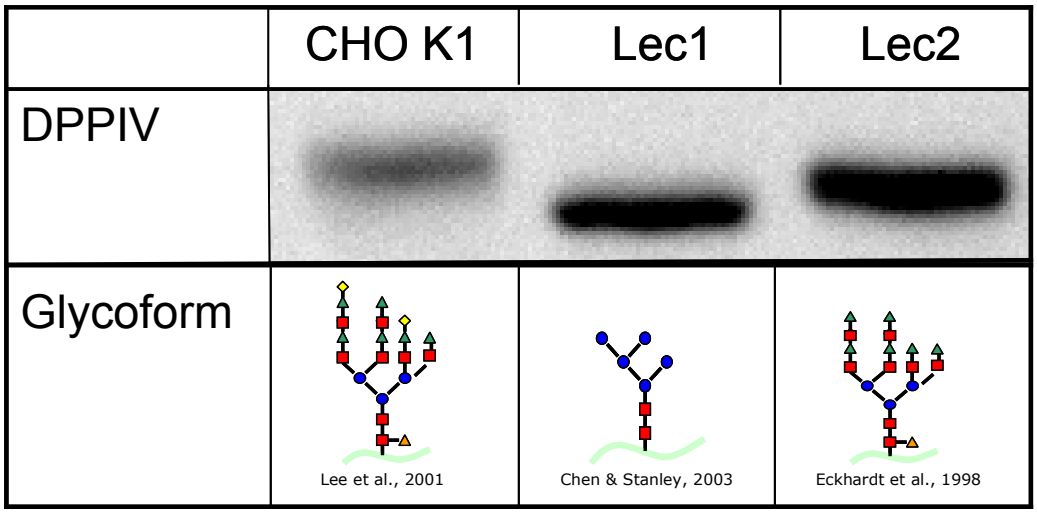

Figure 3.2 Western blot analysis of DPPIV-GFP in CHO K1, Lec1, and Lec2 cells. Immunostaining was conducted with mAb HBB 3/775/42 directed against DPPIV. The first lane represents CHO K1 with the highest molecular weight of ~137 kDa. Lane 2 shows the protein band for DPPIV-GFP in Lec1 cells with a lower molecular weight. DPPIV-GFP expressed in Lec2 cells is shown in lane three with a slightly lower molecular weight in comparison to CHO K1 cells. The different terminal glycoforms which are expressed in the cell lines are shown below the corresponding protein band.

However, taken together the results show that DPPIV-GFP is expressed in all three cell lines. The confocal data obtained that DPPIV-GFP achieves a normal transport competence in all three cell lines, irrespectively of glycosylation defect (Fig. 3.1). The Western blot analysis verify the predicted glycosylation defects of Lec1 and Lec2 cells based on the smaller size of the expressed protein DPPIV-GFP (Fig. 3.2, lane 2 and 3). Therefore, this cell model can be used for further experiments concerning the interaction of DPPIV-GFP with VIP36.

3.2 VIP36 is expressed in different cell lines

To analyze the defined aims of this study concerning VIP36, different VIP36-expressing cell lines were used. It is known from other studies, that VIP36 is expressed in many different cell lines e.g. MDCK cells, NIH 3T3 fibroblasts, rat parotid acinar cells, and GH3 cells (Fiedler et al. 1994, Fiedler & Simons 1995, Shimada et al. 2003a, Shimada et al. 2003b). The cell lines that were used in this study were Caco-2 cells, CHO K1 cells, Lec1 cells, and Lec2 cells.
To confirm the expression of VIP36 in the used cell lines Western blot analysis were conducted. For the experiment cells were lysed and 50 µg protein amount, measured by

protein assay, were separated on SDS-PAGE. Immunostaining was conducted by using the rbAb sc-67131 (H-90) directed against VIP36.

The result showed a clear protein band at the predicted size of 36 kDa in all tested cell lines (Fig. 3.3). In Lec1 and Lec2 cells, a slightly lower band appeared. This is a result of the incomplete glycan processing at the single N-glycosylation site of VIP36, since it is known that this N-glycosylation site is normally complex glycosylated (Füllekrug et al. 1999). The protein band for Caco-2 cells appeared almost at the same height than in the CHO K1 cell line.

With this experiment, I could show that VIP36 is expressed endogenously in the tested cell lines. Therefore, all selected cell types can be used for the examination of interaction with glycoproteins and DRM-association of VIP36.

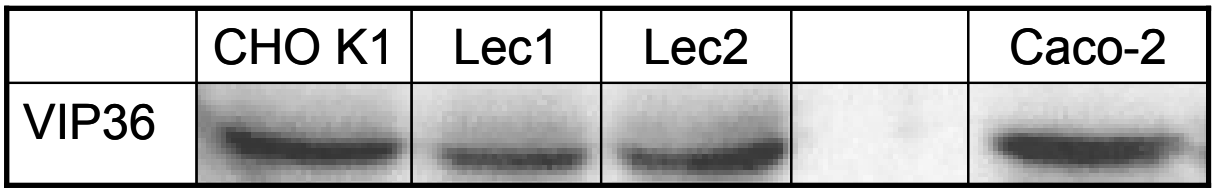

Figure 3.3 VIP36 expressed in different cell lines. Caco-2 cells, CHO K1, Lec1, and Lec2 cells were lysed and preceded by SDS-PAGE. Western blot analysis were conducted using rbAb sc-67131 (H-90) directed against VIP36. The image shows protein bands at the height of 36 kDa, corresponding to VIP36 for the four cell lines

3.3 Interaction of VIP36 with glycoproteins in Caco-2 cells

Since it is known that VIP36 is interacting with different glycoproteins like custerin, α-amylase and α-1-antitrypsin (Hara-Kuge et al. 2002, Hara-Kuge et al. 2004, Reiterer et al. 2010), I was searching for further interaction partners of VIP36.

In the past it has been shown that VIP36 recognize more apical than basolateral sorted glycoproteins (Hara-Kuge et al. 2002), and that it bind to membrane proteins (Hara-Kuge et al. 1999). Therefore, I focused on highly glycosylated transmembrane proteins which are apically sorted.

Caco-2 cell lysates were used to immunoprecipitate the glycoproteins DPPIV, SI, LPH and APN, which are all N- and O-glycosylated transmembrane proteins. One lysate was treated with protein A-Sepharose alone, to proof that protein bands which will appear when VIP36 was binding to one of the immunoprecipitated glycoproteins were not due to an unspecific

binding of the VIP36 antibody to protein A-Sepharose. This procedure was followed by Western blot analysis with rbAb sc-67131 (H-90) directed against VIP36.

Figure 3.4 shows the Western blot analysis of the immunoprecipitation experiment. The first lane shows the negative control, were only protein A-Sepharose was added to the lysate without a specific antibody. Here, no band can be detected. The immunoprecipitated samples are shown in lanes 2 to 5. A band corresponding to VIP36 was detected for the two immunoprecipitated glycoproteins SI (Fig 3.4, lane 2) and DPPIV (Fig. 3.4, lane 3), but no band could be detected for APN and LPH (Fig. 3.4, lanes 4 and 5). This experiment reveals that VIP36 is precipitated together with the two glycoproteins SI and DPPIV. Due to the intensity of the bands, VIP36 might bind more DPPIV proteins than SI proteins.

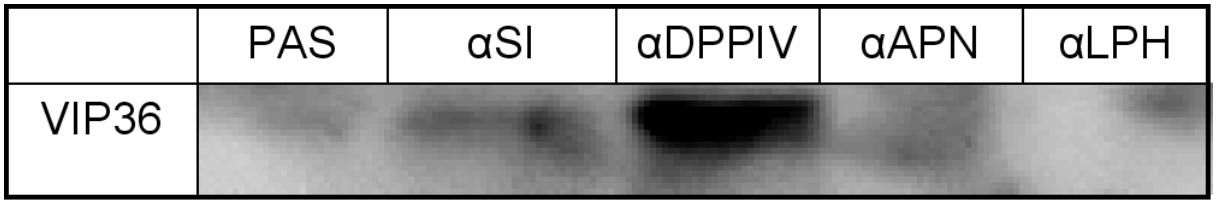

Figure 3.4 Interaction of VIP36 with glycoproteins in Caco-2 cells. Cells were lysed and immunoprecipitated with mAbs directed against SI, DPPIV, APN or LPH. One sample was treated with protein A-Sepharose without any antibody as a negative control. Immunoisolates were further processed by Western blot analysis with rbAb directed against VIP36. The experiment revealed a faint band for the binding of SI and a strong band for binding of DPPIV. No band can be detected for the negative control and the immunoprecipitated proteins APN and LPH.

This experiment was repeated for the proteins DPPIV and SI to proof if there is a difference in binding of VIP36 to DPPIV and SI. As a reference for protein amount of VIP36, DPPIV, and SI, 50 µg of Caco-2 cell lysate was loaded on SDS-PAGE.

The results show a clear band detectable for VIP36 in the lysate (Fig. 3.5a, lane 1). The amount of VIP36 which binds to DPPIV is larger than in the lysate (Fig. 3.5a, lane 2) and the band intensity for VIP36 which binds to SI is weaker (Fig. 3.5a, lane 3). However, when the protein bands for DPPIV and SI were compared in Fig. 3.5b, it is shown that there is a much greater amount of DPPIV in 50 µg of the lysate detectible than for SI. This indicates that the stronger binding of VIP36 is due to the greater amount of DPPIV in Caco-2 cells.

With these experiments I could identify DPPIV and SI as new interaction partners of VIP36. VIP36 binds different amounts of DPPIV and SI, which might be due to the greater protein amount of DPPIV in the cell lysates.

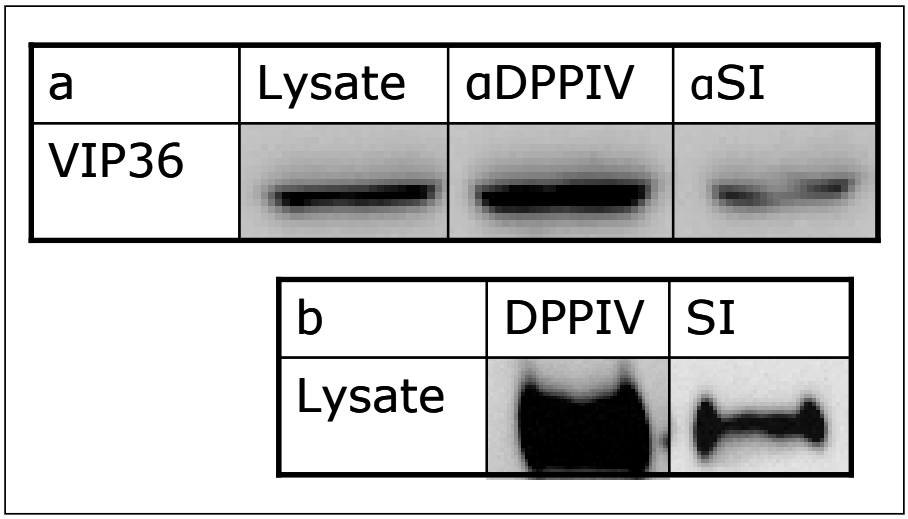

Figure 3.5 Interaction of VIP36 with DPPIV and SI in Caco-2 cells. a: Cells were lysed and immunoprecipitated with mAbs directed against DPPIV or SI or directly loaded on SDS-PAGE. Western blot analysis showed a protein band for VIP36 in the lysate of Caco-2 cells. The second and third lanes represent VIP36 isolated by immunoprecipitation of DPPIV and SI, respectively. b: Cell lysates were processed on SDS-PAGE followed by Western blotting with immunostaining of DPPIV and SI.

3.4 Interaction of VIP36 with DPPIV under glycosylation-deficient conditions

For the investigation of interaction between VIP36 and DPPIV under glycosylation-deficient conditions, the CHO K1 cells and Lec cells, which were stably transfected with DPPIV-GFP, were used. Therefore, Western blot analysis (processed as in 3.2) as well as confocal laser microscopy was conducted. Figure 3.6 shows the Western blot analysis of the three different cell lines. A specific protein band which corresponds to VIP36 can be visualized. This experiment revealed an interaction of VIP36 with DPPIV-GFP in the control cells and also in the glycosylation-deficient cells. However, the binding properties of VIP36 to DPPIV in the glycosylation-defective cell lines differ in comparison to the CHO control cells. For Lec1 and Lec2 cells I obtained an increased binding, represented by the stronger protein band for Lec1 and Lec2 cells (Fig. 3.6). However, this increased binding is possibly caused by the higher expression level in the Lec cells as it was shown in chapter 3.1.

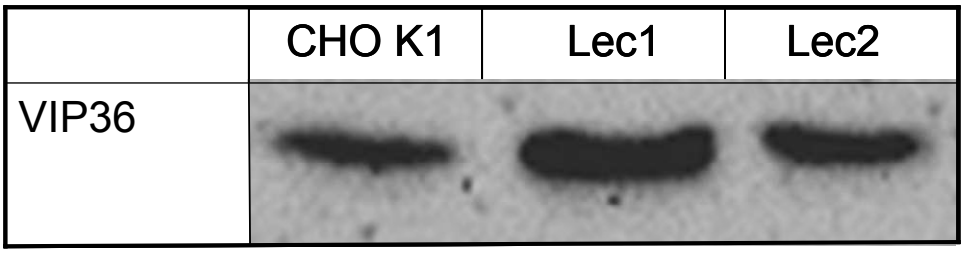

Figure 3.6 Interaction of VIP36 with DPPIV-GFP in CHO K1 and Lec cells. CHO K1 and Lec cells were lysed and DPPIV was immunoprecipitated followed by Western blot analysis with immunostaining of VIP36. Lane 1-3 represent the protein band for VIP36, interacting with DPPIV-GFP in the three cell lines CHO K1, Lec1, and Lec2.

The interaction of VIP36 with DPPIV could also be confirmed by confocal laser microscopy. Therefore, the CHO K1 cells and Lec cells which are stably transfected with DPPIV-GFP were used to visualise VIP36 by immunofluorescense microscopy. For detection of the endogenous VIP36 the rbAb sc-67131 (H90) was used followed by immunostaining with AlexaFlour568 as a secondary antibody, which labelled the protein in red.

Figure 3.7 showed that there are a few colocalization spots of VIP36 and DPPIV, which appeared in yellow, in the different cell lines. The single channel pictures for DPPIV-GFP showed a staining of the cell surface and intracellular compartments (Fig. 3.7a-c, DPPIV-GFP) in all three cell lines as it was already shown in Fig. 3.1. VIP36 is localized intracellularly and no cell surface staining can be observed in the three cell lines (Fig. 3.7 a-c, VIP36-AlexaFlour568).

The control cell line displayed colocalization of the two proteins which appear intracellularly (Fig. 3.7a, merge). Some of these interactions seem to be near the cell surface, the other in the region of the Golgi.

The colocalization for Lec1 is shown in figure 3.7b (merge). Here, the colocalizations which can be detected are localized intracellularly, near the cell surface.

The colocalization of VIP36 and DPPIV-GFP in Lec2 cells is also intracellularly, in the Golgi region (Fig.3.7c, merge). Here no interaction near the cell surface was observed.

In conclusion, the above mentioned interaction studies for DPPIV-GFP and VIP36 in CHO K1 and Lec cells showed that VIP36 is binding to this glycoproteins also when the glycosylation is inhibited at a later step along the secretory pathway, beyond the cis-Golgi.

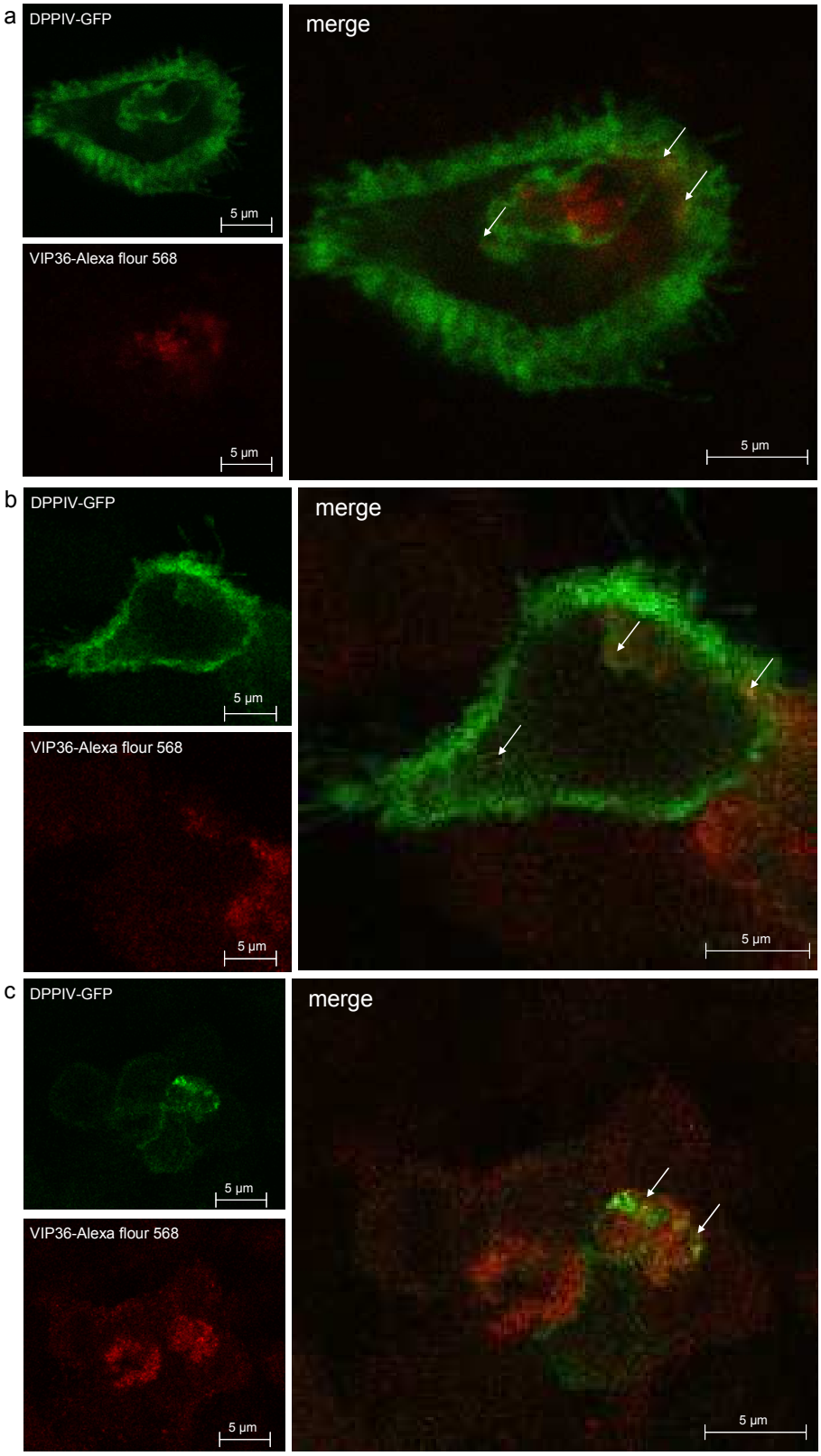

Figure 3.7 Colocalization of VIP36 and DPPIV-GFP in CHO K1 and Lec cells. The stably transfected cells were labelled with anti-VIP36 Ab followed by treatment with AlexaFlour568 as a second antibody. DPPIV-GFP appeared in green, VIP36 in red. Merge visualize the overlay of both laser channels and show colocalizations, which are marked by white arrows, appearing in yellow. a: CHO K1, b: Lec1, c: Lec2.

3.5 Binding properties of VIP36 during glycoprotein maturation

As a next step, the transport kinetics of DPPIV and SI as well as the binding of VIP36 to these two proteins was examined by pulse chase experiments.

To investigate if there is a change in the binding of VIP36 to DPPIV and SI over time, Caco-2 cells were labelled with [^{35}S]methionine for 30 min followed by different chase time points. Afterwards an immunoprecipitation with the mAbs HBB 3/775/42 or HSI2 directed against DPPIV or SI, respectively, was performed. One sample of each time point was then further processed by SDS-PAGE on 6 % gels to show the maturation and the glycosylation stage of DPPIV and SI over time. The other part of each sample was then treated with 0.5 % SDS at 37°C for 1 h to destroy the binding of DPPIV or SI to VIP36 and protein A-Sepharose. This was followed by immunoprecipitation of VIP36, to only isolate VIP36 molecules which bind to DPPIV and SI at the certain time points, followed by SDS-PAGE on 12 % gels.

The pulse chase experiment for DPPIV showed a strong band at 100 kDa at time point 0 min, corresponding to its mannose-rich form (DPPIV$_h$, Fig. 3.8, lane 1). After 30 min of chase, there is a second band at 124 kDa which correspond to the complex form of this protein (DPPIV$_c$, Fig. 3.8, lane 2). The mannose-rich form is weaker in comparison to the preceding time point. At time point 60 min the mannose-rich form is again weaker and the complex band gets stronger (Fig. 3.8, lane 3). From time point 90 min the mannose-rich form could not be detected and DPPIV appeared only complex glycosylated (Fig. 3.8, lane 3-5).

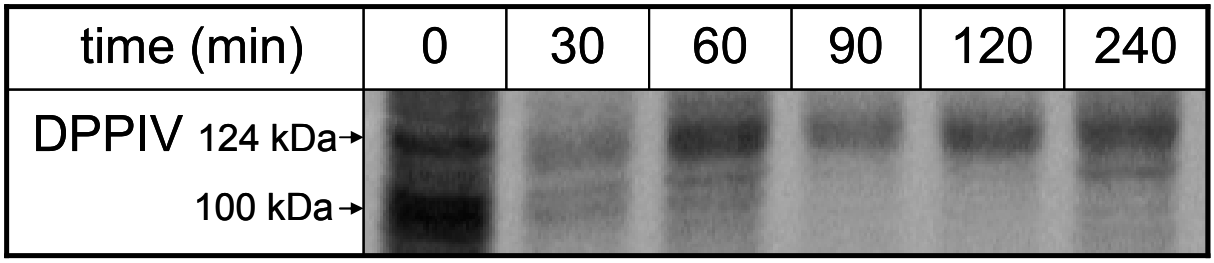

Figure 3.8 Maturation of DPPIV. Caco-2 cells were biosynthetically labelled for 30 min and then lysed at the six different time points. Samples were immunoprecipitated with mouse anti-DPPIV antibody. The figure shows protein maturation of DPPIV. The bands were detected at the size of 100 kDa for mannose-rich DPPIV and 124 kDa for complex glycosylated DPPIV.

For SI, a very faint protein band at 210 kDa, which correspond to the mannose-rich form, could be detected at time point 0 min (pro-SI$_h$, Fig. 3.9, lane 1). The following time point (30 min) this 210 kDa band appeared stronger (Fig. 3.9, lane 2). At time point 60 min the pro-SI$_h$

band again become stronger and a second weaker band appeared at 245 kDa, indicating the complex form of SI (pro-SI_c, Fig. 3.9, lane 3). The next time point (90 min), pro-SI_h appears slightly weaker than the proceeding, whereas pro-SI_c band grows stronger (Fig. 3.9, lane 4). There are almost equal band intensities for pro-SI_h and pro-SI_c at time point 120 min (Fig. 3.9, lane 5). This corresponds into a slightly reduction of pro-SI_h and an increase of pro-SI_c. At the last time point (240 min) only pro-SI_c could be detected, indicating that the labelled pro-SI is fully matured.

The results show that DPPIV reaches its complex glycosylated form earlier than SI, which is in agreement with already published data (Hauri et al. 1985).

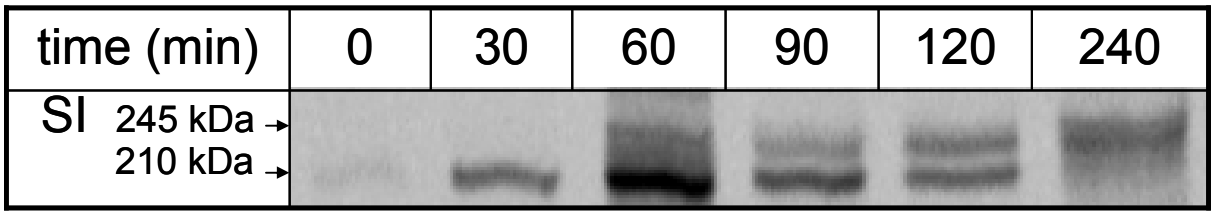

Figure 3.9 Maturation of SI. Caco-2 cells were biosynthetically labelled for 30 min and then lysed at the six different time points. Samples were immunoprecipitated with HSI2 antibody. The figure shows protein maturation of SI. The bands were detected at the size of 210 kDa for mannose-rich SI and 245 kDa for complex glycosylated SI.

The co-immunoprecipitation experiment showed that VIP36 binds to DPPIV at the first time points. As shown in Fig. 3.10, a band at 36 kDa is shown in the first four lanes which correspond to VIP36. Therefore, VIP36 can be detected at the first four time points 0, 30, 60, and 90 min with an increasing binding, reaching its maximum at 90 min of chase. This corresponds to a binding of VIP36 to DPPIV when the mannose-rich form ($DPPIV_{h)}$ is existent at the first two time points and also at the later time points (60 and 90 min) when DPPIV is complex glycosylated (Fig. 3.8).

The binding of VIP36 to SI appeared at different time points. At time points 0 and 30 min, VIP36 binds to SI (Fig. 3.10, lane 1-3). Therefore, VIP36 binds when pro-SI_h is existent (Fig. 3.9). However, at the following time point (60 min) VIP36 can not be detected (Fig 3.10, lane 3), indicating that the association of the two proteins untie. After 90 min of chase, there is again a binding between VIP36 and SI since there is a band detectable in lane 4 (Fig. 3.10). This binding gets stronger, due to a stronger band at time point 120 min (Fig. 3.10, lane 5), which is the strongest band corresponding to the strongest binding between VIP36 and its cargo. The association again unties and can no longer be observed at the last time point (Fig 3.10, lane 6) when there is only complex glycosylated SI detectable (Fig. 3.9).

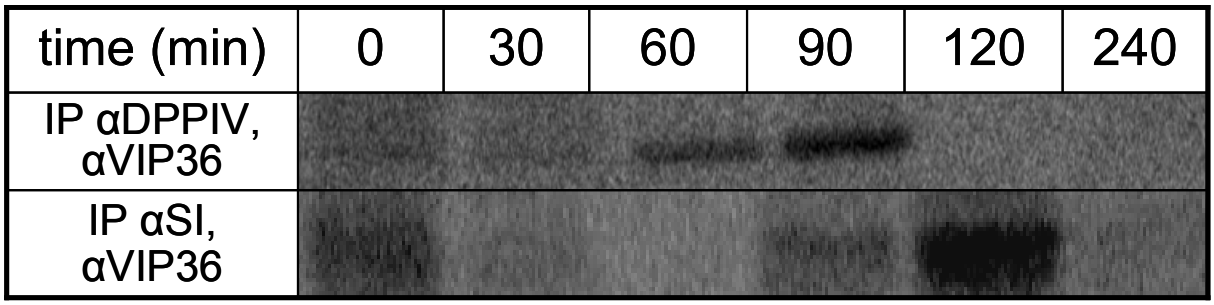

Figure 3.10 Binding of VIP36 to the glycoproteins DPPIV and SI during protein maturation. Caco-2 cells were biosynthetically labelled for 30 min and then lysed at the six different time points. Samples were immunoprecipitated with anti-DPPIV or anti-SI and then treated with 0.5 % SDS for 1 h at 37°C. A second immunoprecipitation was conducted using anti-VIP36 antibody.

These results suggests an interaction of VIP36 with these two proteins at an early stage of development in the ER/ERGIC when the protein has left the CNX/CRT cycle and also later in the Golgi or TGN for both proteins.

3.6 Influence of N-glycosylation on VIP36 binding properties

To examine if binding of VIP36 is influenced when N-glycosylation is inhibited in the early steps of protein transport, the glycosylation inhibitors 1-deoxynojirimycin (dNM) and 1-deoxymannojirimycin (dMM) were used. Treatment with dNM modulates the N-glycosylation since it inhibits α-glucosidase I and II in the ER, which prevents binding of CNX and CRT. For the modulation of complex glycosylation, dMM was used which inhibits α-mannosidase I in the cis-Golgi, resulting into $Man_8GlcNAc_2$ glycans.

Caco-2 cells were treated either with dNM or dMM for 24h with a change of the medium after 12h. Afterwards, an immunoprecipitation of DPPIV and SI was performed, followed by Western blotting with anti-VIP36 Ab.

The results show that the amount of VIP36 in the treated cells is reduced for both treatments (Fig. 3.11a). For the dMM treatment a reduction of VIP36 expression of 16.5 % can be observed (Fig. 3.11b). The dNM treatment causes a reduction of 23 % of VIP36 expression (Fig. 3.11b).

Comparison of the amount of VIP36 which binds to DPPIV in the treated and non-treated cells revealed a reduction of 39.3 % and 38.5 % for the dMM and dNM treatments, respectively (Fig. 3.11a and b, lanes 4-6). This shows that VIP36 might not bind to all DPPIV

proteins which are synthesized when only early glycosylation forms are present, since it might also bind to complex glycosylated proteins (Fig. 3.10).

By comparing the amount of VIP36 which binds to SI, a bigger difference between the two treatments could be detected. The treatment with dMM results in a reduction of 36.8 % in comparison to untreated cells, which is the least observed reduction (Fig. 3.11a and b, lane 8). However, there is a strong decrease of binding to SI in the dNM-treated cells (Fig. 3.11a, lane 9). This reduction was identified as 64.7 % (Fig. 3.11 b). This indicates a requirement of the first N-glycosylation processing steps for a proper binding of VIP36 to SI.

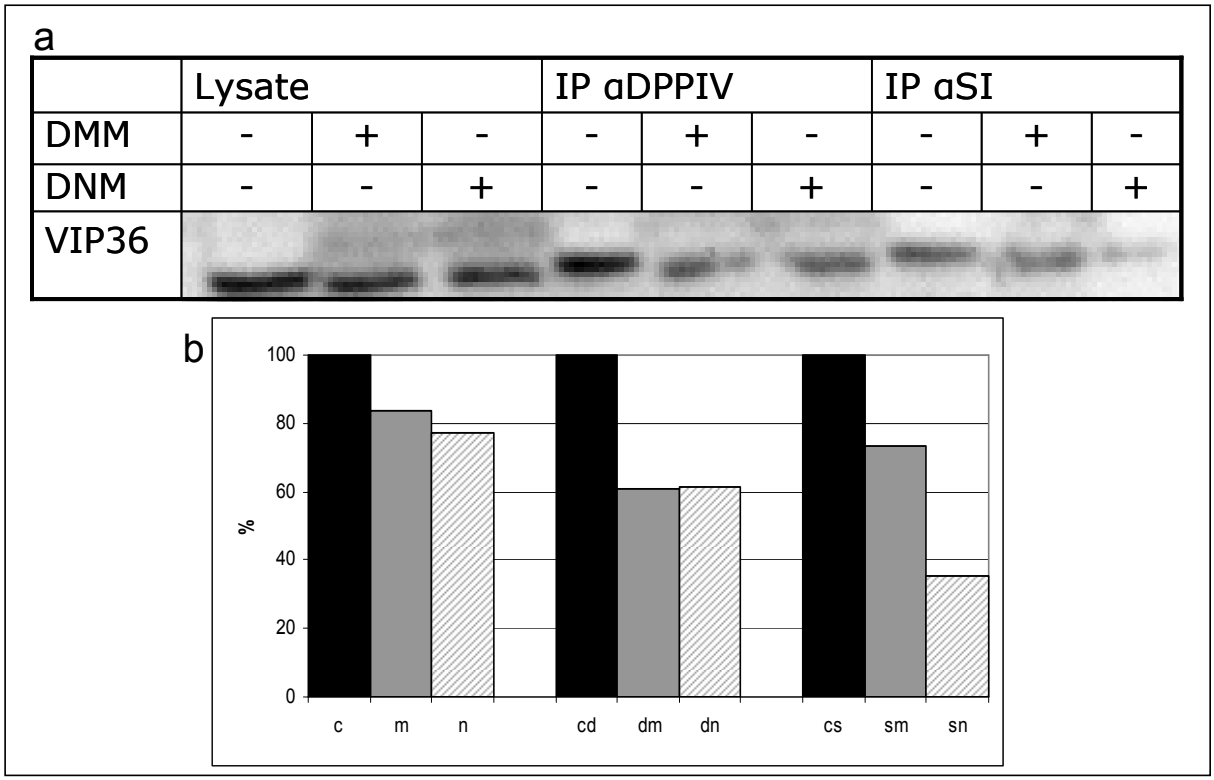

Figure 3.11 Inhibition of N-glycosylation. a: Caco-2 cells were treated with dMM or dNM for 24 h. The first three lanes show Western blot analysis with immunostaining of VIP36 of the cell lysates without and with dMM or dNM treatment. The following three lines represent the Western blot analysis of VIP36 after IP with HBB 3/775/42 directed against DPPIV again without and with dMM or dNM treatment. The same procedure was conducted for SI using mAb HSI2, which is shown in the last three lanes. b: The quantification of the band intensities was conducted for the lysates and the IP for DPPIV and SI. The untreated sample was set as 100 % (x-axis) in comparison to the treated samples (y-axis). c: control, m: dMM treatment, n: dNM treatment, d: IP DPPIV, s: IP SI.

To investigate the binding properties when later steps of N-glycosylation are inhibited, DPPIV was stably transfected into Lec1 and Lec2 cells (see chapter 3.1). As already reported, immunoprecipitation experiments revealed that the binding of VIP36 to DPPIV increases in

the Lec cells (Fig. 3.6). However, this increased binding could be a result of the different expression levels in the different cell lines, as was shown in Fig. 3.1 and Fig. 3.2.

3.7 Influence of N-glycosylation on SI folding

In the previous section, it was shown that there is a strong reduction of the binding between VIP36 and SI, when N-glycosylation is hampered by dNM treatment, and a moderate reduction for the dMM treatment. Therefore, the question arises if VIP36 might bind to SI to a lesser extent because of its incorrect folding, which might be caused by incomplete glycosylation due to the treatments. To reconsider this assumption, Caco-2 cells were treated with trypsin. It is known that SI is digested by trypsin into the two subunits sucrase and isomaltase (Hauri et al. 1985, Naim et al. 1988b). When SI is not folded correctly, the protein subunits are trypsin-sensitive and will be degraded.

Caco-2 cells were treated with 100 mM dMM or dNM in the presence of methionine-free medium for 3 h followed by biosynthetic labelling with additional dMM or dNM treatment for 4 h. Then samples were immunoprecipitated with two antibodies detecting SI. HSI2 detects the sucrase subunit of SI, whereas the HBB 3/705/60 detects early stages and partially folded SI molecules (Hauri et al. 1985, Beaulieu et al. 1989). The immunoisolates were then treated with 500 µg trypsin for 1 h at 37°C and processed on 6 % SDS-PAGE.

The results show that the trypsin digestion worked for the three samples but not the whole amount of SI molecules were digested (Fig. 3.12).

In Figure 3.12, the control pattern is shown in the first lane. The upper bands at 210 and 245 kDa represent pro-SI_h and pro-SI_c, respectively. Part of SI is cleaved by trypsin into sucrase and isomaltase. The bands which are at the predicted size of 145 kDa for isomaltase and 130 kDa for sucrase are blurred. This is a result of the digestion, which leads also into a separation on the SDS gel of complex and mannose-rich sucrase and isomaltase.

The second lane shows the dMM treated SI. The upper band corresponds to pro-SI_h. However, no band at the size of 245 kDa, corresponding to pro-SI_c could be detected. Therefore the dMM treatment completely hampered mannosidase I in the Golgi. The trypsin digestion showed that there are two bands, which represents the mannose-rich form of sucrase and isomaltase.

The third lane shows the dNM treatment. For this treatment, SI showed a strong mannose-rich band as well as a weaker complex form. This pattern revealed that the dNM treatment, which

hampered the α-glucosidase I and II in the ER, was not completely successful. After trypsin digestion, there is a strong band at 130 kDa which corresponds to the sucrase subunit. The second band at 145 kDa corresponds to the isomaltase subunit and is again blurred due to separation of complex and mannose-rich forms of sucrase and isomaltase.
This results show that SI is correctly folded when treated with dMM or dNM and is therefore digested into the two subunits sucrase and isomaltase by trypsin.

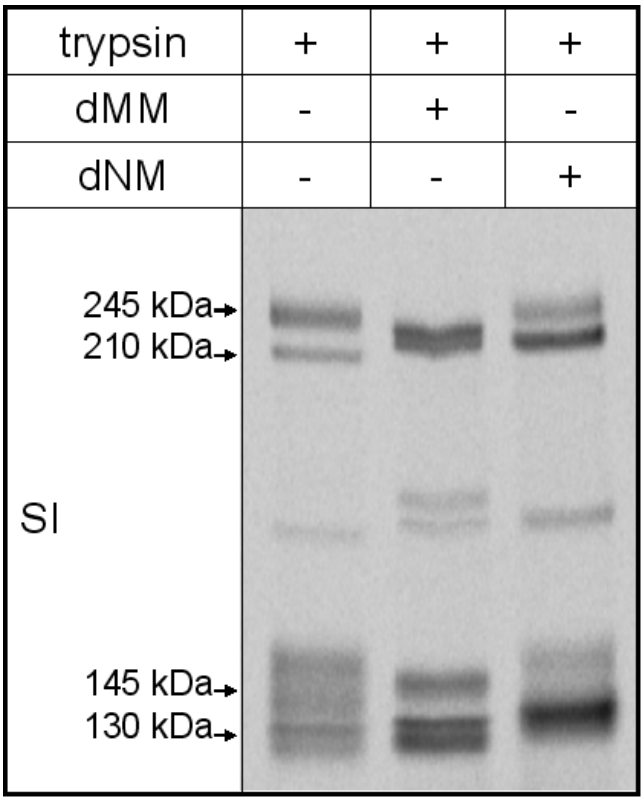

Figure 3.12 Trypsin digestion of SI. Caco-2 cells were biosynthetically labelled for 4 h concomitant with dMM or dNM treatment. Samples were immunoprecipitated with mAbs HSI2 and HBB 3/705/60 directed against SI. Immunoisolates were then incubated with trypsin. SI is cleaved into the two subunits sucrase and isomaltase. The upper bands represent uncleaved mannose-rich (210 kDa) and complex (245 kDa) SI. The lower bands are the result of trypsin digestion and show the separated subunits sucrase (130 kDa) and isomaltase (145 kDa).

3.8 DRM-association of VIP36 and interaction with glycoproteins

Association with DRMs plays a crucial role for the trafficking, sorting and function of the two glycoproteins DPPIV and SI. It is known that they associate with late (extracted with Triton X-100 or Lubrol WX) and early DRMs (extracted with Tween 20) along the secretory

pathway (Alfalah et al. 2002, Jacob et al. 2003, Alfalah et al. 2005). Since VIP36 was first isolated from CHAPS DRMs (Fiedler et al. 1994) and is interacting with DPPIV and SI, which was discovered in the previous experiments, the question arises if VIP36 is also associated with other types of DRMs, and further, if there is an interaction with cargo in DRMs.

For the investigation of DRM-association of VIP36, Caco-2 cells were lysed with 1 % of one of the three non-ionic detergents Triton X-100, Lubrol WX, or Tween 20, followed by a discontinuous sucrose-density gradient centrifugation. Nine fractions, ranging from 5 % to 40 % sucrose, were collected and analysed by Western blotting with immunostaining of VIP36. The two proteins flotillin-2 and rohA were used as controls for the DRM-fractions and the non-DRM-fractions, respectively. The DRM-fractions were expected in the three first fractions of the gradient, whereas the non-DRM-fractions remain at the bottom of the gradient in the three lower fractions (above the 80 % sucrose cushion).

When DRMs were extracted with Triton X-100, the discontinuous sucrose-density gradient pattern shows that VIP36 is not found in the floating-fractions of the gradient. Figure 3.13 (line 1) shows that protein bands for VIP36 are only detected in the non-floating-fractions 7 and 8. This pattern could also been shown for DRMs extracted with Lubrol WX (Fig. 3.13, line 4), where protein bands which correspond to VIP36 appeared in the fractions 8 and 9. However, the extraction of Tween 20 DRMs displays an association of VIP36 with these microdomains, since there are strong protein bands detected in the floating-fractions 1 and 2 (Fig. 3.13, line 7). Therefore, VIP36 is associated with these types of microdomains, which can be found early in the secretory pathway.

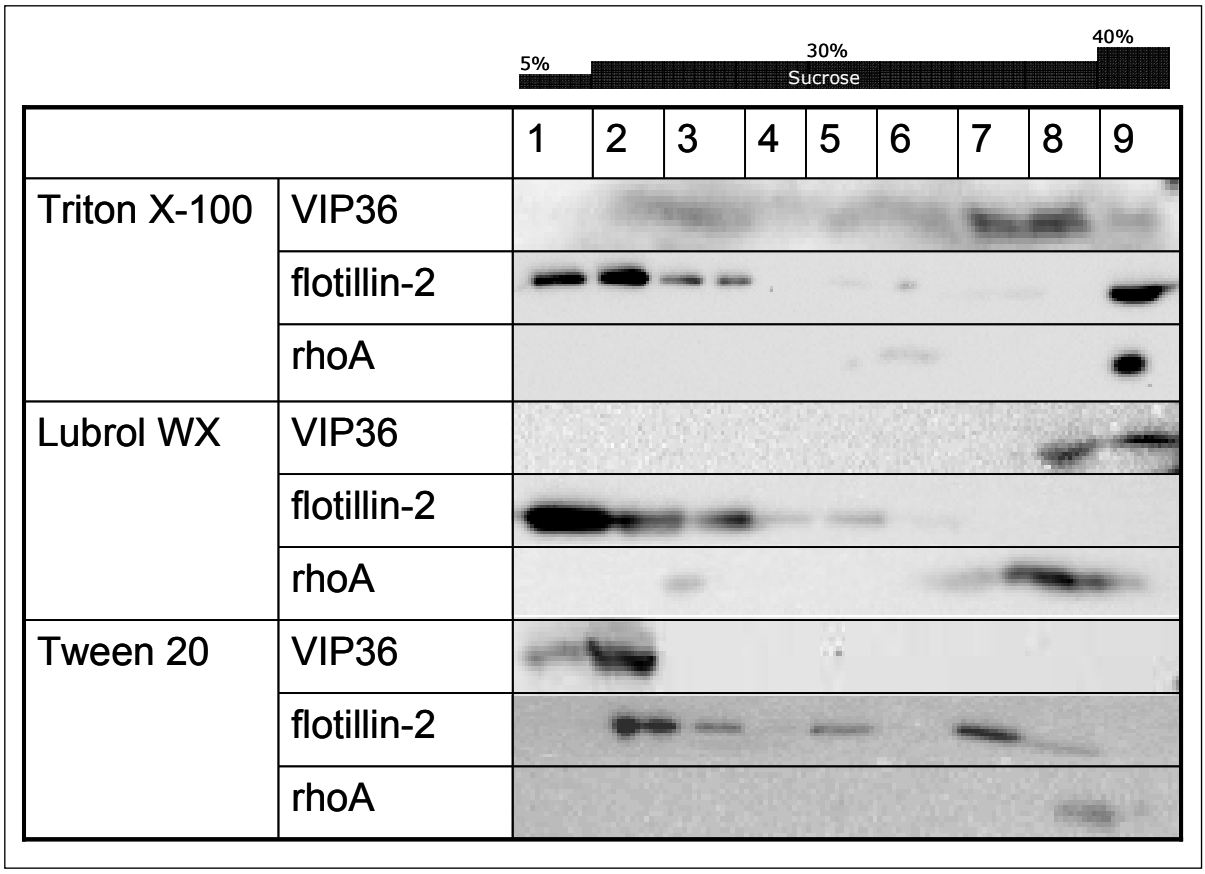

Figure 3.13 DRM-association of VIP36 in Caco-2 cells. Caco-2 cell lysates were processed by sucrose-density gradients. Nine fractions were collected from the top, ranging from 5 % sucrose in the upper fraction to 40 % sucrose in the lowest fraction. The figure shows the DRM extraction with Triton X-100, Lubrol WX, and Tween 20 followed by Western blotting with immunostaining of VIP36, flotillin-2, and rhoA. Flotillin-2 and rhoA are controls for the DRM-fractions and the non-DRM-fractions, respectively.

The extraction of Tween 20 DRMs from Caco-2 cells reveals that DPPIV and SI are transported into these microdomains, like VIP36 (Fig. 3.14) and can be found in the DRM-fractions of the gradient. This association with early DRMs along the secretory pathway was already reported for these two proteins (Alfalah et al. 2005).

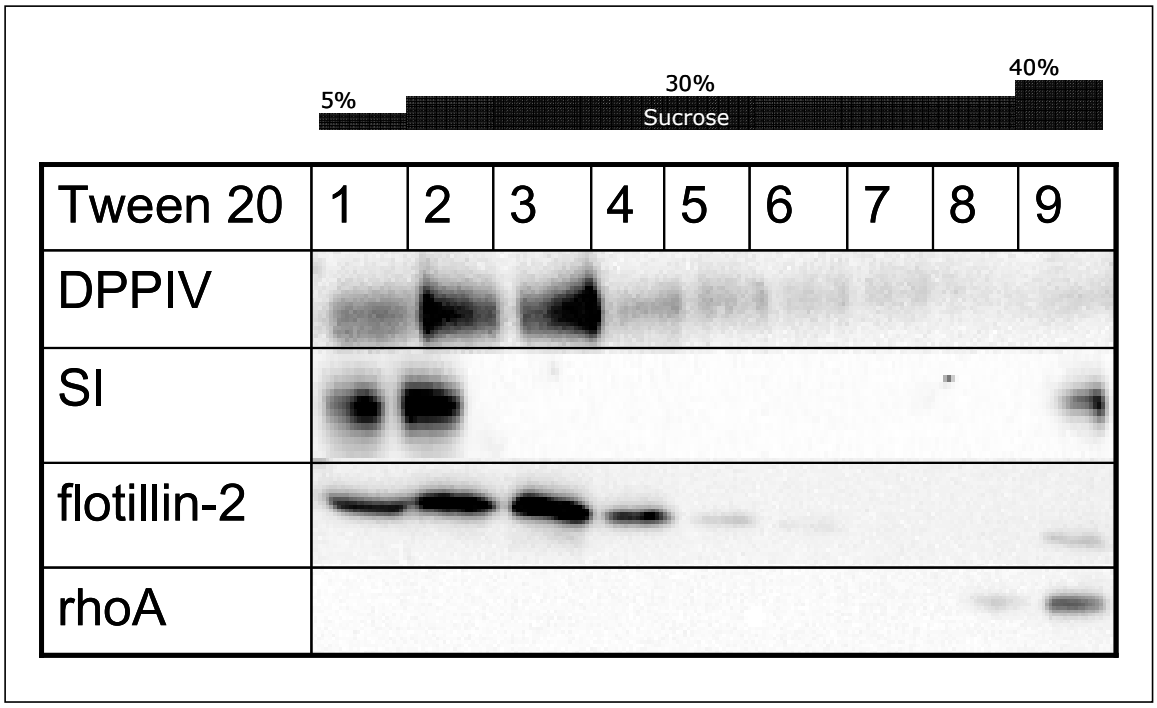

Figure 3.14 Association of DPPIV and SI with Tween 20 DRMs. Caco-2 cells were lysed with Tween 20 and a discontinuous sucrose-density gradient was performed. Nine fractions were collected from the top, ranging from 5 % sucrose in the upper fraction to 40 % sucrose in the lowest fraction. The figure shows the DRM extraction with Tween 20 followed by Western blotting with immunostaining of DPPIV, SI, flotillin-2, and rhoA. Flotillin-2 and rhoA are controls for the DRM-fractions and the non-DRM-fractions, respectively.

The localization of two proteins in the same type of DRMs does not automatically imply that they are interacting in these membrane microdomains. Thus, to test if VIP36 is interacting with DPPIV and SI in Tween 20 DRMs immunoprecipitation with antibodies directed against DPPIV and SI of the nine fractions of the sucrose-density gradient followed by Western blot analysis with immunostaining of VIP36 was performed.

This experiment displays an interaction of VIP36 with DPPIV and SI in Tween 20 DRMs, shown by protein bands appearing in the first three fractions of the sucrose-density gradient (Fig.3.15).

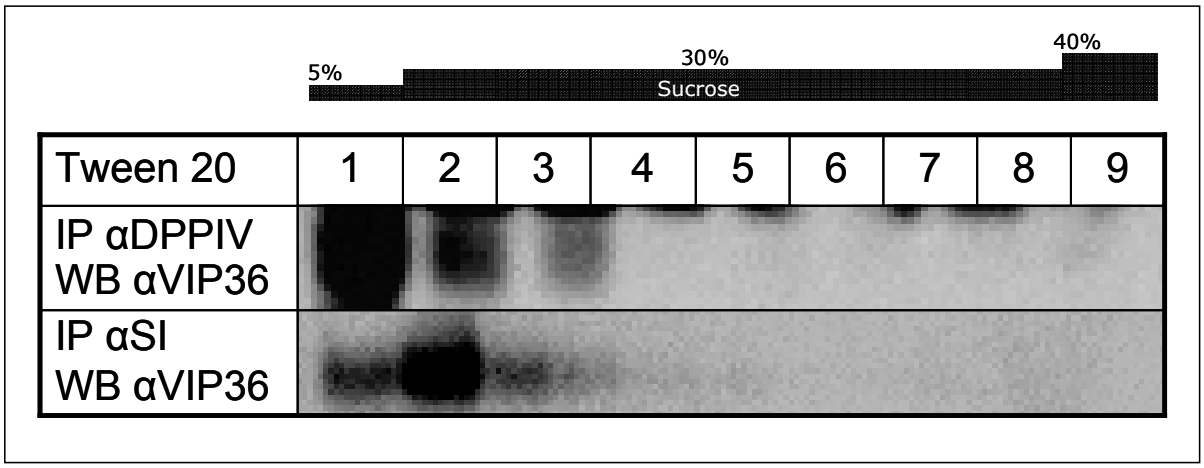

Figure 3.15 Interaction of VIP36 with DPPIV and SI in Tween 20 DRMs. Caco-2 cells were lysed with Tween 20 and a discontinuous sucrose-density gradient was performed. Nine fractions were collected and immunoprecipitated with mAbs directed against DPPIV or SI. This procedure was followed by Western blot analysis with immunostaining of VIP36.

3.9 DRM-association of VIP36 and DPPIV under glycosylation-deficient conditions

Recruiting into DRMs is known to be dependent on glycosylation of certain proteins. For DPPIV efficient association with DRMs requires N- and O-glycosylation (Alfalah et al. 2002). Therefore, it was interesting to find out if VIP36 or the interacting glycoprotein DPPIV are transported into DRMs when there is an incomplete glycosylation, like in Lec1 and Lec2 cells.

For the investigation of DRM-association of VIP36 and DPPIV-GFP, CHO K1 cells, Lec1 cells, and Lec2 cells were treated as reported in chapter 3.8. For the Western blot analysis the antibodies directed against DPPIV, VIP36, flotillin-2 and rhoA were employed.

The extraction of Triton X-100 DRMs shows a similar distribution of VIP36 and DPPIV in CHO K1 and Lec cells. Like in Caco-2 cells, VIP36 can be detected in the non-DRM-fractions (Fig. 3.16, fraction 7-9) in all three cell lines. DPPIV is transported into the DRM-fractions of the gradient, irrespectively of glycosylation stage. The main protein amount is detected in the first three fractions of the gradient, but there are also faint protein bands in the fractions 4 to 8 for the control and Lec2 cells (Fig. 3.16, line 2 and 10). The distribution of DPPIV in the Lec1 cells is restricted to fractions 1 and 2, as well as fractions 6 and 7 (Fig. 3.16, line 6). Flotillin-2 and rhoA are normally distributed in all three cell lines, so that the DRMs seem to be still existent when glycosylation is incomplete in the cell (Fig, 3.16).

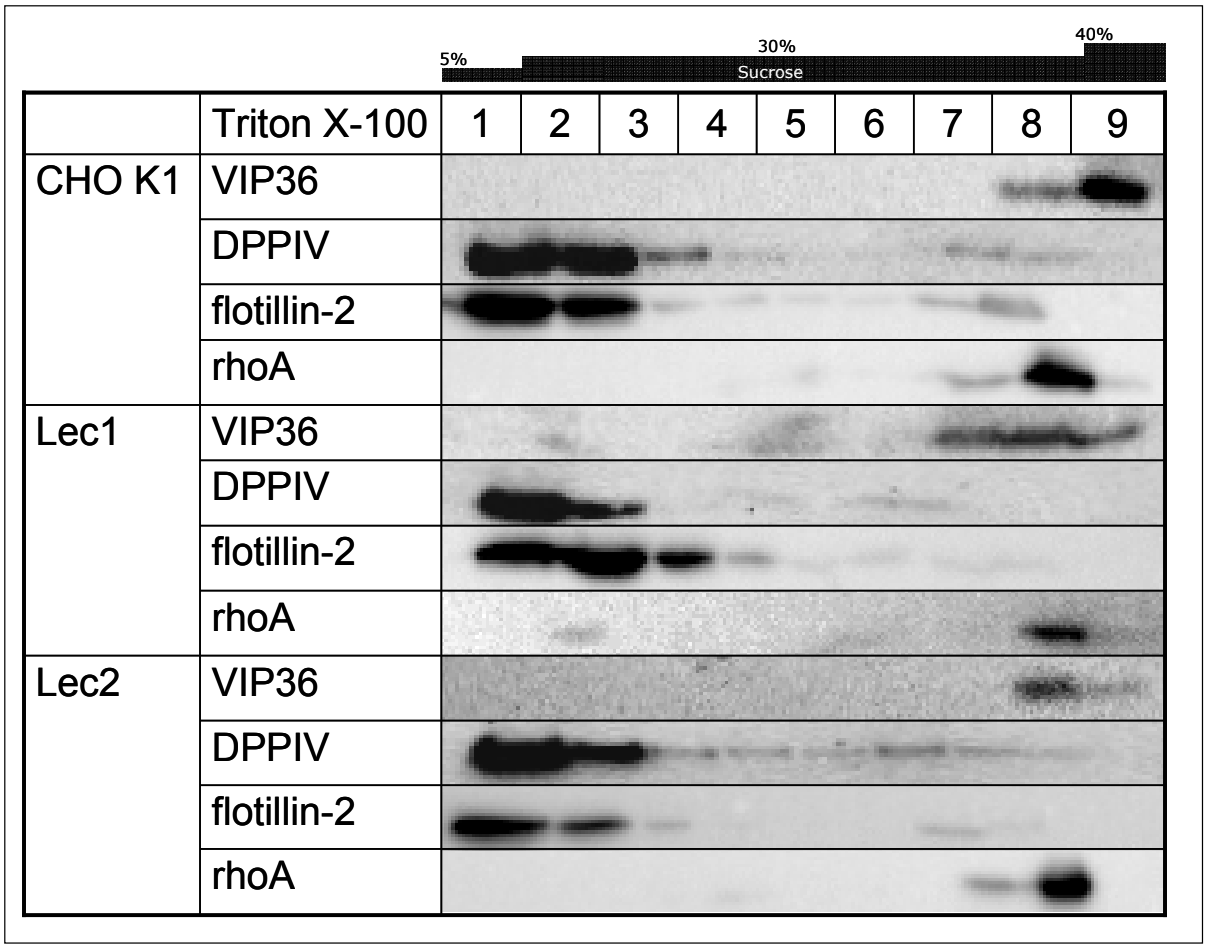

Figure 3.16 Extraction of Triton X-100 DRMs of CHO K1, Lec1, and Lec2 cells. CHO K1, Lec1, and Lec2 cells were lysed with Triton X-100 followed by a discontinuous sucrose-density gradient. Nine fractions were collected from the top, ranging from 5 % sucrose in the upper fraction to 40 % sucrose in the lowest fraction. Western blotting analysis with immunostaining of VIP36, DPPIV, flotillin-2, and rhoA was performed. Flotillin-2 and rhoA are controls for the DRM-fractions and the non-DRM-fractions, respectively.

In Caco-2 cells, an association with Tween 20 DRMs could be shown (Fig. 3.13). When DRM extraction with this detergent was conducted using the CHO K1 and Lec cells, a localization of VIP36 in the floating fractions, irrespectively of the glycosylation defect, can be observed (Fig. 3.17, line 1, 5 and 9). The same was observed for DPPIV (Fig. 3.17, line 2, 6 and 10). The distribution of flotillin-2 and rhoA also remains the same in the CHO Lec cells in comparison to the control cells, still mark the DRM- and non-DRM-fractions (Fig 3.17).

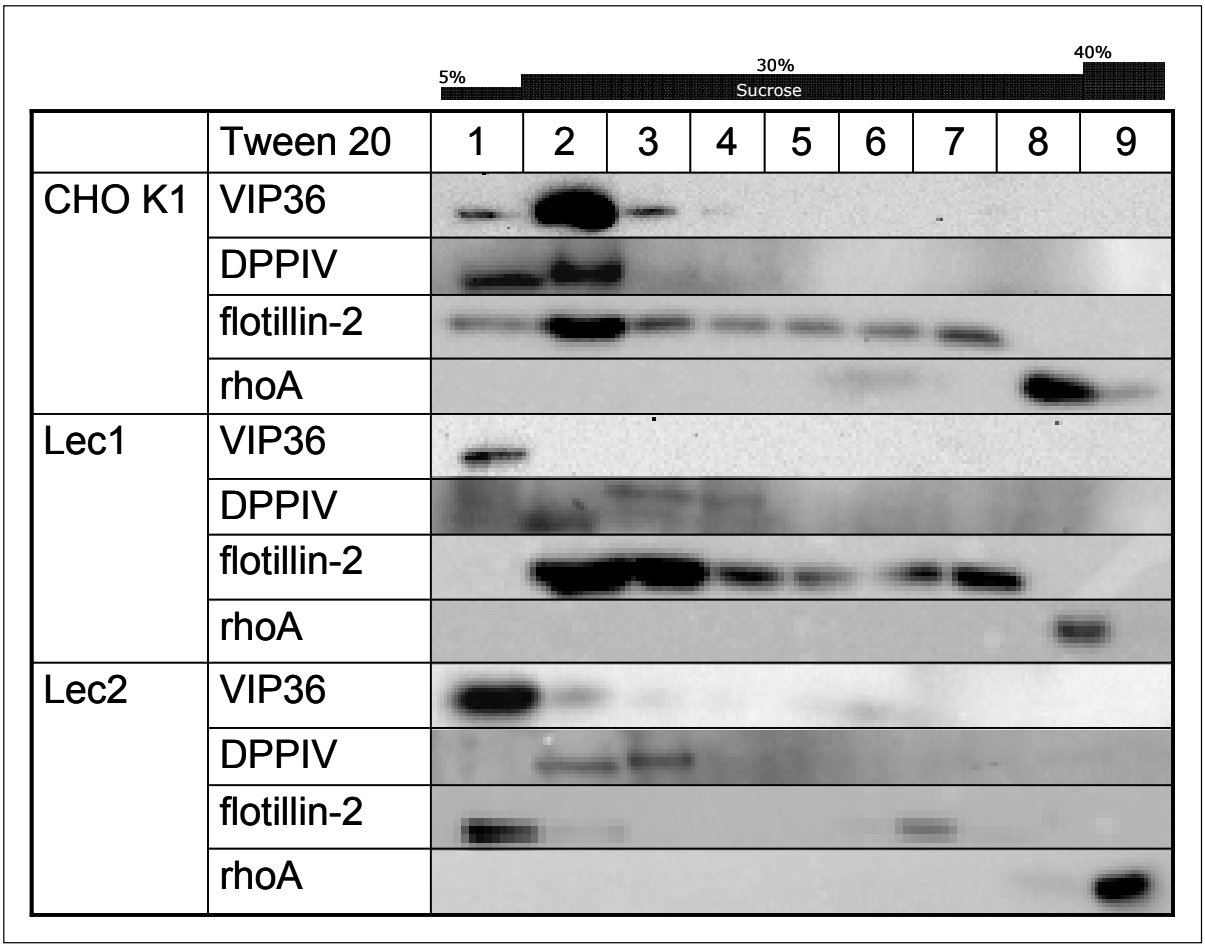

Figure 3.17 Extraction of Tween 20 DRMs of CHO K1, Lec1, and Lec2 cells. CHO K1, Lec1, and Lec2 cells were lysed with Tween 20 followed by a discontinuous sucrose-density gradient. Nine fractions were collected from the top, ranging from 5 % sucrose in the upper fraction to 40 % sucrose in the lowest fraction. Western blot analysis with immunostaining of VIP36, DPPIV, flotillin-2, and rhoA was performed. Flotillin-2 and rhoA are controls for the DRM-fractions and the non-DRM-fractions, respectively.

To verify that VIP36 is also interacting with DPPIV in Tween 20 DRMs in the CHO K1 and Lec cells, immunoprecipitation with isolation of DPPIV of the first four fractions, which refers to the DRM-fractions, were conducted. The immunoisolates were then further processed by Western blotting with immunostaining of VIP36. Figure 3.18 depicts the interaction studies of the three cell lines. As shown for Caco-2 cells, the interaction of VIP36 and DPPIV takes place in Tween 20 DRMs, since protein bands are detectable in these fractions.

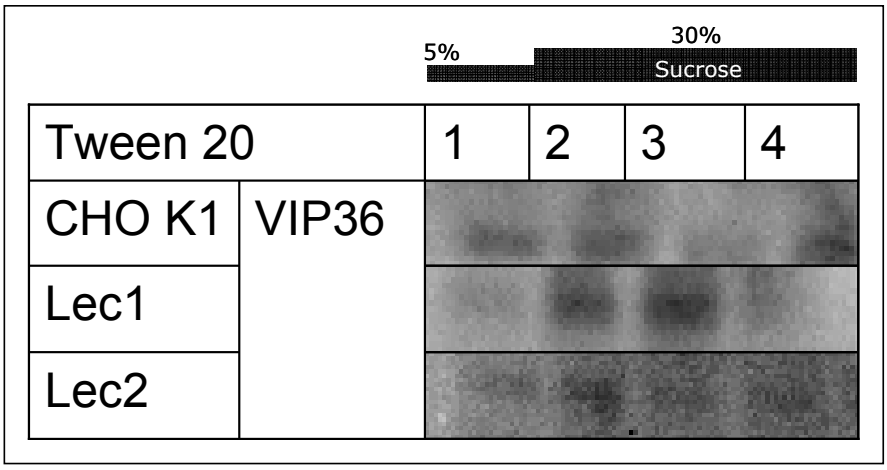

Figure 3.18 Interaction of VIP36 with DPPIV in Tween 20 DRMs. CHO K1, Lec1, and Lec2 cells were lysed with Tween 20 and a discontinuous sucrose-density gradient was performed. Nine fractions were collected and the first four fractions, corresponding to the DRM-fractions were immunoprecipitated with mAb directed against DPPIV. This procedure was followed by Western blot analysis with immunostaining of VIP36.

Extraction of Lubrol WX DRMs of the Lec cells, obtained a different band pattern of VIP36 in comparison to the control cells. In the CHO K1 cells, VIP36 is mainly found in the non-DRM-fractions (Fig. 3.19, line 1) as expected. It can be found in fraction 3-9. Therefore, it is distributed over many fractions and some VIP36 proteins are floating in the third fraction. However, there is a peak for this protein in fraction 7 to 9, which represents the non-DRM-fractions as shown by the distribution of rhoA (Fig. 3.19, line 4). DPPIV can be detected in the DRM-fractions as well as in the non-DRM-fractions. The strongest bands can be observed in fraction 1 and 2, indicating that the main part of this protein is transported into Lubrol WX DRMs (Fig.3.19, line 2).

In Lec1 cells, VIP36 is also distributed over many fractions (fraction 1-7) of the gradient. However, there are strong protein bands in the first three fractions, which represent the DRM-fractions (Fig. 3.19, line 5). The distribution of DPPIV is comparable to that in the control cells, with strong protein bands in the DRM-fractions 1-3 and weaker bands in the last two fractions (Fig. 3.19, line 6). Flotillin-2 and rhoA show also a normal distribution (Fig. 3.19, line 7 and 8).

When Lubrol WX DRMs of Lec2 cells were extracted, VIP36 is also distributed differently in comparison to the control cells. VIP36 can be found in fraction 1-7. Therefore, it is also transported in the DRM-fractions and shows a peak of protein content in fractions 3-6 (Fig. 3.19, line 9). Again, the pattern of DPPIV did not change and is comparable to the CHO K1

and Lec1 cells (Fig. 3.19, line 10). The distribution of the marker proteins flotillin-2 and rhoA also remains unchanged in this cell line (Fig. 3.19, line 11 and 12).

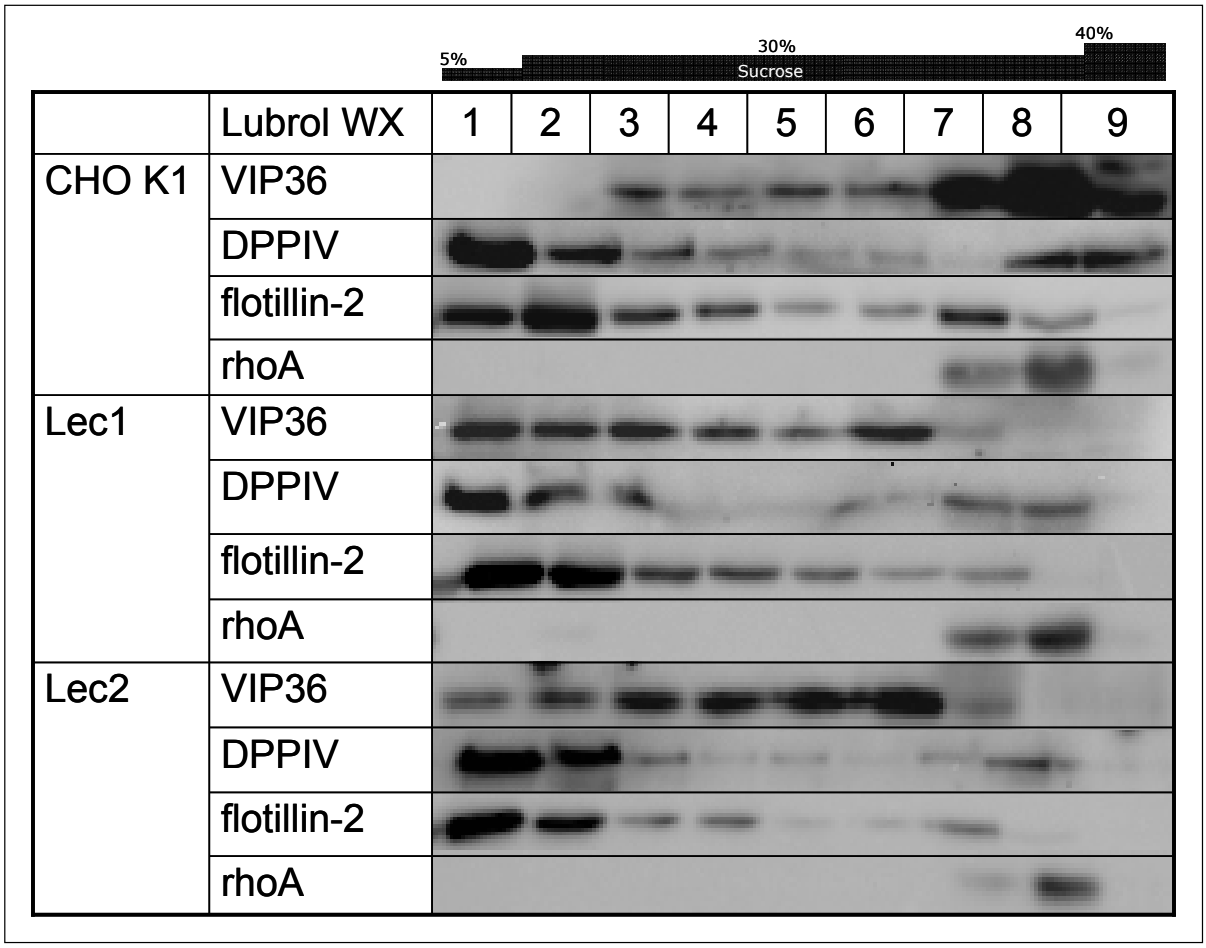

Figure 3.19 Extraction of Lubrol WX DRMs of CHO K1, Lec1, and Lec2 cells. CHO K1, Lec1, and Lec2 cells were lysed with Lubrol WX followed by a discontinuous sucrose-density gradient. Nine fractions were collected from the top, ranging from 5 % sucrose in the upper fraction to 40 % sucrose in the lowest fraction. Western blot analysis with immunostaining of VIP36, DPPIV, flotillin-2, and rhoA was performed. Flottilin-2 and rhoA are controls for the DRM-fractions and the non-DRM-fractions, respectively.

The experiment reveals that distribution of VIP36 changes in Lubrol WX DRMs when the glycosylation is incomplete, like in the Lec1 and Lec2 cells. This redistribution was not observed for the proteins DPPIV, flotillin-2 and rhoA. Therefore, VIP36 is transported into Lubrol WX DRMs when the glycosylation is incomplete. This suggests an interaction of VIP36 with its cargo at later steps of the secretory pathway when the N-glycosylation is incomplete and a potential role in the post-ER quality control.

3.10 Lipid-analysis of DRMs

A defect in glycosylation, like in the CHO-Lec cells, might influence the composition of lipids in DRMs. To reject the hypothesis that the obtained differences in the distribution of VIP36 are only due to a difference in lipid composition, lipid-analysis of the different DRMs were conducted.

For the lipid analysis of the three CHO cell lines, DRMs were extracted by using 1 % of either one of the detergents Triton X-100, Lubrol WX and Tween 20. The isolated DRM pellet was used for lipid extraction which was followed by TLC. Dried TLC plates (see 6.4) were scanned and then analyzed by the program "ImageJ 1.41i". The quantification of the different lipids in µg was then calculated with "Microsoft Office Exel 2003" (see 6.5). The values of eight samples were used for each cell line per lipid component and DRM extraction. To test for significant difference between the amount of the different lipid components in µg for CHO K1 and the two different Lec cell lines, the Mann-Whitney U test was used. The working hypothesis was defined as H_0: $Values_{CHO} = Values_{Lec1}$ or $Values_{CHO} = Values_{Lec2}$ for the different lipid components. The hypothesis was rejected if p-value was ≤ 0.05.

Twelve lipid components were analyzed for the three different detergents (see 6.6). L-choline was not detected for any of the three cell lines when Triton X-100 DRMs were extracted, so that the remaining eleven lipid components were compared.

For the extraction of Triton X-100, significant difference in lipid content was found for both Lec cell lines in comparison to CHO K1 cells. In the Lec1 cells, there was a significant increase of oleic acid (p: 0.002) and a significant decrease of ethanolamine (p: 0.038), serine (p: 0.038), and monoacylglycerol (p: 0.002) (Fig. 3.20). For the Lec2 cell line, a significant increase was also observed for oleic acid (p: 0.001) as well as a significant decrease of monoacylglycerol (p: 0.002) like in the Lec1 cells (Fig. 3.20). For the other lipid components, no significant difference was observed.

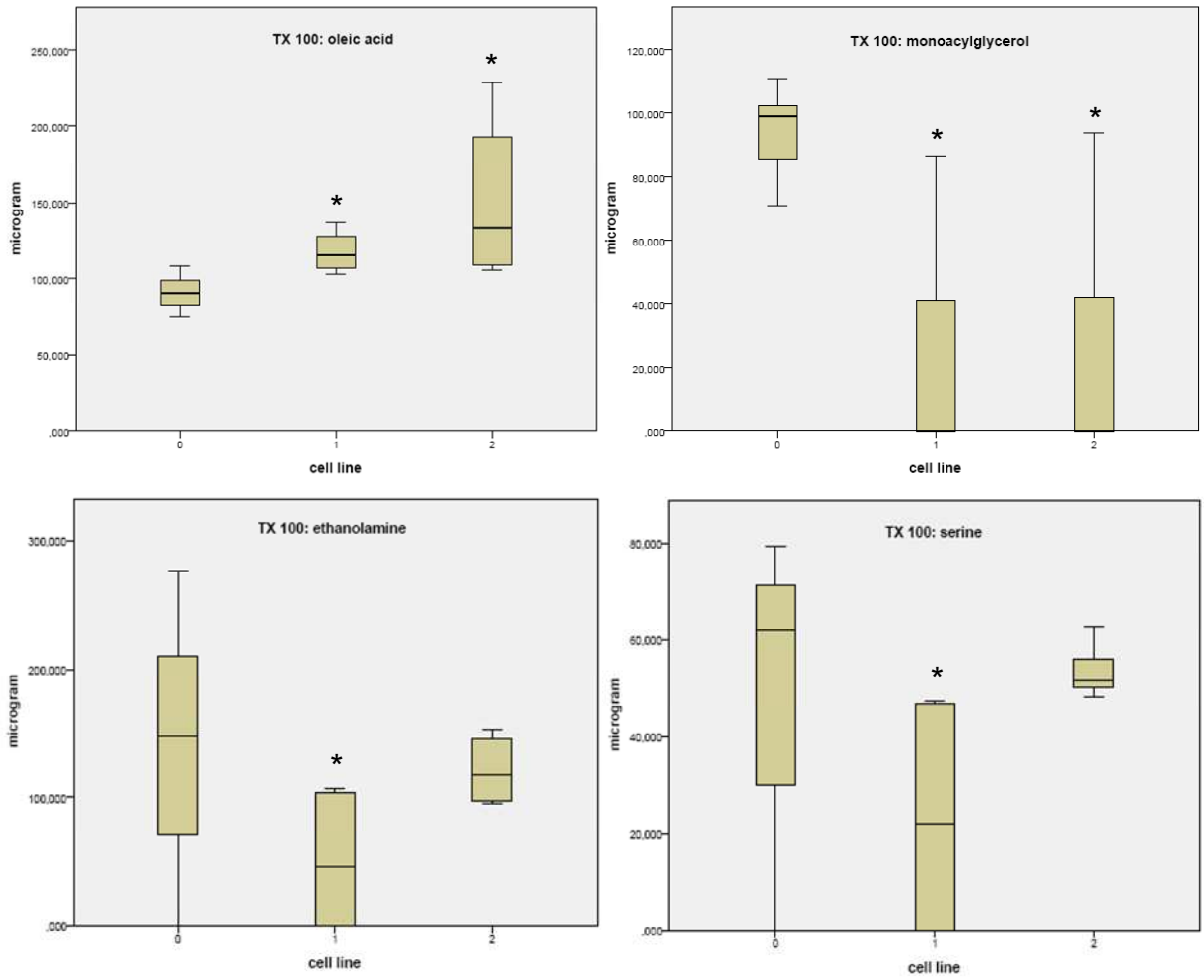

Figure 3.20 Analysis of Triton X-100 DRM composition. DRMs were extracted from CHO K1, Lec1, and Lec2 cells using the detergent Triton X-100. Lipid components were separated on TLC. Eight values for every cell line per detergent and lipid component were consulted for statistical analysis, using the Mann-Whitney U test. The figure depicts the eight values in a boxplot for the different cell lines and lipid components. The cross beams in every boxplot represent the median of the values. A star marks the significant difference of either Lec1 or Lec2 in comparison to the CHO K1 cell line. 0: CHO K1, 1: Lec1, 2: Lec2.

When Lubrol WX DRMs were extracted, there were also differences in lipid composition for both Lec cell lines in comparison to CHO K1 cells. Lec1 DRM composition differs due to a significant increase of ethanolamine (p: 0.001) and a significant decrease of sphingomyelin (p: 0.003) (Fig. 3.21). Lec2 DRMs contain significant less cardiolipin (p: 0.003), cholesterol (p: 0.038), choline (p: 0.038), serine (p: 0.015), and sphingomyelin (p: 0.0001) (Fig. 3.21).

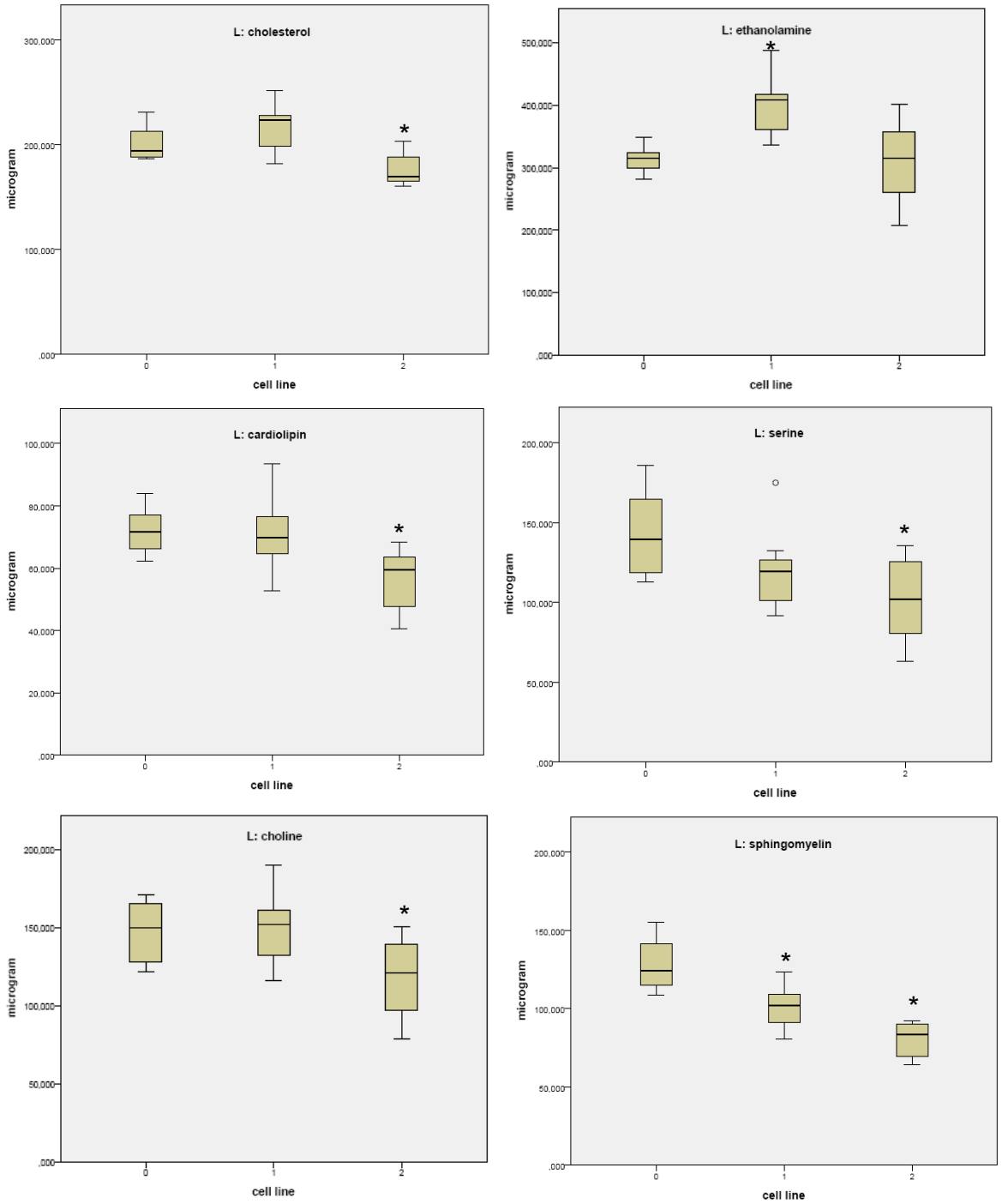

Figure 3.21 Analysis of Lubrol WX DRM composition. DRMs were extracted from CHO K1, Lec1 and, Lec2 cells using the detergent Lubrol WX. Lipid components were separated on TLC. Eight values for every cell line per detergent and lipid component were consulted for statistical analysis, using the Mann-Whitney U test. The figure depicts the eight values in a boxplot for the different cell lines and lipid components. The cross beams in every boxplot represent the median of the values. A circle marks an outliner, defined as a value which is between 1.5 and 3 length of a box outside the box of all values. A star marks the significant difference of either Lec1 or Lec2 in comparison to the CHO K1 cell line. 0: CHO K1, 1: Lec1, 2: Lec2.

The extraction of Tween 20 DRMs also revealed significant differences in lipid content between CHO K1 and Lec1 or Lec2 cells. For Lec1 cells, a significant increase could be shown for ethanolamine (p: 0.010) and choline (p: 0.003) (Fig. 3.22). A significant decrease of galactosyl cerebroside (0.038) and monoacylglycerol (p: 0.028) was observed for the Lec2 cell line (Fig. 3.22).

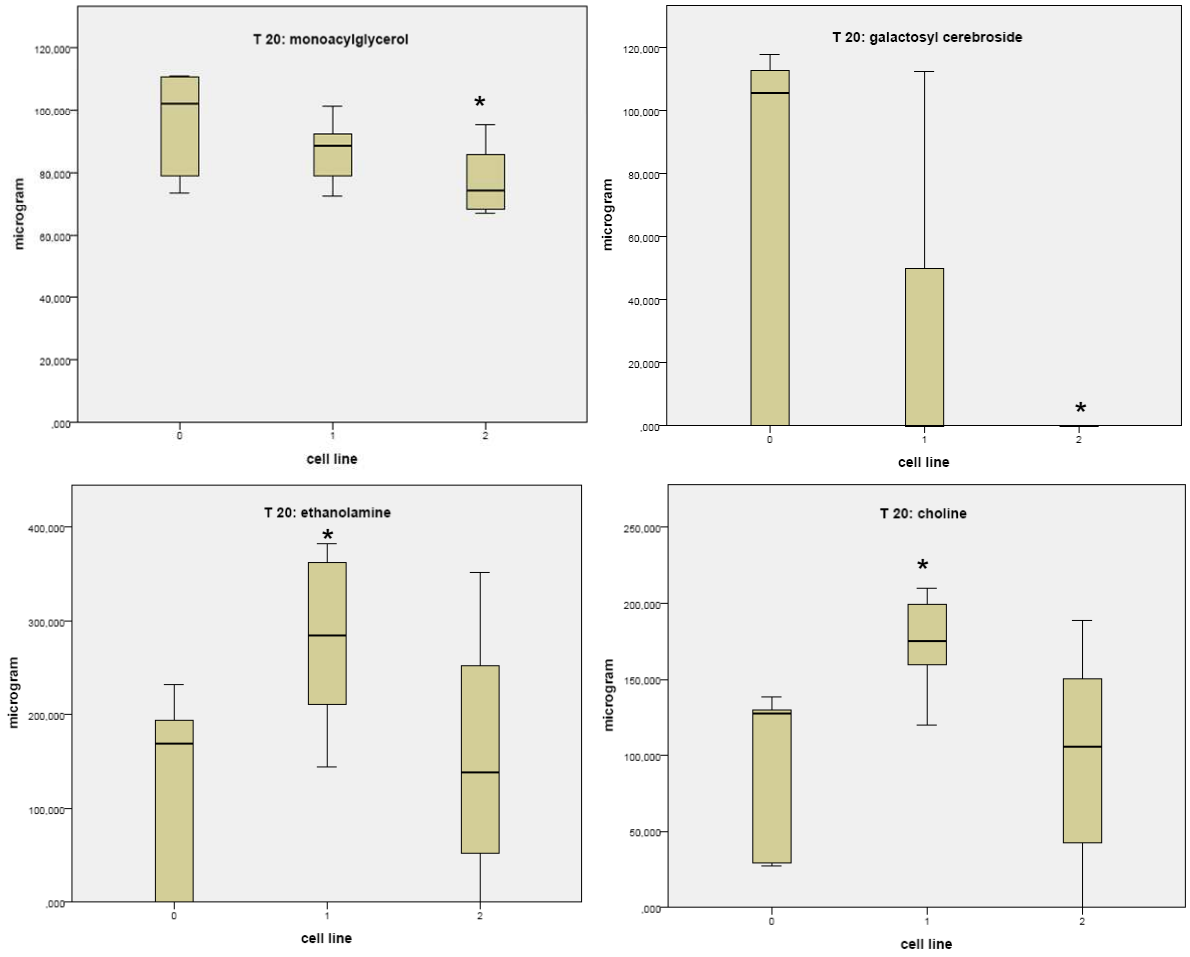

Figure 3.22 Analysis of Tween 20 DRM composition. DRMs were extracted from CHO K1, Lec1 and, Lec2 cells using the detergent Tween 20. Lipid components were separated on TLC. Eight values for every cell line per detergent and lipid component were consulted for statistical analysis, using the Mann-Whitney U test. The figure depicts the eight values in a boxplot for the different cell lines and lipid components. The cross beams in every boxplot represent the median of the values. A star marks the significant difference of either Lec1 or Lec2 in comparison to the CHO K1 cell line. 0: CHO K1, 1: Lec1, 2: Lec2.

The lipid analysis showed that there are some differences in DRM composition between CHO K1 and the two Lec cell lines. The biggest difference could be observed for Lec1 when Triton X-100 extraction was performed and for Lec2 in the Lubrol WX DRMs, with four or five

significant alterations in the lipid content, respectively. For Tween 20 DRMs there was only a minor difference, only two lipid contents altered for each cell line. Since there are twelve lipids which were compared, the main composition of DRMs seems to be unchanged, which is in line with the sucrose density-gradients, where the localisation of the marker proteins flotillin-2 and rhoA did not change in the cell lines with glycosylation defects. Taken together, incomplete glycosylation has an effect on lipid composition of DRMs, but the DRMs itself seem to be still existent.

3.11 Summary of the results in regard to the specific aims of the study

1. By focussing on apical transmembrane glycoproteins as VIP36 interaction partners, the two proteins DPPIV and SI could be identified, interacting with VIP36. However, no interaction with the glycoproteins APN and LPH was observed.
2. The interaction of VIP36 with the glycoproteins DPPIV and SI takes place when mannose-rich as well as complex glycosylated proteins are present. However, no interaction at the cell surface could be observed. Further, the interaction with these two proteins is glycosylation-dependent. When early stages of glycosylation were inhibited by using dNM or dMM, the binding of VIP36 to DPPIV and SI is decreased. The most obvious reduction of binding was found for SI when dNM treatment was used. A possible increase of binding could be observed for DPPIV when later steps of the glycosylation were inhibited, revealed in the two Lec cell lines.
3. A DRM-association of VIP36 was found in Caco-2, CHO K1, and Lec cells by using the detergent Tween 20. In these microdomains, which represent DRMs of early compartments (e.g. ER and ERGIC), an interaction with DPPIV and SI could be observed. This interaction was also shown in the glycosylation-deficient Lec cell lines. No association with DRMs of the Golgi, extracted with Triton X-100 and Lubrol WX, could be shown for Caco-2 and CHO K1 cells. However, a change in the distribution was obtained in Lec1 and Lec2 cells, where VIP36 is associated with Lubrol WX DRMs.

   The lipid analysis of DRMs revealed significant differences in all three DRM-types for Lec1 and Lec2 cells. However, the main composition of DRMs seems to be unchanged, and also the localisation of the marker proteins flotillin-2 and rhoA did not change in the cell lines with glycosylation defects.

4. Discussion

VIP36 is an intracellular lectin which is proposed to play a role in protein sorting and post-ER quality control. It was first discovered in 1994 (Fiedler et al. 1994) and isolated from MDCK cells, but to date its function is still not fully understood. Many studies were conducted to analyze sugar binding properties, cellular localization and possible cargo for this intracellular lectin. The aim of this study was to further characterize the function and localization of VIP36 along the secretory pathway. Finally, I was able to identify two glycoproteins as new interaction partners for VIP36. Further, I could show DRM-association of this protein in different cellular compartments and a possible attendance of VIP36 in the early polarized sorting as well as in the post-ER quality control machinery.

4.1 Intracellular localization of VIP36

The cellular distribution found for VIP36 is very wide spread. It was found that this protein is localized mainly in the Golgi apparatus (e.g. Fiedler et al. 1994, Shimada et al. 2003b). Localization beyond the Golgi was found by several groups. Some showed VIP36 in endosomal and vesicular structures and at the basolateral and apical cell surface with overexpression models (Fiedler et al. 1994, Dahm et al. 2001), others identified endogenous VIP36 in the TGN, granules in rat parotid acinar cells, and at the apical and basolateral cell surface in MDCK cells (Hara-Kuge et al. 2002, Shimada et al. 2003a). However, a distribution in early cellular compartments was also found, identifying VIP36 in the ER and ERGIC (Füllekrug et al. 1999, Dahm et al. 2001). All these studies used different cell lines for their investigations, indicating that VIP36 localization might be cell dependent.
In this study, it was shown that VIP36 is localized in early as well as late compartments along the secretory pathway. Western blot analysis revealed an appearance of VIP36 in Caco-2 and CHO K1 cells as well as in the glycosylation-defective cell lines Lec1 and Lec2, which were further used in this study. The staining of VIP36 in CHO K1 and Lec cells obtained a wide spread distribution of this lectin in the cell. However, no association with the cell surface was observed (Fig. 3.7). Pulse chase experiments using Caco-2 cells revealed that VIP36 binds to mannose-rich and complex glycosylated proteins, which indicate a localization of VIP36 in early cellular compartments like the ER and ERGIC and also in later compartments e.g. Golgi and TGN.

These data confirmed the statements made so far for VIP36 localization (Fiedler et al. 1994, Füllekrug et al. 1999, Hara-Kuge et al. 2002) and suggests that VIP36 might play more than one role in the intracellular sorting machinery due to its localization in distinct cellular compartments.

4.2 VIP36 and its interaction with glycoproteins

Since VIP36 is an intracellular lectin, recognizing N-linked glycans of glycoproteins, specific cargo or interaction partners must exist along the secretory pathway. In the past, it was found that VIP36 interacts with different proteins along the secretory pathway. A glycosylation-dependent interaction of VIP36 was shown for the proteins clusterin (Hara-Kuge et al. 2002), α-amylase (Hara-Kuge et al. 2004), and α-1-antitrypsin (Reiterer et al. 2010), identifying them as cargo for VIP36. The association with the ER-resident chaperone BiP was found to be glycosylation independent (Nawa et al. 2007).

BiP binds to various nascent and newly synthesized proteins in the ER, assisting their folding and participate in quality control processes together with CNX and CRT (Haas 1994, Kleizen & Braakman 2004). However, it was shown that it has in part access to post-ER compartments (Hammond & Helenius 1994). The binding of VIP36 was shown to be independent of folding processes (Nawa et al. 2007). Therefore, it is suggested that VIP36 might interact with BiP, handing over misfolded proteins which VIP36 relocated back to the ER.

The cargo identified so far for VIP36 are all soluble proteins (α-1-antitrypsin: Travis & Salvesen 1983, clusterin: Urban et al. 1987, α-amylase: Humphreys-Beher et al. 1982). Alpha-1-antitrypsin inactivates the serine proteases in blood plasma (Travis & Salvesen 1983). Its interaction with VIP36 occurs in the early secretory pathway, when α-1-antitrypsin is mannose-rich glycosylated before the medial-Golgi, and this complex can be recycled back from the Golgi to the ER (Reiterer et al. 2010). VIP36 retards the transport of α-1-antitrypsin and is involved in retrograde transport, which suggests an involvement in quality control of VIP36 beyond the ER.

Clusterin is released as a disulfide-linked heterodimeric complex from the apical surface of MDCK cells (Urban et al. 1987). It was shown that overproduction of VIP36 results into an increased transport of clusterin, suggesting an involvement of VIP36 in the anterograde transport of this protein (Hara-Kuge et al. 2002). VIP36 binds to clusterin carrying high

mannose-type glycans. This proposes an involvement of VIP36 in sorting events early in the secretory pathway.

Alpha-amylase interacts with VIP36 in secretory vesicles in parotid gland cells (Hara-Kuge et al. 2004), indicating a localization later along the secretory pathway.

Moreover, it was found that VIP36 has a higher affinity to bind membrane proteins and apically sorted proteins (Hara-Kuge et al. 1999, Hara-Kuge et al. 2002) and that the apical delivery of VIP36-recognized glycoproteins was increased due to VIP36 overexpression. Taken together, the studies conducted to date demonstrate a localization and lectin function in the early as well as in the late secretory pathway. But to date no transmembrane protein was identified as cargo.

In this study, I could identify the two glycoproteins DPPIV and SI as new interaction partners of the mammalian L-type lectin VIP36. The two N- and O-glycosylated transmembrane proteins, which are apically sorted in polarized cells, are raft-associated and need this association for a correct targeting (reviewed in Schuck & Simons 2004). These are the first transmembrane glycoproteins which are defined as a possible cargo for VIP36. No binding activity of VIP36 could be detected for the two glycoproteins APN and LPH. These proteins are also apically sorted in polarized cells but their sorting is Triton X-100 raft-independent (Jacob & Naim 2001, Alfalah et al. 2005). It is known that raft-associated and raft-independent proteins take distinct routes to the apical membrane (Jacob & Naim 2001, Jacob et al. 2003, Cresawn et al. 2007). For apical delivery they interact with different lectins (e.g. galectin-3 and galectin-4) in the final steps of the secretory pathway (Delacour et al. 2005, Delacour et al. 2006). It might be possible that there also exist two distinct lectins which distinguish between raft-associated and raft-independent proteins earlier in the secretory pathway which leads to the assumption that VIP36 is involved in the transport of apical raft-associated proteins. An involvement in the apical sorting was already proposed by Fiedler and Simons in 1995 but was rejected by finding VIP36 in early cellular compartments (Füllekrug et al 1999). However, Hara-Kuge et al. (2002) proposed also an involvement of VIP36 in apical sorting events.

Another explanation for the missing binding of VIP36 to APN could be that APN sorting is carbohydrate-independent (Naim et al. 1999). VIP36 might play no role for its sorting since there must be other mechanisms for this protein to reach its final destination. For LPH transport, its dimerization plays a major role, since failure leads to an ER retention followed by degradation (Naim & Naim 1996). VIP36 might not play a role in the sorting of LPH

because other proteins will initiate ER exit when it dimerizes and takes care for sorting in the right vesicles designated to the cell surface.
The immunoprecipitation experiments obtained a stronger band for VIP36 when binding to DPPIV than to SI. However, when the expression levels of DPPIV and SI were compared, a much higher amount of DPPIV was found in Caco-2 cells, which is in agreement with the literature (Hauri et al. 1985). Therefore, the increased binding may be due to the higher expression level of DPPIV.
It is also known that VIP36 binds to basolateral transported proteins (Hara-Kuge et al. 2002) and soluble proteins (Hara-Kuge et al. 2002, Hara-Kuge et al. 2004, Reiterer et al. 2010). Therefore, VIP36 might be involved in distinct transport routes along the secretory pathway and distinguish between apical and basolateral proteins, as well as between DRM-associated and DRM-independent proteins.

The intracellular localization and glycosylation state of proteins, when binding to VIP36, was investigated, using confocal laser microscopy and pulse chase experiments. Confocal data obtained an association of VIP36 with DPPIV intracellularly, in vesicular structures, possibly in the ER and Golgi region. However, only a few colocalizations could be observed. A major problem in identifying cargo glycoproteins of animal lectins is their low affinity and transient binding (Lee & Lee 2000). This might explain the few overlapping spots in the immunofluorescence. The images display a steady state situation and could therefore only represent the binding of VIP36 to DPPIV at one time point in the cell. Since there is only a short time window when single VIP36 molecules interact with DPPIV or glycoproteins in general, it seems normal to detect only one or two interactions in a single cell.
The pulse chase experiments revealed a binding of VIP36 to different glycoforms of interacting proteins. VIP36 can be found in early cellular compartments, like the ER and ERGIC (Füllekrug et al. 1999) which is in agreement with the data of this study. The interaction with DPPIV and SI was shown in the beginning of glycoprotein maturation where the mannose-rich form of the proteins is expressed. This support the findings of Hara-Kuge et al. (2002) and Reiterer et al. (2010), identifying VIP36 binding to cargo with high mannose-type glycans in early cellular compartments. There was also binding at later stages of the secretory pathway shown. Binding to DPPIV occurred when the complex glycosylated form of this protein was present. However, in the last two chase time points there was no binding. At this time, DPPIV is already reaching the cell surface, showing that VIP36 releases its cargo in the Golgi or TGN. The same could be observed for SI, where binding was not

observed at the last time point. Since maturation of SI remains slower than of DPPIV (Hauri et al. 1985), VIP36 binds most likely at the same glycosylation stage and localization of these two proteins. Therefore, VIP36 might also be active as a lectin in later sorting and transport processes, which supports the studies of Hara-Kuge et al. (2004) and Reiterer et al. (2010).

The studies conducted so far (including this one) have demonstrated that VIP36 binds only a restricted set of proteins, which have different tasks in the cell and function in blood plasma, glands or the intestine (Travis & Salvesen 1983, Humphreys-Beher et al. 1983, Matter et al. 1990, Matter & Hauri 1991). The same was found for ERGIC-53, interacting with proteins of blood cells and immune cells (Nichols et al. 1998, Vollenweider et al. 1998, Appenzeller et al. 1999, Cortini & Sitia 2010). Hara-Kuge et al. (2002) obtained, that VIP36 binds to several glycoproteins but the only identified cargo to date are the three proteins clusterin, α-amylase, and α-1-antitrypsin (Hara-Kuge et al. 2002, Hara-Kuge et al. 2004, Reiterer et al. 2010). The two glycoproteins DPPIV and SI are also interacting with VIP36 and this might play a role for its sorting. Since it is known that ERGIC-53 is acting as a cargo receptor for a limited set of proteins and transports them from the ER to the ERGIC, VIP36 might have the same role for its identified cargo in the early secretory pathway.

Binding of VIP36 to DPPIV and SI was shown to be glycosylation-dependent due to the glycosylation-inhibitor experiments. Treatment with either dNM or dMM obtained a decreased binding of VIP36 to the two glycoproteins. This makes SI and DPPIV possible candidates for VIP36 cargo since the binding of cargo identified so far is also glycosylation-dependent (Hara-Kuge et al. 2002, Hara-Kuge et al. 2004, Reiterer et al. 2010).
The inhibition with dMM showed similar reductions of 39.3 % and 36.8 % for VIP36 binding to DPPIV and SI, respectively. DMM hampers α-mannosidase I in the cis-Golgi, preventing further processing of $Man_8GlcNAc_2$ glycans. It was shown that the inhibition with dMM also results in impaired O-glycosylation of SI and DPPIV (Naim et al. 1999). The accessibility of potential O-glycosylation sites to GalNAc requires a reduced number of mannose residues of neighbouring N-glycosylation chains (Naim et al. 1999) processed by α-mannosidase I in the Golgi. When O-glycosylation is hampered by steric hindrance due to dMM treatment, DPPIV and SI are randomly transported to the apical and basolateral cell membrane in Caco-2 cells. Binding could be decreased due to the hampered O-glycosylation of SI and DPPIV. The two proteins may be localized distinctly already at early stages in the secretory pathway when not sorted to the apical surface (Alfalah et al. 2005) and therefore VIP36 fails to bind to the

basolateral transported proteins or bind only a smaller amount as it was shown by Hara-Kuge et al. (2002). Normally it was expected that VIP36 binding is increased since high mannose-type glycans are the favoured bound sugar chains (Kamiya et al. 2005). Further, the interaction is increased when cells were treated with kifunesine, which inhibits α-mannosidase I in the cis-Golgi and ER mannosidase (Reiterer et al. 2010). The binding might be disturbed since VIP36 could not bind to later glycoforms which were not processed due to the treatment.

When the dNM treatment for the two glycoproteins was compared, it was shown that VIP36 binding was decreased either 38.5 % or 64.7 % for DPPIV and SI, respectively. As shown in the pulse chase experiments, VIP36 is interacting with both glycoproteins when they are mannose-rich glycosylated. However, retaining of glucose on the D1-arm of the glycans results into a weak binding of VIP36 (Kamiya et al. 2005). Therefore, it might be possible that VIP36 is not able to identify and bind its cargo. Binding shortly after release from the CNX/CRT cycle might be more important for SI since there was a more severe reduction observable.

The proposal that SI might not be correctly folded due to the treatments and therefore fails binding to VIP36 could be rejected by the trypsin digestion experiment. Neither the dMM treatment nor the dNM treatment affected SI folding, since it was cleaved by trypsin in its subunits sucrase and isomaltase. However, it obtained that dNM treatment did not fully work in the cells, not hampering the whole amount of α-glucosidase I and II. This inefficient treatment has also been reported by Butters et al. (1999). They reported that only 12% of total protein being fully endoglycosidase H-sensitive in dNM-treated CHO cells. Therefore they suggest the combined usage of dNM and CHO Lec3.2.8.1 cells to resolve this problem since these Lec cells express the same glycan processing as it is achieved with dNM treatment (Butters et al. 1999). However, the Lec cell model is not always suitable for investigation of the defined hypothesis, like in this study. Since there was only a partial inhibition of α-glucosidase I and II it is interesting that binding of VIP36 to SI is decreased to such a great extent. In regard to the strong reduction of the binding it might be likely, that VIP36 cannot bind to SI when the N-glycosylation is hampered at a step when CNX (and CRT) are unable to assist SI folding. This is also in agreement with binding assays conducted by Kamiya et al. (2005). Since the dNM treatment only hampers part of the N-glycosylation, VIP36 might bind only to the SI molecules which were further bound by the lectins CNX and CRT. When the remaining glucose on the D1-arm is still present, VIP36 is unable to detect glycoproteins as cargo. The reduction suggests a main interaction of VIP36 shortly after the CNX/CRT-cycle

(and after binding of VIPL) as it was proposed by other studies (Kawasaki et al. 2007, Kamiya et al. 2008). Moreover, VIP36 binding to SI could require the previous binding of the mannose-rich form. As shown in the pulse chase experiment the association between SI and VIP36 untie before complex glycosylation is achieved. Since VIP36 cannot bind to the early forms of the glycosylated protein, it is likely that SI is not identified as potential cargo in later cellular compartments. This could result in the much weaker binding in comparison to DPPIV, where association is stable over the first four chase time points.

When VIP36 does not bind to SI this glycoprotein might be missorted. The association of SI with Triton X-100 DRMs is important since its enzymatic activity is 3-fold higher in DRMs (Wetzel et al. 2009). It was shown that treatment with dMM impairs the transport of SI to these microdomains, reducing it's enzymatically activity (Wetzel et al. 2009). DMM treatment also hampers the binding of VIP36 to SI. This suggests a function of VIP36 as a sorting receptor for SI routing it into the right way that it is transported into Triton X-100 DRMs as it was found by Jacob et al. (2003).

The results show that VIP36 require the quality control of CNX and CRT and the action of α-glucosidase I and II to identify its cargo as interaction partners and that avoidance of protein maturation in the cis-Golgi results into a weaker binding.

Inhibition of later stages of glycosylation, beyond the cis-Golgi, was examined by using Lec1 and Lec2 cells with a defect in N-acetylglucosaminyltransferase I and CMP-sialic acid transporter, respectively. The immunoprecipitation revealed an increased binding of DPPIV by VIP36 in both cell lines. This might be a hind for VIP36 involved in post-ER quality control, binding to incorrect glycosylated proteins and transport them back to the ER for an additional round of folding or glycosylation as was shown by Reiterer et al. (2010). However, the expression levels of DPPIV in the Lec1 and Lec2 cells are increased in comparison to CHO K1 cells. Therefore, it cannot be excluded that VIP36 binds to a larger extend to DPPIV due to more DPPIV proteins expressed in the cell lines, as it was shown for Caco-2 cells.

4.3 DRM-association of VIP36

VIP36 was first isolated as a component of glycolipid rafts, isolated with CHAPS (Fiedler et al. 1994). However, later studies showed that VIP36 might not be associated with DRMs (Füllekrug et al. 1999). Since the cargo of VIP36 I identified in this study are two raft-

associated proteins, I wanted to determine if there is an association with different types of DRMs and if they might serve as interaction platforms for VIP36 and its cargo.

First, DRMs of Caco-2 cells were extracted using different detergents. This obtained no association with DRMs, extracted with Triton X-100 or Lubrol WX for VIP36. Lubrol WX extracts microdomains of the inner leaflet of Golgi membranes, whereas Triton X-100 DRMs are localized more to the outer leaflet of the Golgi and to the TGN (Delaunay et al. 2008). This indicates that VIP36 is not associated with DRMs which appear later along the secretory pathway. Since there is an interaction of VIP36 with DPPIV and SI, which are associated with this type of DRMs, this interaction might be DRM-independent for VIP36 and only dependent on N-glycosylation of cargo.

However, a localization of VIP36 was found in DRMs which were extracted with Tween 20. This type of DRMs represents microdomains of the ER and ERGIC, meaning a DRM-association of VIP36 in the early secretory pathway as was also found for DPPIV and SI (Alfalah et al. 2005). Alfalah et al. (2005) found, that an early polarized sorting takes place in Tween 20 DRMs, identifying only apical sorted proteins in these microdomains. Immunoprecipitation experiments revealed an interaction of VIP36 with its cargo in these DRMs. Therefore, it might be possible that VIP36 functions as a sorting receptor in these DRMs, routing apical, raft-associated proteins on their way to the apical surface. The sorting hypothesis of VIP36 is supported by the studies of Hara-Kuge et al. (2002), who found that VIP36 is interacting with more apical than basolateral sorted proteins. Further, they found that overexpression of VIP36 results into a more efficient apical sorting of glycoproteins, recognized by VIP36. A possible function of VIP36 in this purpose might be cooperation with galectin-4, which sorts proteins into DRMs and deliver them to the apical surface (Delaunay et al. 2005, Stechly et al. 2009). VIP36 might hand proteins, like DPPIV, in the TGN to galectin-4 for further raft-dependent apical delivery of its cargo beyond the TGN. Dependence of DPPIV and other raft-associated proteins on galectin-4 for reaching the apical surface was already shown (Stechly et al. 2009). This has to be verified also for SI. Moreover, there is evidence that more than one mechanism of apical sorting is existent, and that a discrimination of lipid raft-associated and non-associated proteins take place. This was shown for the two glycoproteins SI and LPH, which were routed into distinct vesicles to reach the apical surface (Jacob & Naim 2001, Jacob et al. 2003). Since an early polarized sorting was shown in early cellular compartments (Alfalah et al. 2005) it might be likely that lectins are involved in it like galectin-4 for raft-dependent or galectin-3 for raft-independent proteins (Delacour et al. 2005, Delacour et al. 2006) involving VIP36 for the raft-dependent proteins.

Since the glycosylation plays a role for binding of VIP36 to glycoproteins the question arises if DRM-association was also affected. The interaction studies in the two Lec cell lines indicate a stronger binding of VIP36 to DPPIV when late N-glycan processing was hampered. The association of VIP36 with Tween 20 DRMs should not be affected since these membrane microdomains are present in earlier compartments, but the other two DRM-types appear in the Golgi where the defects are developed. By extraction of Triton X-100 and Tween 20 DRMs of the two Lec cell lines, I couldn`t observe any difference in the distribution of VIP36, DPPIV or the marker proteins flotillin-2 and rhoA. Therefore, it could be shown for these two extractions that inhibition of N-glycosylation beyond the cis-Golgi does not disturb the association with DRMs, and the DRM integrity remains intact referred to the distribution of marker proteins.

The DRM extraction with Lubrol WX reveals that VIP36 is usually not found in these microdomains as shown for Caco-2 and CHO K1 cells. However, in both Lec cell lines VIP36 can be found more in the DRM fractions of the sucrose-density gradient. Delaunay et al. (2008) found that Lubrol WX DRMs represent more the inner leaflet of the Golgi membrane, indicating that VIP36 is located on this side of the membrane in this cellular compartment.

This binding might also explain the stronger bands in the Western blot experiments after immunoprecipitation of DPPIV.

It might be likely that VIP36 is recruited into these microdomains because of an incomplete glycosylation either of itself, or of its cargo. Since this redistribution was not found in Triton X-100 DRMs under the same conditions it can be excluded that the glycosylation of VIP36 plays a role. Moreover, it was shown that VIP36 showing normal localization and binding properties when its N-glycosylation side was removed (Reiterer et al. 2010).

It is questionable why VIP36 is recruited into these specific microdomains. One possible explanation could be that VIP36 might interact more with DPPIV when glycosylation is incorrect and is therefore recruited due to the interaction with DPPIV, since not all VIP36 was found exclusively in the DRM fractions of the gradient. The hypothesis that redistribution might be due to a change in lipid composition was also followed up. The TLC experiments revealed differences in some of the lipid components in Lec1 and Lec2 cells for all the extractions. However, no clear model for increase or decrease of special components for the different detergents and cell lines was observed. In addition, the major part of the investigated components showed no significant change for the two cell lines and different extractions, indicating DRM integrity in Lec1 and Lec2 cell membranes. For Lubrol WX DRMs a decrease in cholesterol for Lec2 cells and sphingomyelin for Lec1 and Lec2 cells was

observed, which are the main components of DRMs or lipid rafts (Simons & Ikonen 1997, Brown & London 1998). This might be the most severe change in lipid composition, which could result into a redistribution of DRMs. However, it was shown that complete depletion of DRM components e.g. sphingolipids or cholesterol do not affect lipid raft integrity (Ostermeyer et al. 1999, Klappe et al. 2010). Moreover, the marker proteins for DRM- and non-DRM-fractions in the sucrose-density gradient still mark the expected fractions. Therefore, it is likely that changes in distribution of VIP36 in Lubrol WX DRMs are not due to the changes in the lipid composition but to the incomplete N-glycosylation of its cargo in the Golgi.

It is suggested that VIP36 might play an important role in post-ER quality control (Reiterer et al. 2010). The observed redistribution might also be a hind for quality control of VIP36 binding to DPPIV and possibly transport it back to earlier compartments for an additional round of glycosylation. Post-ER quality control is mentioned a lot in the literature, since it was found that some misfolded or incomplete glycosylated proteins escape the ER and are further transported through the secretory pathway (VanSlyke et al. 2000, Ashok & Hegde 2009, Reiterer et al. 2010). This was also found for DPPIV in Lec cells. To date, the mechanisms behind and the involved proteins of post-ER quality control are poorly understood and only some proteins are suggested to play a role in this mechanism. Some of these proteins which are involved in retrieval mechanisms to the ER are known to be localized in the ERGIC (e.g. KDEL receptor: Yamamoto et al. 2001), others can be found in the Golgi (Vps10p: Jorgensen et al. 1999, Rab6: White et al. 1999, Tul1p (for membrane proteins): Reggiori & Pelham 2002, Wsc1p: Wang & Ng 2010). Since a retrograde transport was found for VIP36 together with its cargo (Füllekrug et al. 1999, Reiterer et al. 2010), it is likely that VIP36 is involved in this step of the sorting machinery, also indicated by the glycosylation-independent interaction with the chaperone BiP which was also shown in retrograde vesicles directed to the ER and also in the ER (Nawa et al. 2007).

4.4 Lectin function of VIP36 in the secretory pathway

My data, in combination with known features of VIP36 leads to the following model (Fig. 4.1) for the interaction with glycoproteins like DPPIV and SI:

VIP36 binds to correctly folded proteins directly after the CNX/CRT cycle and binding of VIPL in the ER. Here, it functions as a cargo receptor for a set of glycoproteins, in the same

manner as the lectin ERGIC-53. It traffics with its cargo to the ERGIC, where binding is still existent. In the ERGIC it is associated with Tween 20 DRMs and is involved in the apical sorting machinery, possibly for raft-dependent proteins like DPPIV and SI. After this step, VIP36 transports its cargo to the Golgi. In the Golgi, the interaction with cargo might separate temporarily as shown for SI or remains also in this compartment. When VIP36 binds to glycoproteins in the medial- and trans-Golgi it scans them for their proper glycosylation. If the interacting glycoprotein is not correctly glycosylated, it is recycled back by VIP36 to earlier compartments for an additional round of glycan processing. For this step it might be recruited into DRMs of the inner leaflet of the Golgi. Finally, in the TGN VIP36 might hand terminal glycosylated proteins to other lectins, like galectin-4 for raft-associated proteins, which then transport them to their final destination, e.g. the apical cell surface for DPPIV and SI.

In conclusion, my data showed that VIP36 may exert its functions at different sites of the secretory pathway.

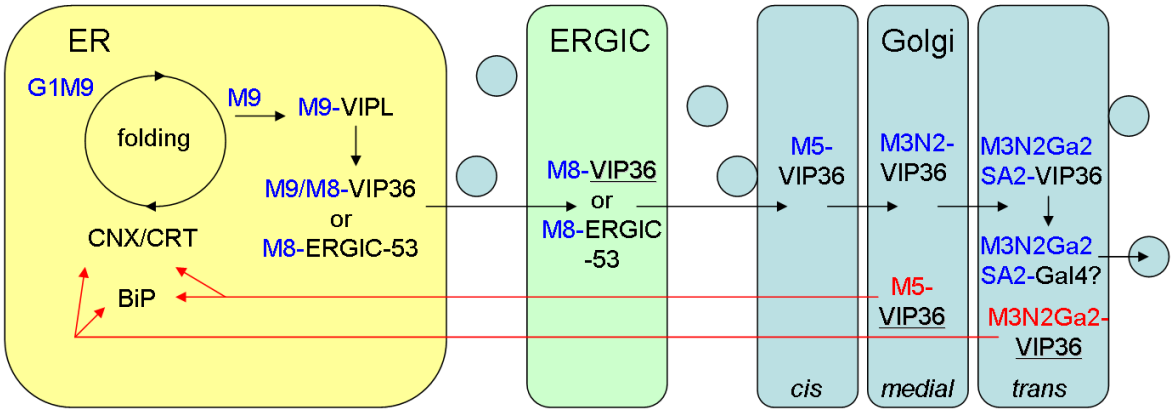

Figure 4.1 VIP36 and its interaction with glycoproteins along the secretory pathway. VIP36 binds to high-mannose type glycans on glycoproteins in the ER after the action of CNX/CRT and VIPL. It traffics with cargo to the ERGIC, like ERGIC-53. In the ERGIC, VIP36 is associated with Tween 20 DRMs and is possibly involved in early polarized sorting for apical proteins. The lectin-glycoprotein complex travels to the Golgi. Here, VIP36 scans its cargo for correct glycosylation, not associated with DRMs. When proteins are not correctly glycosylated, VIP36 might relocated them back to earlier compartments (e.g. ER) and is possibly recruited into Lubrol WX DRMs. Terminal glycosylated proteins are released in the TGN and possibly handed to other lectins e.g. galectin-4 for raft-associated proteins. G: glucose, M: mannose, N: GlcNAc, Ga: galactose, SA: sialic acid, Gal-4: galectin-4, underlined VIP36: DRM-associated.

4.5 Concluding remarks and outlook

In this study, it could be shown that VIP36 is interacting with the transmembrane glycoproteins DPPIV and SI in a glycosylation-dependent manner. These two proteins are raft-associated, which is crucial for their proper sorting and trafficking. Since no interaction with raft-independent proteins could be shown in this study, VIP36 might play a role in the sorting of raft-dependent proteins. It was found that VIP36 recognize and bind to DPPIV and SI in their mannose-rich and complex glycosylated form. This indicates an interaction in the ER and ERGIC as well as in the Golgi and TGN. No interaction could be observed at the cell surface and also pulse chase experiments showed no binding of VIP36 to the two glycoproteins when they supposed to reach the cell surface. Therefore, VIP36 might play a role in early sorting events and release the proteins in the TGN, where it might hand its cargo to other lectins like galectin-4 for raft-associated proteins (e.g. DPPIV). The inhibition of early steps of glycosylation obtained a decreased binding for VIP36 to its cargo. Therefore, VIP36 might require the previous quality control of the lectins CNX and CRT. The inhibiton of glycosylation beyond the cis-Golgi showed a possible increase in binding of VIP36 to DPPIV and SI, suggesting a binding to incomplete glycosylated proteins for retrograde transport to earlier compartments and with this involvement in post-ER quality control.
An association of VIP36 with DRMs along the secretoy pathway was also shown in this study. VIP36 was isolated from Tween 20 DRMs, which represent sorting platforms for apical trafficking. Therefore, it might play a role in early polarized sorting of raft-associated proteins, since an interaction with DPPIV and SI in these DRMs could be shown. No association of VIP36 with DRMs of the Golgi, extracted with Lubrol WX or Triton X-100, could be observed. This suggests that the interaction with glycoproteins is only glycosylation dependent later along the secretory pathway. When the glycosylation was inhibited beyond the cis-Golgi, VIP36 could be found in Lubrol WX DRMs. However, DRM integrity seems to be intact. This suggests recruitment of VIP36 into these microdomains, binding to incorrect glycosylated proteins for a retrograde transport and post-ER quality control.

Taken together, in this work more information about VIP36 was obtained, supporting its involvement in early sorting, apical sorting and post-ER quality control. Although it seems hard-to-believe that one protein can have so many functions in the cell; I think that my data together with the studies conducted so far are a good hind that VIP36 is a multifunctional

intracellular lectin. However, more studies are necessary to define the processes in which VIP36 is involved.

Since the absence of CNX and CRT in mice caused lethality (reviewed in Anelli & Sitia 2008) and mutation in ERGIC-53 bleeding disorder (Nichols et al. 1998) it would be interesting to generate a VIP36 knockout cell line or mouse model to investigate the effects on protein sorting and apical delivery of proteins. Knockdown of VIP36 was conducted by Reiterer et al. (2010) in HepG2 cells. They found a difference in trafficking of α-1-antitrypsin, showing an increasing transport. It would be interesting to investigate DPPIV and SI in a VIP36 knockout Caco-2 cell line. With this it could be determine if VIP36 directly influences apical targeting of DPPIV and SI or not. Further, the interaction with other lectins at later steps of the secretory pathway should be investigated to determine if VIP36 might hand its cargo to other lectins which transport them to the cell surface.

The study gave an additional insight into sorting events along the secretory pathway. Such studies are important to learn more about the complicated sorting machinery which can be found in cells and with this to enhance our understanding of cellular processes which are influenced or altered by certain pathomechanisms.

5. References

Abbott CA, Baker E, Sutherland GR, McCaughan GW (1994): Genomic organization, extract localization, and tissue expression of the human CD26 (dipeptidyl peptidase IV) gene. Immunogenetics 40: 331-338.

Alberts B, Johnson A, Lewis J, Raff M, Roberts K, Walter P, Jaenicke L (2004): Molekularbiologie der Zelle. In: WILEY-VCH Verlag GmbH & Co. KgaA.

Alfalah M, Jacob R, Preuss U, Zimmer KP, Naim H, Naim HY (1999): O-linked glycans mediate apical sorting of human intestinal sucrase-isomaltase through association with lipid rafts. Curr Biol 9: 593-596.

Alfalah M, Jacob R, Naim HY (2002): Intestinal dipeptidyl-peptidase IV is efficiently sorted to the apical membrane through the concerted action of N- and O-glycans as well as association with lipid microdomains. J Biol Chem 277: 10683-10690.

Alfalah M, Wetzel G, Fischer I, Busche R, Sterchi EE, Zimmer KP, Sallmann HP, Naim HY (2005): A novel type of detergent-resistant membranes may contribute to an early protein sorting event in epithelial cells. J Biol Chem 280: 42636-42643.

Anderson RG, Jacobson K (2002): A role for lipid shells in targeting proteins to caveolae, rafts, and other lipid domains. Science 296: 1821-1825.

Anelli T, Sitia R (2008): Protein quality control in the early secretory pathway. EMBO J 27: 315-327.

Appenzeller C, Anderson H, Kappeler F, Hauri HP (1999): The lectin ERGIC-53 is a cargo transport receptor for glycoproteins. Nat Cell Biol 1: 330-334.

Apweiler R, Hermjakob H, Sharon N (1999): On the frequency of protein glycosylation, as deduced from analysis of the SWISS-PROT database. Biochim Biophys Acta 1473: 4-8.

Arar C, Carpentier V, Le Cear J-P, Monsigny M, Legrand A, Roche A-C (1995): ERGIC-53, a membrane protein of the ER-Golgi intermediate compartment is identical to MR60, an intracellular mannose-specific lectin of myelomonocytic cells. J Biol Chem 270: 3551-3553.

Ashok A, Hegde RS (2009): Selective processing and metabolism of disease-causing mutant prion proteins. PLoS Pathog 5: e1000479.

Babiychuk EB, Draeger A (2006): Biochemical characterization of detergent-resistant membranes: a systematic approach. Biochem J 397: 407-416.

Bannykh SI, Nishimura N, Balch WE (1998): Getting into the Golgi. Trends Cell Biol 8: 21-25.

Beaulieu JF, Nichols B, Quaroni A (1989): Posttranslational regulation of sucrase-isomaltase expression in intestinal crypt and villus cells. J Biol Chem 264: 20000-20011.

Benting JH, Rietveld AG, Simons K (1999): N-glycans mediate the apical sorting of a GPI-anchored, raft-associated protein in Mardin-Darby canine kidney cells. J Cell Biol 146: 313-320.

Bligh EG, Dyer WJ (1959): A rapid method of total lipid extraction and purification. Can J Biochem Physiol 37: 911-917.

Blobel G (1980): Intracellular protein topogenesis. Proc Natl Acad Sci U S A 77: 1496-1500.

Bradford MM (1976): A rapid and sensitive method for the quantitation of microgram quantities of protein utilizing the principle of protein-dye binding. Anal Biochem 72: 248-254.

Brockmeier A, Williams BD (2006): Potent lectin-independent chaperone function of calnexin under conditions prevalent within the lumen of the endoplasmic reticulum. Biochemistry 45: 12906-12916.

Browman DT, Resek ME, Zajchowski LD, Robbins SM (2006): Erlin-1 and erlin-2 are novel members of the prohibiting family of proteins that define lipid-raft-like domains of the ER. J Cell Sci 119: 3149-3160.

Brown DA, Rose JK (1992): Sorting of GPI-anchored proteins to glycolipid-enriched membrane subdomains during transport to the apical cell surface. Cell 68: 533-544.

Brown DA, London E (1998): Structure and origin of ordered lipid domains in biological membranes. J Membr Biol 164: 103-114.

Butters TD, Sparks LM, Harlos K, Ikemizu S, Stuart D, Jones EY, Davis SJ (1999): Effects of N-butyldeoxynojirimycin and the Lec3.2.8.1 mutant phenotype on N-glycan processing in Chinese hamster ovary cells: Application to glycoprotein crystallization. Prot Sci 8: 1696-1701.

Campbell SM, Crowe SM, Mak J (2001): Lipid rafts and HIV-1: from viral entry to assembly of progeny virions. J Clin Virol 22: 217-227.

Castelletti D, Alfalah M, Heine M, Hein Z, Schmitte R, Fracasso G, Colombatti M, Naim HY (2008): Different glycoforms of prostate-specific membrane antigen are intracellularly transported through their association with distinct detergent-resistant membranes. Biochem J 409: 149-157.

Chen W, Stanley P (2003): Five Lec1 CHO cell mutants have distinct Mgat1 gene mutations that encode truncated N-acetylglucosaminyltransferase I. Glycobiology 13: 43-50.

Cortini M, Sitia R (2010): ERp44 and ERGIC-53 synergize in coupling efficiency and fidelity of IgM polymerization and secretion. Traffic 11: 651-659.

Cresawn KO, Potter BA, Oztan A, Guerriero CJ, Ihrke G, Goldenring JR, Apodaca G, Weisz OA (2007): Differential involvement of endocytic compartments in the biosynthetic traffic of apical proteins. EMBO J 26: 3737-3748.

Dahm T, White J, Grill S, Füllekrug J, Stelzer EHK (2001): Quantitative ER – Golgi transport kinetics and protein separation upon Golgi exit revealed by vesicular integral-membrane protein 36 dynamics in live cells. Mol Biol Cell 12: 1481-1498.

Dahms NM, Lobel P, Kornfeld S (1989): Mannose-6-phosphate receptors and lysosomal enzyme targeting. J Biol Chem 264: 12115-12118.

Darmoul D, Lacasa M, Baricault L, Marguet D, Sapin C, Trotot P, Barbat A, Trugnan G (1992): Dipeptidyl peptidase IV (CD26) gene expression in enterocyte-like colon cancer cell lines Ht-29 and Caco-2. Cloning of the complete human coding sequence and changes of dipeptidyl peptidase IV mRNA levels during cell differentiation. J Biol Chem 267: 4824-4833.

Delacour D, Gouyer V, Zanetta JP, Drobecq H, Leteurtre E, Grard G, Moreau-Hannedouche O, Maes E, Pons A, André S, Le Bivic A, Gabius HJ, Manninen A, Simons K, Huet G (2005): Galectin-4 and sulfatides in apical membrane trafficking in enterocyte-like cells. J Cell Biol 169: 491-501.

Delacour D, Cramm-Behrens CI, Drobecq H, Le Bivic A, Naim HY, Jacob R (2006): Requirement for galectin-3 in apical protein sorting. Curr Biol 16: 408-414.

Delaunay J-L, Breton M, Trugnan G, Maurice M (2008): Differential solubilisation of inner plasma membrane leaflet components by Lubrol WX and Triton X-100. Biochem Biophys Acta 1778: 105-112.

De Meester I, Vanhoof G, Hendriks D, Demuth HU, Yaron A, Scharpe S (1992): Characterization of dipeptidyl peptidase IV (CD26) from human lymphocytes. Clin Chim Acta 210: 23-34.

De Meester I, Korom S, Van Damme J, Scharpe S (1999): CD26, let it cut or cut it down. Immunol Today 20: 367-375.

Deutscher SL, Nuwayhid N, Stanley P, Briles IE, Hirschberg CB (1984): Translocation across Golgi vesicle membranes: A CHO glycosylation mutant deficient in CMP-sialic acid transport. Cell 39: 295-299.

Drobnik W, Borsukova H, Böttcher A, Pfeiffer A, Liebisch G, Schütz GJ, Schindler H, Schmitz G (2002): Apo AI/ABCA1-dependent and HDL3-mediated lipid efflux from compositionally distinct cholesterol-based microdomains. Traffic 3: 268-278.

Eckhardt M, Gotza B, Gerardy-Schahn R (1998): Mutants of the CMP-sialic acid transporter causing the Lec2 phenotype. J Biol Chem 273: 20189-20195.

Edidin M (2003): The state of lipid rafts: from model membranes to cells. Annu Rev Biophys Biomol Struct 32: 257-283.

Ellgaard L, Helenius A (2003): Quality control in the endoplasmic reticulum. Nat Rev Mol Cell Biol 4: 181-191.

Fan H, Meng W, Kilian C, Grams S, Reuter W (1997): Domain-specific N-glycosylation of the membrane glycoprotein dipepitdylpeptidase IV (CD26) influences its subcellular trafficking, biological stability, enzyme activity and protein folding. Eur J Biochem 246: 243-251.

Fiedler K, Parton RG, Kellner R, Simons K (1994): VIP36, a novel component of glycolipid rafts and exocytic carrier vesicles in epithelial cells. EMBO Journal 13: 1729-1740.

Fiedler K, Simons K (1995): Characterization of VIP36, an animal lectin homologous to leguminous lectins. J Cell Sci 109: 271-276.

Field KA, Holowka D, Barid B (1995): Fc(epsilon)RI-mediated recruitment of p53/56lyn to detergent-resistant membrane domains accompanies cellular signalling. Proc Natl Acad Sci U S A 92: 9201-9205.

Fitzner D, Schneider A, Kippert A, Möbius W, Willig KI, Hell SW, Bunt G, Gaus K, Simons M (2006): Myelin basic protein-dependent plasma membrane reorganization in the formation of myelin. EMBO J 25: 5037-5048.

Frickel EM, Riek R, Jelesarov I, Helenius A, Wuthrich K, Ellegaard L (2002): TROSY-NMR reveales interaction between ERp57 and the tip of the calreticulin P-domain. Natl Acad Sci U S A 99: 1954-1959.

Füllekrug J, Scheiffele P, Simons K (1999): VIP36 in the early secretory pathway. J Cell Sci 112: 2813-2821.

Giuliano AR, Wood RJ (1991): Vitamin D-regulated calcium transport in Caco-2 cells: A unique in virto model. Am J Physiol 260: 207-212.

Gut A, Kappeler F, Hyka N, Balda MS, Hauri HP, Matter K (1998): Charbohydrate-mediated Golgi to cell surface transport and apical targeting of membrane proteins. EMBO J 17: 1919-1929.

Haas IG (1994): BiP (GRP78), an essential hsp70 resident protein in the endoplasmic reticulum. Experientia 50: 1012-1020.

Haltiwanger RS, Lowe JB (2004): Role of glycosylation in development. Annu Rev Biochem 73: 491-537.

Hammond C, Helenius A (1994): Folding of VSV G protein: sequential interaction with BiP and calnexin. Science 266: 456-458.

Hara-Kuge S, Ohkura T, Seko A, Yamashita K (1999): Vesicular-integral membrane protein, VIP36, recognizes high-mannose type glycans containing α1-2 mannosyl residues in MDCK cells. Glycobiology 9: 833-839.

Hara-Kuge S, Ohkura T, Ideo H, Shimada O, Atsumi S, Yamashita K (2002): Involvement of VIP36 in intracellular transport and secretion of glycoproteins in polarized Mardin-Darby canine kidney (MDCK) cells. J Biol Chem 277: 16332-16339.

Hara-Kuge S, Seko A, Shimada O, Tosaka-Shimada H, Yamashita K (2004): The binding of VIP36 and α-amylase in the secretory vesicles via high-mannose type glycans. Glycobiology 14: 739-744.

Hauri HP, Sterchi EE, Bienz D, Fransen JA, Marxer A (1985): Expression and intracellular transport of microvillus membrane hydrolases in human intestinal epithelial cells. J Cell Biol 101: 838-851.

Hauri HP, Schweizer A (1992): The endoplasmic reticulum: Golgi intermediate compartment. Curr Opin Cell Biol 4: 600-608.

Hauri HP, Appenzeller C, Kuhn F, Nufer O (2000): Lectins and traffic in the secretory pathway. FEBS Lett 476: 32-37.

Havre PA, Abe M, Urasaki Y, Ohnuma K, Morimoto C, Dang NH (2008): The role of CD26/dipeptidyl peptidase IV in cancer. Front Biosci 13: 1634-1645.

Hebert DN, Molinari M (2007): In and out of the ER: protein folding, quality control, degradation, and related human diseases. Physiol Rev 87: 1377-1408.

Hein Z, Hooper NM, Naim HY (2009): Association of GPI-anchored protein with detergent-resistant membranes facilitates its trafficking through the early secretory pathway. Exp Cell Res 315: 348-356.

Helenius A, Aebi M (2001): Intracellular functions of N-linked glycans. Science 291: 2364-2369.

Helenius A, Aebi M (2004): Roles of N-linked glycans in the endoplasmic reticulum. Annu Rev Biochem 73: 1019.

Henderson RM, Edwardson JM, Geisse NA, Saslowsky DE (2004): Lipid rafts: feeling is believing. News Physiol Sci 19: 39-43.

Herscovics A (2001): Structure and function of class I alpha 1,2-mannosidases involved in glycoprotein synthesis and endoplasmic reticulum quality control. Biochimie 83: 757-762.

Holowka D, Barid B (2001): Fc(epsilon)RI as a paradigm for a lipid raft-dependent receptor in hematipoietic cells. Semin Immunol 13: 99-105.

Hong W, Piazza GA, Hixson DC, Doyle D (1989): Expression of enzymatically active rat dipeptidyl peptidase IV in Chinese hamster ovary cells after transfection. Biochemistry 28: 8474-8478.

Horstmann H, Ng CP, Tang BL, Hong W (2002): Ultrastructural characterization of endoplasmic reticulum-Golgi transport containers (EGTC). J Cell Sci 115: 4263-4273.

Hosokawa N, Wada I, Hasegawa K, Yorihuzi T, Tremblay LO, Herscovics A, Nagata K (2001): A novel ER alpha-mannosidase-like protein accelerates ER-associated degradation. EMBO Rep 2: 415-422.

Hosokawa N, Kamiya Y, Kamiya D, Kato K, Nagata K (2009): Human OS-9, a lectin required for glycoprotein endoplasmic reticulum-associated degradation, recognizes mannose-trimmed N-glycans. J Biol Chem 284: 17061-17068.

Huet G, Hennebicq-Reig S, de Bolos C, Ulloa F, Lesuffleur T, Barbat A, Carrière V, Kim I, Real FX, Delannoy P, Zweibaum A (1998): GalNAc-α-*O*-benzyl inhibits NeuAcα2-3 glycosylation and blocks the intracellular transport of apical glycoproteins and mucus in differentiated HT-29 cells. J Cell Biol 141: 1311-1322.

Humphreys-Beher MG, Hollis DL, Carlson DM (1982): Comparative developmental analysis of the parotid, submandibular and sublingual glands in the neonatal rat. Biochem J 204: 673-679.

Hunziker W, Spiess M, Semenza G, Lodish HF (1986): The sucrase-isomaltase complex: Primary structure, membrane-orientation, and evolution of a stalked, intrinsic brush border protein. Cell 46: 227-234.

Ikehara Y, Ogata S, Misumi Y (1994): Dipeptidyl-peptidase IV from rat liver. Methods Enzymol 244: 215-227.

Ioffe E, Stanley P (1994): Mice lacking N-acetylglucosaminyltransferase I activity die at mid-gestation, revealing an essential role for complex or hybrid N-linked carbohydrates. Proc Natl Acad Sci U S A 91: 728-732.

Itin C, Kappeler F, Linstedt AD, Hauri HP (1995a): A novel endocytosis signal related to KKXX ER-retrieval signal. EMBO J 14: 2250-2256.

Itin C, Schindler R, Hauri HP (1995b): Targeting of protein ERGIC-53 to the ER/ERGIC/cis-Golgi recycling pathway. J Cell Biol 131: 57-67.

Itin C, Roche A-C, Monsigny M, Hauri HP (1996): ERGIC-53 is a functional mannose-selective and calcium-dependent human homologue of leguminous lectins. Mol Biol Cell 7: 483-493.

Iwaki-Egawa S, Watanabe Y, Kikuya Y, Fujimoto Y (1998): Dipeptidyl peptidase IV from human serum: Purification, characterization, and N-terminal amino acid sequence. J Biochem 124: 428-433.

Jacob CA, Bodmer D, Spirig U, Battig P, Marcil A, Dignard D, Bergeron JJ, Thomas DY, Aebi M (2001): Htm1p, a mannosidase-like protein, is involved in glycoprotein degradation in yeast. EMBO Rep 2: 423-430.

Jacob R, Alfalah M, Grünberg J, Obendorf M, Naim HY (2000): Structural determinants required for apical sorting of an intestinal brush-border membrane protein. J Biol Chem 275: 6566-6572.

Jacob R, Naim HY (2001): Apical membrane proteins are transported in distinct vesicular carriers. Curr Biol 11: 1444-1450.

Jacob R, Heine M, Alfalah M, Naim HY (2003): Distinct cytoskeletal tracks direct individual vesicle populations to the apical membrane of epithelial cells. Curr Biol 13: 607-612.

Jaeken J, Matthijs G (2007): Congenital disorders of glycosylation: a rapidly expanding disease family. Annu Rev Genom Hum Genet 8: 261-278.

Janes PW, Ley SC, Magee AI, Kabouridis PS (2000): The role of lipid rafts in T cell antigen receptor (TCR) signalling. Smin Immunol 12: 23-34.

Jascur T, Matter K, Hauri HP (1991): Oligomerization and intracellular protein transport: Dimerization of intestinal dipeptidylpeptidase IV occurs in the Golgi apparatus. Biochemistry 30: 1908-1915.

Jorgensen MU, Emr SD, Winther JR (1999): Ligand recognition and domain structure of Vps10p, a vacuolar protein sorting receptor in *Saccharomyces cerevisidae*. Eur J Biochem 260: 461-469.

Kamiya Y, Yamaguchi Y, Takahashi N, Arata Y, Kasai K-I, Ihara Y, Matsuo I, Ito Y, Yamamoto K, Kato K (2005): Sugar-binding properties of VIP36, an intracellular animal lectin operating as a cargo receptor. J Biol Chem 280: 37178-37182.

Kamiya Y, Kamiya K, Yamamoto K, Nyfeler B, Hauri HP, Kato K (2008): Molecular basis of sugar recognition by the human L-type lectins ERGIC-53, VIPL and VIP36. J Biol Chem 283: 1857-1861.

Kappeler F, Klopfenstein DR, Foguet M, Paccaud JP, Hauri HP (1997): The recycling of ERGIC-53 in the early secretory pathway: ERGIC-53 carries a cytosolic endoplasmic reticulum-exit determinant interacting with COPII. J Biol Chem 272: 31801-31808.

Kawasaki N, Matsuo I, Totani K, Nawa D, Suzuki N, Yamaguchi D, Matsumoto N, Ito Y, Yamamoto K (2007): Detection of weak sugar binding activity of VIP36 using VIP36-streptavidin complex and membrane-based sugar chains. J Biochem 141: 221-229.

Khalkhall Z, Marshall RD (1975): Glycosylation of ribonuclease A catalysed by rabbit liver extracts. Biochem J 146: 299-307.

Kimura Y, Nakazawa M, Yamada M (1998): Cloning and characterization of three isoforms of OS-9 cDNA and expression of the OS-9 gene in various human tumor cell lines. J Biochem 123: 876-882.

Klappe K, Dijkhus AJ, Hummel I, van Dam A, Ivanova PT, Milene SB, Myers DS, Brown HA, Permentier H, Kok JW (2010): Extensive sphingolipid depletion does not affect lipid raft integrity or lipid raft localization and efflux function of the ABC transporter MRP1. Biochem J 430: 519-529.

Kleizen B, Braakman I (2004): Protein folding and quality control in the endoplasmic reticulum. Curr Opin Cell Biol 16: 343-349.

Klumperman I, Schweizer A, Clausen H, Tang BL, Hong W, Oorschot V, Hauri HP (1998): The recycling pathway of protein ERGIC-53 and dynamics of the ER-Golgi intermediate compartment. J Cell Sci 111: 3411-3425.

Kornfeld R, Kornfeld S (1985): Assembly of asparagine-linked oligosaccharides. Annu Rev Biochem 54: 631-664.

Kornfeld S (1992): Structure and function of the mannose 6-phosphate/insulin-like growth factor receptors. Annu Rev Biochem 61: 307-330.

Kozlov G, Maattanen P, Schrag JD, Pollock S, Cygler M, Nagar B, Thomas DY, Gehring K (2006): Crystal structure of the bb' domains of the protein disulfide isomerase ERp57. Structure 14: 1331-1339.

Kozlov G, Pocaschi CL, Rosenauer A, Bastos-Aristizabal S, Gorelik A, Williams DB, Gehring K (2010): Structural basis of carbohydrate recognition by calreticulin. J Biol Chem 285: 38612-38620.

Kuokkanen M, Kokkonen J, Enattah NS, Ylisaukko-Oja T, Komu H, Varilo T, Peltonen L, Savilahti E, Jarvela I (2006): Mutations in the translated region of the lactase gene (LCT) underlie congenital lactase deficiency. Am J Hum Genet 78: 339-344.

Kusumi A, Koyama-Honda I, Suzuki K (2004): Molecular dynamics and interactions for creation of stimulation-induced stabilized rafts from small unstable steady-state rafts. Traffic 5: 213-230.

Kwik J, Boyle S, Fooksman D, Margolis L, Sheetz MP, Edidin M (2003): Membrane cholesterol, lateral mobility, and the phosphatidylinositol 4,5-bisphosphate-dependent organization of cell actin. Proc Natl Acad Sci U S A 100: 13964-13969.

Lackie PM, Adam EC (2006): Sweet talking-cellular carbohydrates and epithelial repair. Clin Exp Allergy 36: 560-652.

Laemmli UK (1970): Cleavage of structural proteins during the assembly of the head of bacteriophage T4. Nature 227: 755-725.

Le Bivic A, Quaroni A, Nichols B, Rodriguez-Boulan E (1990): Biogenetic pathways of plasma membrane proteins in Caco-2, a human intestinal epithelial cell line. J Cell Biol 111: 1351-1361.

Lederkremer GZ (2009): Glycoprotein folding, quality control and ER-associated degradation. Curr Opin Struct Biol 19: 515-523.

Lee J, Sundaram S, Shaper NL, Raju TS, Stanley P (2001): Chinese hamster ovary (CHO) cells may express six beta 4-galactosyltransferases (beta 4GalTs). Consequences of the loss of functional beta 4GalT-1, beta 4GalT-6, or both in CHO glycosylation mutants. J Biol Chem 276: 13924-13934.

Lee RT, Lee YC (2000): Affinity enhancement by multivalent lectin-carbohydrate interaction. Glycoconj J 17: 543-551.

Leitner K, Ellinger I, Grill M, Brabec M, Fuchs R (2006): Efficient apical IgG recycling and apical-to-basolateral transcytosis in polarized Bewo cells overexpressing Hfcrn. Placenta 27: 799-811.

Lindner R, Naim HY (2009): Domains in biological membranes. Exp Cell Res 315: 2871-2878.

Lippincott-Schwartz J, Donaldson JG, Schweizer A, Berger EG, Hauri HP, Yuan LC, Klausner RD (1990): Microtubule-dependent retrograde transport of proteins into the ER in the presence of brefeldin A suggests an ER recycling pathway. Cell 60: 821-836.

Lodish HF, Berk A, Zipursky SL, Matsudaira PT, Baltimore D, Darnell J (2000): Molecular cell biology. In: WH Freeman and Company.

Low SH, Wong SH, Tang BL, Hong WJ (1991): Involvement of both vectorial and transcytotic pathways in the preferential apical cell surface localization of rat dipeptidyl peptidase IV in transfected Llc-Pk1 cells. J Biol Chem 266: 19710-19716.

Lübbehusen J, Thiel C, Rind N, Ungar D, Prinsen BHCMT, de Koning TJ, van Hasselt PM, Körner C (2010): Fatal outcome due to deficiency of subunit 6 of the conserved oligomeric Golgi complex leading to new type of congenital disorders of glycosylation. Hum Mol Gen 19: 3623-3633.

Maiuri L, Raia V, Potter J, Swallow D, Ho MW, Fiocca R, Finzi G, Cornaggia M, Capella C, Quaroni A, et al. (1991): Mosaic pattern of lactase expression by villous enterocytes in human adult-type hypolactasia. Gastroenterology 100: 359-369.

Mann H, Whitney D (1947): On a test of whether one of two random variables is stochastically larger than the other. Ann Math Stat 18: 50-60.

Marth JD, Grewal PK (2008): Mammalian glycosylation in immunity. Nat Rev Immunol 8: 874-887.

Martinez-Menarguez JA, Geuze HJ, Slot JW, Klumperman J (1999): Vesicular tubular clusters between the ER and Golgi mediate concentration of soluble secretory proteins by exclusion from COPI-coated vesicles. Cell 98: 81-90.

Matter K, Brauchbar K, Bucher K, Hauri HP (1990): Sorting of endogenous plasma membrane proteins occurs from two sites in cultured human intestinal epithelial cells (Caco-2). Cell 60: 429-437.

Matter K, Hauri HP (1991): Intracellular transport and conformational maturation of intestinal brush border hydrolases. Biochemistry 30: 1916-1923.

Mikami K, Yamaguchi D, Tateo H, Hu D, Qin S-Y, Kawasaki N, Yamada M, Matsumoto N, Hirabayashi J, Ito Y, Yamamoto K (2010): The sugar-binding ability of human OS-9 and its involvement in ER-associated degradation. Glycobiology 20: 310-321.

Misumi Y, Hayashi Y, Arakawa F, Ikehara Y (1992): Molecular cloning and sequence analysis of human dipeptidyl peptidase IV, a serine proteinase on the cell surface. Biochim Biophys Acta 1131: 333-336.

Moussalli M, Pipe SW, Hauri HP, Nichols WC, Ginsburg D, Kaufman RJ (1999): Mannose-dependent ERGIC-53-mediated ER to Golgi trafficking of coagulation factors V and VIII. J Biol Chem 274: 32539-32542.

Munro S (2001): The MRH domain suggests a shared ancestry for the mannose 6-phosphate receptors and other N-glycan-recognising proteins. Curr Biol 11: 499-501.

Naim HY, Roth J, Sterchi EE, Lentze M, Milla P, Schmitz J, Hauri HP (1988a): Sucrase-isomaltase deficiency in humans. Different mutations disrupt intracellular transport, processing, and function of an intestinal brush border enzyme. J Clin Invest 82: 667-679.

Naim HY, Sterchi EE, Lentze MJ (1988b): Biosynthesis of the human sucrase-isomaltase complex. Differential O-glycosylation of the sucrase subunit correlates with its position within the enzyme complex. J Biol Chem 263: 7242-7253.

Naim HY, Lacey SW, Sambrook FJ, Gething MJ (1991): Expression of a full-length cDNA coding for human intestinal lactase-phlorizin hydrolase reveals an uncleaved, enzymatically active, and transport-competent protein. J Biol Chem 266: 12313-12320.

Naim HY, Naim H (1996): Dimerization of lactase-phlorizin hydrolase occurs in the endoplasmic reticulum, involves the putative membrane spanning domain and is required for an efficient transport of the enzyme to the cell surface. Eur J Cell Biol 70: 198-208.

Naim HY, Joberty G, Alfalah M, Jacob R (1999): Temporal association of the N- and O-linked glycosylation in the polarized sorting of intestinal brush border sucrase-isomaltase, aminopeptidase N, and dipeptidyl peptidase IV. J Biol Chem 274: 17961-17967.

Nakada C, Ritchie K, Oba Y, Nakamura M, Hotta Y, Iino R, Kasai RS, Yamaguchi K, Fujiwara T, Kusumi A (2003): Accumulation of anchored proteins forms membrane diffusion barriers during neuronal polarization. Nat Cell Biol 5: 626-632.

Nauseef WM, McCormick SJ, Clark RA (1995): Calreticulin functions as a molecular chaperone in the biosynthesis of myeloperoxidase. J Biol Chem 270: 4741-4747.

Nawa D, Shimada O, Kawasaki N, Matsumoto N, Yamamoto K (2007): Stable interaction of the cargo receptor VIP36 with molecular chaperone BiP. Glycobiology 17: 913-921.

Neve EPA, Svensson K, Fuxe J, Pettersson R (2003): VIPL, a VIP36-like membrane protein with a putative function in the export of glycoproteins from the endoplasmic reticulum. Exp Cell Res 288: 70-83.

Nichols WC, Seligson U, Zivelin A, Terry VH, Hertel CE, Wheatley MA, Moussalli MJ, Hauri HP, Ciavarella N, Kaufman RJ, Ginsburg D (1998): Mutations in the ER-Golgi intermediate compartment protein ERGIC-53 cause combined deficiency of coagulation factors V and VIII. Cell 93: 61-70.

Nicolau DV, Burrage K, Parton RG, Hancock JF (2006): Identifying optimal lipid raft characteristics required to promote nanoscale protein-protein interactions on the plasma membrane. Mol Cell Biol 26: 313-323.

Nufer O, Mitrovic S, Hauri HP (2003): Profile-based data scanning for animal L-type lectins and characterization of VIPL, a novel VIP36-like endoplasmic reticulum protein. J Biol Chem 278: 15886-15896.

Nyfeler B, Reiterer V, Wendeler MW, Stefan E, Zhang B, Michnick SW, Hauri HP (2008): Identification of ERGIC-53 as an intracellular transport receptor of {alpha}1-antitrypsin. J Cell Biol 180: 705-712.

Ostermeyer AG, Beckrich BT, Ivarson KA, Grove KE, Brown DA (1999): Glycosphingolipids are not essential for formation of detergent-resistant membrane rafts in melanoma cells. J Biol Chem 274: 34459-34466.

Ou WJ, Cameron PH, Thomas DY, Bergeron JJ (1993): Association of folding intermediates of glycoproteins with calnexin during protein maturation. Nature 364: 771-776.

Paladino S, Sarnataro D, Pillich R, Tivodar S, Nitsch L, Zurzolo C (2004): Protein oligomerization modulates raft partitioning and apical sorting of GPI-anchored proteins. J Cell Biol 167: 699-709.

Pang S, Urquhart P, Hooper NM (2004): N-glycans, not the GPI-anchor, mediate the apical targeting of a naturally glycosylated, GPI-anchored protein in polarised epithelial cells. J Cell Sci 177: 5079-5086.

Peretti N, Marcil V, Drouin E, Levy E (2005): Mechanisms of lipid malabsorbtion in cystic fibrosis: the impact of essential fatty acids deficiency. Nutr Metab (Lond) 2:11.

Peterson JR, Helenius A (1999): In vitro reconstitution of calreticulin-substrate interactions. Cell Sci 112: 2775-2784.

Pike LJ (2003): Lipid rafts: bringing order to chaos. J Lipid Res 44: 655-667.

Pike LJ (2006): Rafts defined: a report on the keystone symposium on lipid rafts and cell function. J Lipid Res 47: 1597-1598.

Pinto M, Robine-Leon S, Appay M-D, Kedinger M, Triadou N, Dussaulx E, Lacroix B, Simon-Assmann P, Haffen K, Fogh J, Zweibaum A (1983): Enterocyte-like differentiation and polarization of the human colon carcinoma cell line Caco-2 in culture. Biol Cell 47: 323-330.

Presley JF, Cole NB, Schroer TA, Hirschberg K, Zaal KJ, Lippincott-Schwartz J (1997): ER-to-Golgi transport visualized in living cells. Nature 389: 81-85.

Puck TT, Cieciura SJ, Robinson A (1958): Genetics of somatic mammalian cells, III. Long-term cultivation of euploid cells from human and animal subjects. J Exp Med 108: 945-956.

Reggiori F, Pelham HR (2002): A transmembrane ubiquitin ligase required to sort membrane proteins into multivesicular bodies. Nat Cell Biol 4: 117-123.

Reiterer V, Nyfeler B, Hauri HP (2010): Role of the lectin VIP36 in post-ER quality control of human α-1-antitrypsin. Traffic 11:1044-1055.

Riordan JR, Rommens JM, Kerem B, Alon N, Rozmahel R, Grzelczak Z, Zielenski J, Lok S, Plavsic N, Chou JL, et al. (1989): Identification of the cystic fibrosis gene: cloning and characterization of complementary DNA. Science 245: 1066-1073.

Röper K, Corbeil D, Huttner WB (2000): Retention of prominin in microvilli reveals distinct cholesterol-based lipid microdomains in the apical plasma membrane. Nat Cell Biol 2: 582-592.

Saraste J, Svensson K (1991): Distribution of the intermediate elements operating in ER to Golgi transport. J Cell Sci 100: 415-430.

Satoh T, Cowieson NP, Hakamata W, Ideo H, Fukushima K, Kurihara M, Kato R, Yamashita K, Wakatsuki S (2007): Structural basis for recognition of high mannose type glycoproteins by mammalian transport lectin VIP36. J Biol Chem 282: 28246-28255.

Scheiffele P, Peranen J, Simons K (1995): N-glycans as apical sorting signals in epithelial cells. Nature 378: 96-98.

Schuck S, Honsho M, Ekroos M, Shevchenko A, Simons K (2003): Resistance of cell membranes to different detergents. Proc Natl Acad Sci U S A 100: 5795-5800.

Schuck S, Simons K (2004): Polarized sorting in epithelial cells: raft clustering and the biogenesis of the apical membrane. J Cell Sci 117: 5955-5964.

Schrag JD, Bergeron JJ, Li Y, Borisova S, Hahn M, Thomas DY, Cygler M (2001): The structure of calnexin, an ER chaperone involved in quality control and protein folding. Mol Cell 8: 633-644.

Shaanan B, Lis H, Sharon N (1991): Structure of a legume lectin with an ordered N-linked carbohydrate in complex with lactose. Science 254: 862-866.

Sharon N, Lis H (1990): Legume lectins: A large family of homologous proteins. FASEB J 4: 3198-3208.

Shimada O, Hara-Kuge S, Yamashita K, Tosaka-Shimada H, Yanchao L, Einan L, Atsumi S, Ishikawa H (2003a): Localization of VIP36 in the post-Golgi secretory pathway also in rat parotid acinar cells. J Histochem Cytochem 51: 1057-1063.

Shimada O, Hara-Kuge S, Yamashita K, Tosaka-Shimada H, Yanchao L, Yongnan L, Atsumi S, Ishikawa H (2003b): Clusters of VIP36-positive vesicles between endoplasmic reticulum and Golgi apparatus in GH3 cells. Cell Structure and Function 28: 155-163.

Simons K, Van Meer G (1988): Lipid sorting in epithelial cells. Biochem 27: 6197-6202.

Simons K, Ikonen E (1997): Functional rafts in cell membranes. Nature 387: 569-572.

Simons K, Ehehalt R (2002): Cholesterol, lipid rafts, and disease. J Clin Invest 110: 597-603.

Singer SJ, Nicolson GL (1972): The fluid mosaic model of the structure of cell membranes. Science 175: 720-731.

Soldà T, Galli C, Kaufman RJ, Molinari M (2007): Substrate-specific requirements for UGT1-dependent release from calnexin. Mol Cell 27: 238-249.

Spiro RG, Zhu Q, Bhoyroo V, Söling HD (1996): Definition of the lectin-like properties of the molecular chaperone, calreticulin, and demonstration of its copurification with endomannosidase from rat liver Golgi. J Biol Chem 271: 11588-11594.

Stanley P, Caillibot V, Siminovitch L (1975a): Selection and characterization of eight phenotypically distinct lines of lectin-resistant Chinese hamster ovary cell. Cell 6:121-128.

Stanley P, Narasimhan S, Siminovitch L, Schachter H (1975b): Chinese hamster ovary cells selected for resistance to the cytotoxicity of phytohemagglutinin are deficient in a UDP-N-acetylglucosamine-glycoprotein N-acetylglucosaminyltransferase activity. Proc Natl Acad Sci U S A 72: 3323-3327.

Stechly L, Morelle W, Dessein A-F, André S, Grard G, Trinel D, Dejonghe M-J, Leteurtre E, Drobecq H, Trugnan G, Gabius HJ, Huet G (2009): Galectin-4-regulated delivery of glycoproteins to the brush border membrane of enterocyte-like cells. Traffic 10: 438-450.

Travis J, Salvesen G (1983): Human plasma proteinase inhibitors. Annu Rev Biochem 52: 655-709.

Turk E, Zabel B, Mundlos S, Dyer J, Wright EM (1991): Glucose/galactose malabsorption caused by a defect in the Na^+/glucose cotransporter. Nature 350: 354-356.

Urban J, Parrczyk K, Leutz A, Kayne M, Kondor-Koch C (1987): Constitutive apical secretion of an 80-kD sulfated glycoprotein complex in the polarized epithelial Mardin-Darby canine kidney cell line. J Cell Biol 105: 2735-2743.

Vagin O, Turdikulova S, Sachs G (2004): The H, K-ATPase β subunit as a model to study the role of N-glycosylation in membrane trafficking and apical sorting. J Biol Chem 279: 39026-39034.

Van Meer G (1989): Lipid traffic in animal cells. Annu Rev Cell Biol 5: 247-275.

VanSlyke JK, Deschenes SM, Musil LS (2000): Intracellular transport, assembly, and degradation of wild-type and disease-linked mutant gap junction proteins. Mol Biol Cell 11: 1933-1946.

Varki A, Cummings RD, Esko JD, Freeze HH, Stanley P, Bertozzy CR, Hart GW, Etzler ME (2009): Essentials of glycobiology. In: Cold Spring Harbor Laboratory Press.

Vassilakos A, Michalak M, Lehrman MA, Williams DB (1998): Oligosaccharide binding characteristics of the molecular chaperones calnexin and calreticulin. Biochemistry 37: 3480-3490.

Voet DJ, Voet JG, Pratt CW (2002): Lehrbuch der Biochemie. In: WILEY-VCH Verlag GmbH & Co. KgaA.

Vollenweider F, Kappeler F, Itin C, Hauri HP (1998): Mistargeting of the lectin ERGIC-53 to the endoplasmic reticulum of HeLa cells impairs the secretion of a lysosomal enzyme. J Cell Biol 142: 377-389.

Wang S, Ng DTW (2010): Evasion of endoplasmic reticulum surveillance makes Wsc1p an obligate substrate of Golgi quality control. Mol Biol Cell 21: 1153-1165.

Ware FE, Vassilakos A, Peterson PA, Jackson MR, Lehrman MA, Williams DB (1995): The molecular chaperone calnexin binds Glc1Man9GlcNAc2 oligosaccharide as an initial step in recognizing unfolded glycoproteins. J Biol Chem 270: 4697-4704.

Wetzel G, Heine M. Rohwedder A, Naim HY (2009): Impact of glycosylation and detergent-resistant membranes on the function of intestinal sucrase-isomaltase. Biol Chem 390: 545-549.

White J, Johannes J, Mallard F, Girod A, Grill S, Reinsch S, Keller P, Tzschaschel B, Eckard A, Goud B, Stetzer EH (1999): Rab6 coordinates a novel Golgi to ER retrograde transport in liver cells. J Cell Biol 147: 734-760.

Yamaguchi D, Kawasaki N, Matsuo I, Totani K, Tozawa H, Matsumoto N, Ito Y, Yamamoto K (2007): VIPL has sugar-binding activity specific for high-mannose-type N-glycans, and glucosylation of the α1,2 mannotriosyl branch blocks its binding. Glycobiology 17: 1061-1069.

Yamamoto K, Fuji R, Toyofuku Y, Saito T, Koseki H, Hsu VW, Aoe T (2001): The KDEL receptor mediates a retrieval mechanism that contributes to quality control at the endoplasmic reticulum. EMBO J 20: 3082-3091.

Yamamoto K (2009): Intracellular lectins involved in folding and transport in the endomlasmic reticulum. Biol Pharm Bull 32: 767-773.

Yeaman C, Le Gall AH, Baldwin AN, Monlauzeur L, Le Bivic A, Rodriguez-Boulan E (1997): The O-glycosylated stalk domain is required for apical sorting of neurotrophin receptors in polarized MDCK cells. J Cell Biol 139: 929-940.

Zweibaum A, Hauri HP, Sterchi E, Chantret I, Haffen K, Bamat J, Sordat B (1984): Immunohistological evidence, obtained with monoclonal antibodies, of small intestinal brush border hydrolases in human colon cancers and foetal colons. Int J Cancer 34: 591-598.

Zweibaum A, Laburthe M, Grasset E, Louvard D (1991): Use of cultured cell lines in studies of intestinal cell differentiation and function. In: Field M, Frizzell A: Handbook of physiology: Section 6: The gastrointestinal system vol. 4. Oxford University Press Inc, USA: 223-255.

6. Appendix

6.1 Eidesstattliche Erklärung

Hiermit erkläre ich, dass ich die vorliegende Dissertation mit dem Titel: “The intracellular lectin vesicular integral-membrane protein (VIP36) as a potential sorting receptor for the glycoproteins dipeptidyl peptidase IV and sucrase-isomaltase in the early secterory pathway” selbstständig verfasst habe und die benutzten Hilfsmittel und Quellen sowie die zu Hilfsleistungen herangezogenen Institutionen vollständig angegeben habe.

Diese Dissertation wurde nicht schon als Masterarbeit, Diplomarbeit oder ähnliche Prüfung verwendet.

Die vorliegende Arbeit wurde im Institut für Physiologische Chemie der Stiftung Tierärztliche Hochschule Hannover angefertigt.

Hannover, 15.12.2010

Miriam Wessels

6.2 Curriculum Vitae

Persönliche Daten

Name:	Miriam Wessels
Geburtsdatum:	14.11.1981
Geburtsort:	Hannover
Nationalität:	deutsch

Hochschulausbildung

2007 – 2011	Promotionsstudium an der Leibniz Universität Hannover Doktorarbeit bei Prof. Dr. H.Y. Naim, Institut für Physiologische Chemie, Stiftung Tierärztliche Hochschule Hannover: „The intracellular lectin vesicular integral-membrane protein (VIP36) as a potential sorting receptor for the glycoproteins dipeptidyl peptidase IV and sucrase-isomaltase in the early secretory pathway"
2001 – 2006	Diplomstudium der Biologie an der Leibniz Universität Hannover Diplomarbeit bei Prof. Dr. E. Zimmermann, Institut für Zoologie, Stiftung Tierärztliche Hochschule Hannover: „Social rules in the play behavior of rehabilitated orangutans (*Pongo pygmaeus morio*)"

Schulbildung

1994 – 2001	Tellkampfschule Hannover, Abschluss: Abitur
1988 – 1994	Peter-Petersen-Schule Hannover (Grundschule / Orientierungsstufe)

6.3 Acknowledgements

First of all, I would like to thank Prof. Dr. Hassan Y. Naim for the very interesting and challenging project, for his great supervision and helpful discussions during the last years. I am also very grateful that he supported my participation at international meetings and that he offered me the financial support during the time I spent in the lab.

I am grateful to Prof. Dr. Rita Gerardy-Schahn for being the second examiner of my thesis. I also want to thank Prof. Dr. Anaclet Ngezahayo for being the third examiner of this work.

This is a great opportunity to express my graditude to my collegues. I want to thank all former and present members of the Department of Physiological Chemistry for fruitful discussions, helping advices, proofreading the thesis, and for creating such a nice work atmosphere. They all have been great teachers and provided me with their expertise and assistance. In particular I want to thank Gaby Wetzel and Franziska Schirmer for their technical support.

I am much indebted to Dipl. Biol. Reinhild Gräber for her help on the statistical analysis.

Finally, I want to thank my family and friends for their support over the last years, always encouraged me and helped to overcome motivation problems. Most dearly, I am grateful to Gerrit Dollendorf for his overwhelming motivation, loving support and for keeping me up and standing during the hard times, never lost the confidence in me and my work.

This thesis was financially supported by the SFB 621 “Pathomechanismen der intestinalen Mucosa”.

6.4 TCL-plates of lipid analysis

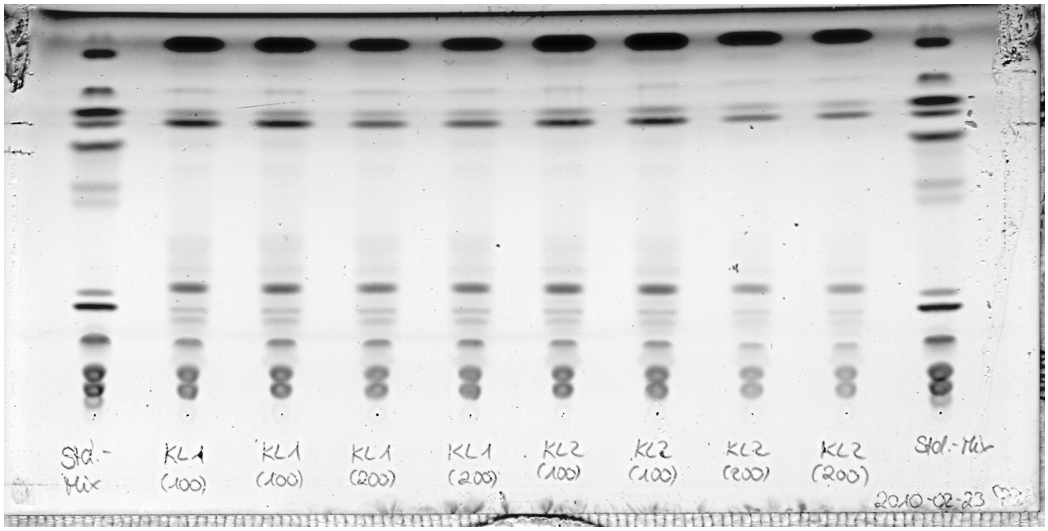

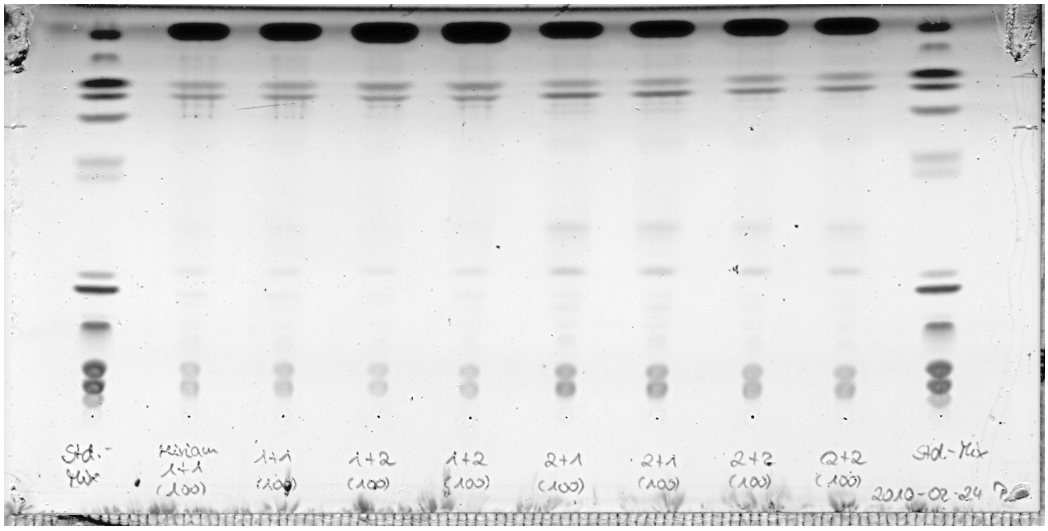

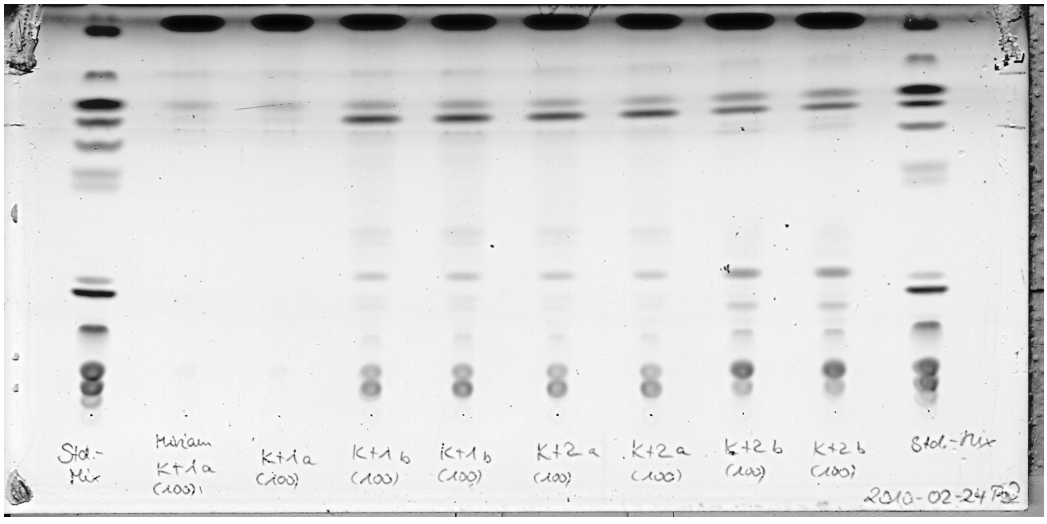

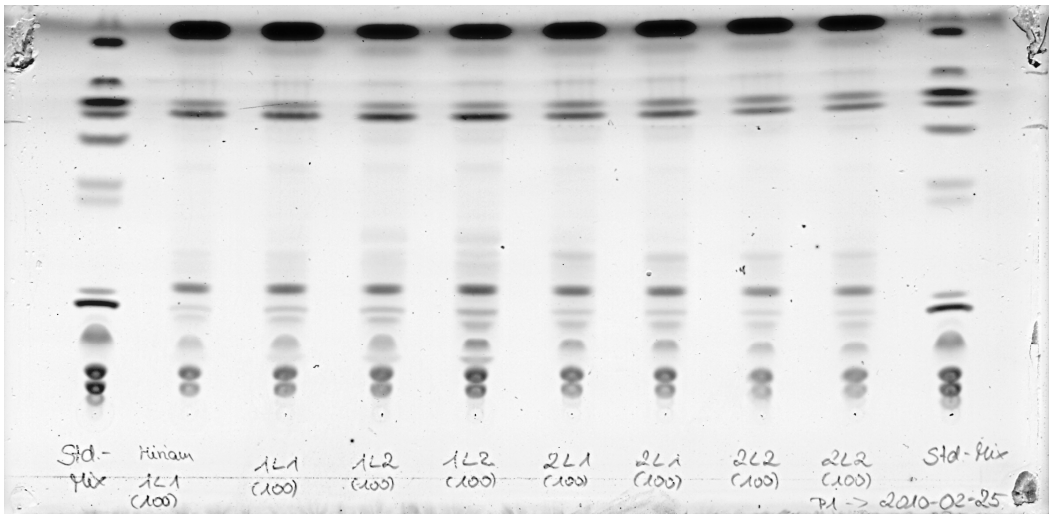
Std.-Mix
Miriam 1L1 (100)
1L1 (100)
1L2 (100)
1L2 (100)
2L1 (100)
2L1 (100)
2L2 (100)
2L2 (100)
Std.-Mix
T1 -> 2010-02-25

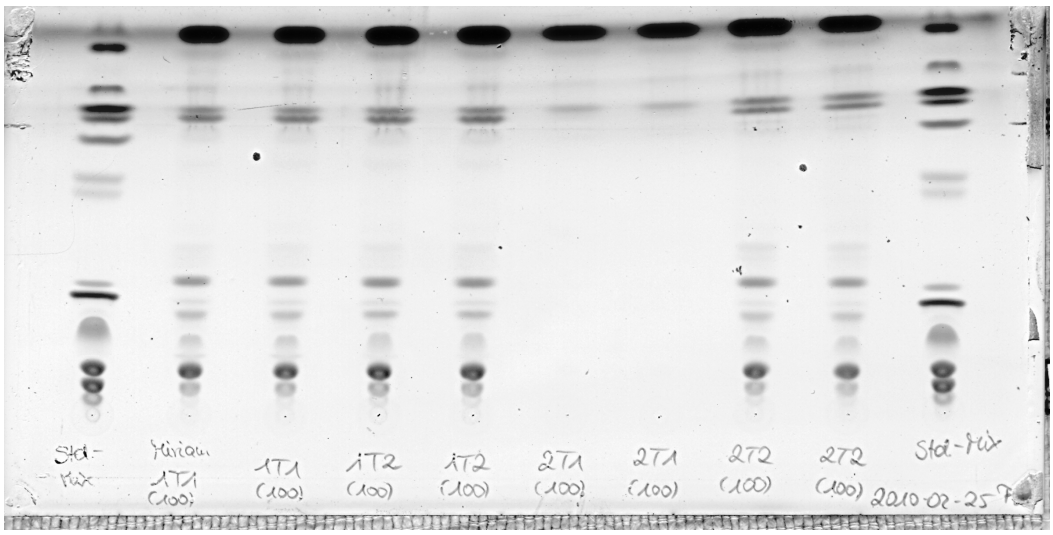
Std.-Mix
Miriam 1T1 (100)
1T1 (100)
1T2 (100)
1T2 (100)
2T1 (100)
2T1 (100)
2T2 (100)
2T2 (100)
Std.-Mix
2010-02-25 T

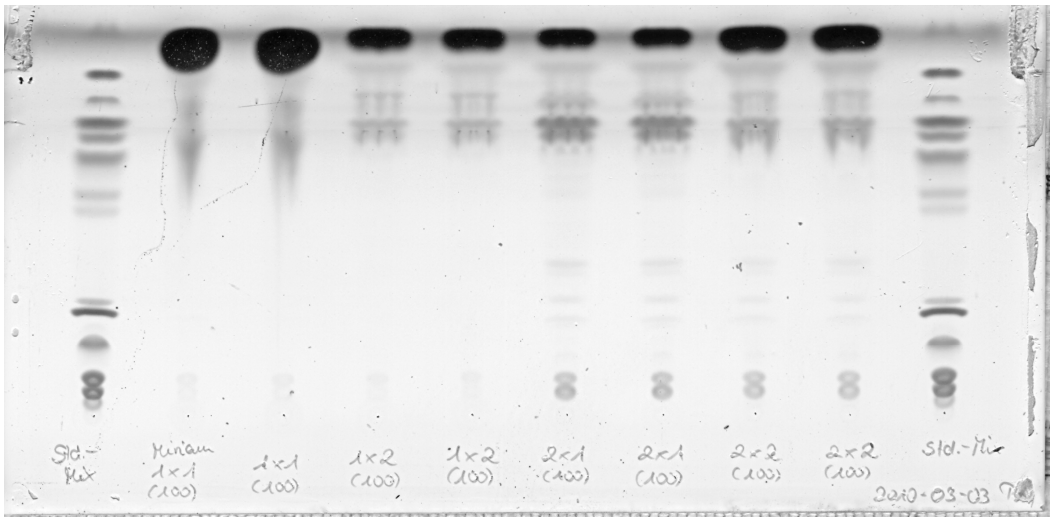
Std.-Mix
Miriam 1x1 (100)
1x1 (100)
1x2 (100)
1x2 (100)
2x1 (100)
2x1 (100)
2x2 (100)
2x2 (100)
Std.-Mix
2010-03-03 T

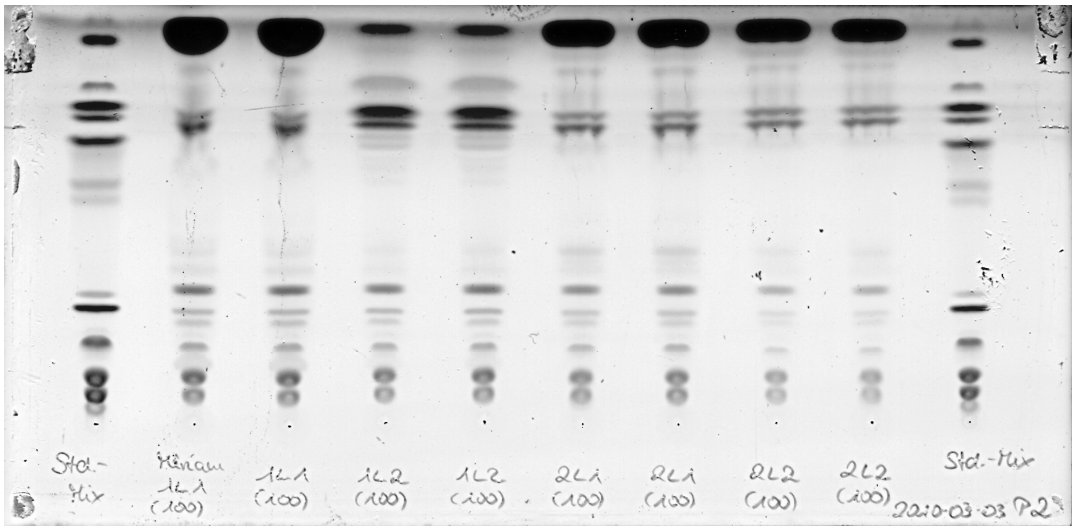
Std.-Mix
Miriam 1L1 (100)
1L1 (100)
1L2 (100)
1L2 (100)
2L1 (100)
2L1 (100)
2L2 (100)
2L2 (100)
Std.-Mix
2010-03-03 P2

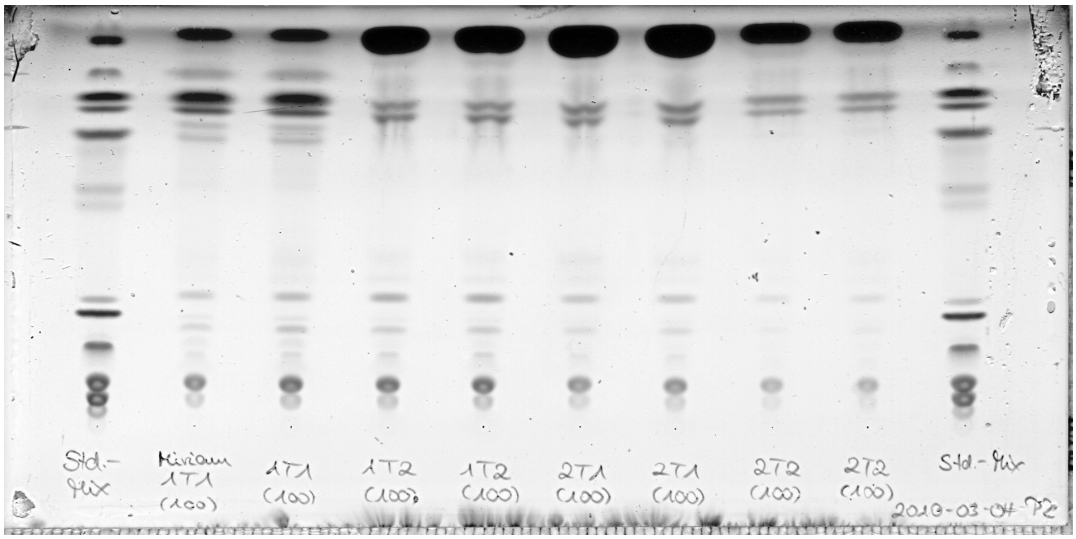
Std.-Mix
Miriam 1T1 (100)
1T1 (100)
1T2 (100)
1T2 (100)
2T1 (100)
2T1 (100)
2T2 (100)
2T2 (100)
Std.-Mix
2010-03-04 P2

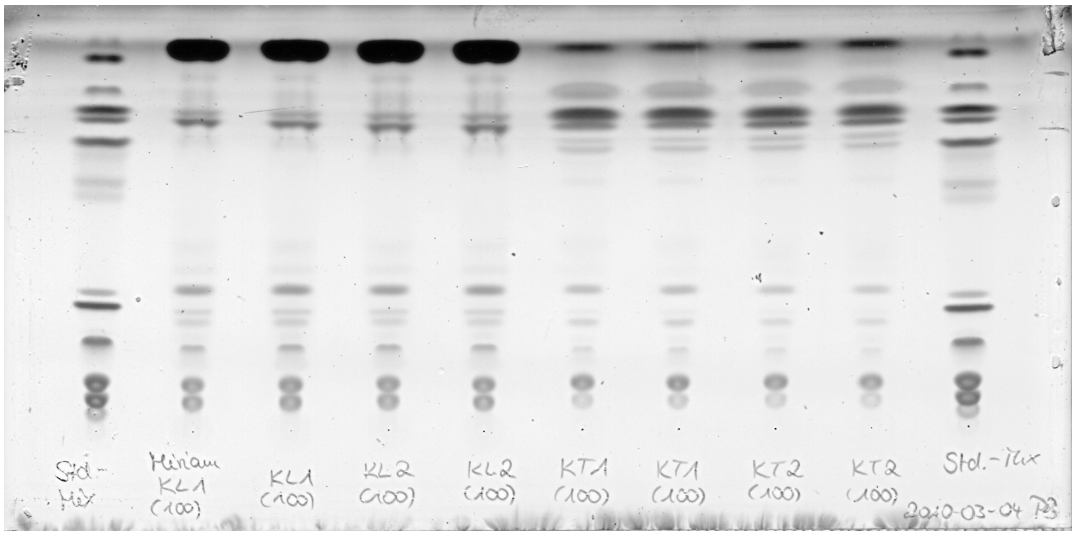
Std.-Mix
Miriam KL1 (100)
KL1 (100)
KL2 (100)
KL2 (100)
KT1 (100)
KT1 (100)
KT2 (100)
KT2 (100)
Std.-Mix
2010-03-04 P3

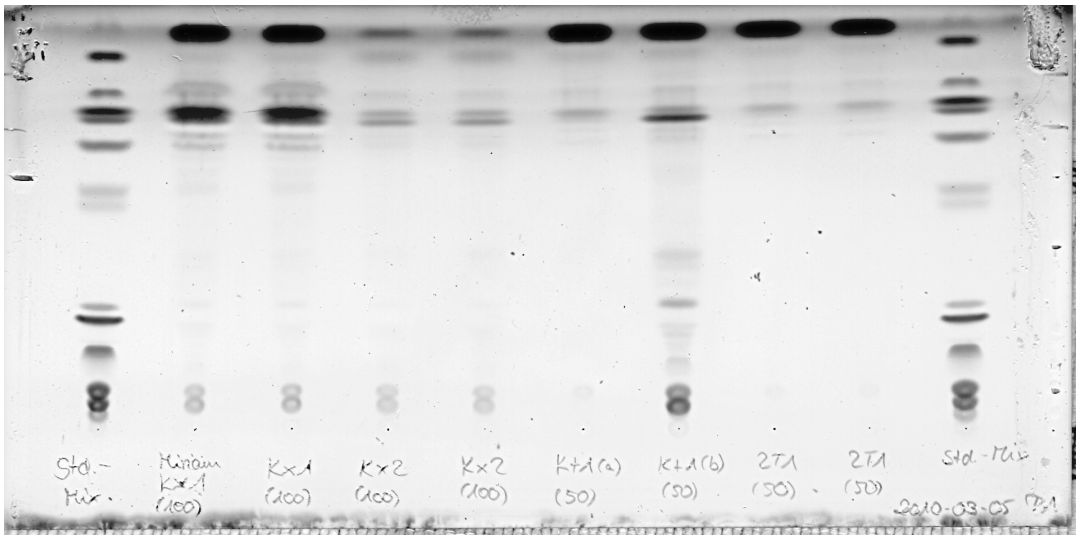

6.5 Lipid content of DRM-fractions of CHO K1, Lec1, and Lec2 cells.

DRMs were isolated from CHO K1, Lec1 and, Lec2 cells with the detergents Triton X 100 (TX 100), Lubrol WX (Lubrol), and Tween 20 (K1: CHO K1, L1: Lec1, L2: Lec2).

Lipid component	**µg**	**cell line**		**µg**	**cell line**		**µg**	**Cell line**
Cholesterol ester	241,213	K1 Tx 100		100,191	K1 Lubrol		90,464	K1 Tween 20
Cholesterol ester	240,837	K1 Tx 100		99,378	K1 Lubrol		102,510	K1 Tween 20
Cholesterol ester	243,854	K1 Tx 100		103,662	K1 Lubrol		89,325	K1 Tween 20
Cholesterol ester	243,342	K1 Tx 100		102,239	K1 Lubrol		90,316	K1 Tween 20
Cholesterol ester	243,051	K1 Tx 100		231,438	K1 Lubrol		124,961	K1 Tween 20
Cholesterol ester	239,290	K1 Tx 100		190,939	K1 Lubrol		113,901	K1 Tween 20
Cholesterol ester	249,910	K1 Tx 100		233,847	K1 Lubrol		106,759	K1 Tween 20
Cholesterol ester	246,355	K1 Tx 100		219,980	K1 Lubrol		109,623	K1 Tween 20
Cholesterol ester	295,895	L1 Tx 100		123,191	L1 Lubrol		92,991	L1 Tween 20
Cholesterol ester	298,837	L1 Tx 100		111,186	L1 Lubrol		89,052	L1 Tween 20
Cholesterol ester	330,605	L1 Tx 100		114,908	L1 Lubrol		95,229	L1 Tween 20
Cholesterol ester	342,773	L1 Tx 100		122,060	L1 Lubrol		94,715	L1 Tween 20
Cholesterol ester	199,947	L1 Tx 100		274,482	L1 Lubrol		123,861	L1 Tween 20
Cholesterol ester	236,825	L1 Tx 100		269,999	L1 Lubrol		125,393	L1 Tween 20
Cholesterol ester	123,063	L1 Tx 100		103,348	L1 Lubrol		245,426	L1 Tween 20
Cholesterol ester	121,275	L1 Tx 100		103,070	L1 Lubrol		210,837	L1 Tween 20
Cholesterol ester	295,333	L2 Tx 100		121,641	L2 Lubrol		79,771	L2 Tween 20
Cholesterol ester	297,758	L2 Tx 100		119,369	L2 Lubrol		81,541	L2 Tween 20
Cholesterol ester	300,646	L2 Tx 100		117,245	L2 Lubrol		101,145	L2 Tween 20
Cholesterol ester	297,663	L2 Tx 100		116,114	L2 Lubrol		96,414	L2 Tween 20
Cholesterol ester	127,445	L2 Tx 100		77,119	L2 Lubrol		222,654	L2 Tween 20
Cholesterol ester	128,496	L2 Tx 100		86,786	L2 Lubrol		212,537	L2 Tween 20
Cholesterol ester	143,623	L2 Tx 100		96,886	L2 Lubrol		98,386	L2 Tween 20
Cholesterol ester	144,267	L2 Tx 100		90,378	L2 Lubrol		108,662	L2 Tween 20
Triglycerides	120,394	K1 Tx 100		110,847	K1 Lubrol		105,767	K1 Tween 20
Triglycerides	116,124	K1 Tx 100		109,103	K1 Lubrol		118,007	K1 Tween 20
Triglycerides	122,888	K1 Tx 100		104,440	K1 Lubrol		101,201	K1 Tween 20

Triglycerides	124,812	K1 Tx 100		105,930	K1 Lubrol		105,011	K1 Tween 20
Triglycerides	124,731	K1 Tx 100		143,862	K1 Lubrol		209,425	K1 Tween 20
Triglycerides	125,959	K1 Tx 100		146,362	K1 Lubrol		209,378	K1 Tween 20
Triglycerides	129,920	K1 Tx 100		163,115	K1 Lubrol		188,633	K1 Tween 20
Triglycerides	137,641	K1 Tx 100		161,056	K1 Lubrol		184,774	K1 Tween 20
Triglycerides	156,742	L1 Tx 100		101,222	L1 Lubrol		107,043	L1 Tween 20
Triglycerides	154,671	L1 Tx 100		102,811	L1 Lubrol		105,040	L1 Tween 20
Triglycerides	0,000	L1 Tx 100		102,288	L1 Lubrol		119,616	L1 Tween 20
Triglycerides	0,000	L1 Tx 100		104,276	L1 Lubrol		111,857	L1 Tween 20
Triglycerides	186,375	L1 Tx 100		155,305	L1 Lubrol		201,169	L1 Tween 20
Triglycerides	207,686	L1 Tx 100		157,364	L1 Lubrol		203,335	L1 Tween 20
Triglycerides	166,444	L1 Tx 100		203,496	L1 Lubrol		132,196	L1 Tween 20
Triglycerides	165,025	L1 Tx 100		203,103	L1 Lubrol		134,466	L1 Tween 20
Triglycerides	0,000	L2 Tx 100		108,708	L2 Lubrol		93,145	L2 Tween 20
Triglycerides	0,000	L2 Tx 100		106,154	L2 Lubrol		93,418	L2 Tween 20
Triglycerides	0,000	L2 Tx 100		105,099	L2 Lubrol		109,054	L2 Tween 20
Triglycerides	0,000	L2 Tx 100		105,414	L2 Lubrol		110,484	L2 Tween 20
Triglycerides	201,150	L2 Tx 100		129,523	L2 Lubrol		126,893	L2 Tween 20
Triglycerides	201,453	L2 Tx 100		130,209	L2 Lubrol		128,826	L2 Tween 20
Triglycerides	171,500	L2 Tx 100		134,614	L2 Lubrol		137,287	L2 Tween 20
Triglycerides	170,847	L2 Tx 100		133,151	L2 Lubrol		144,567	L2 Tween 20
Oleic acid	74,789	K1 Tx 100		126,658	K1 Lubrol		82,136	K1 Tween 20
Oleic acid	77,115	K1 Tx 100		111,015	K1 Lubrol		92,539	K1 Tween 20
Oleic acid	91,982	K1 Tx 100		111,894	K1 Lubrol		73,889	K1 Tween 20
Oleic acid	91,270	K1 Tx 100		117,048	K1 Lubrol		77,961	K1 Tween 20
Oleic acid	87,893	K1 Tx 100		110,085	K1 Lubrol		217,304	K1 Tween 20
Oleic acid	89,675	K1 Tx 100		122,361	K1 Lubrol		209,434	K1 Tween 20
Oleic acid	105,638	K1 Tx 100		122,111	K1 Lubrol		201,696	K1 Tween 20
Oleic acid	108,204	K1 Tx 100		122,313	K1 Lubrol		199,341	K1 Tween 20
Oleic acid	102,481	L1 Tx 100		105,596	L1 Lubrol		100,893	L1 Tween 20
Oleic acid	102,520	L1 Tx 100		111,535	L1 Lubrol		105,638	L1 Tween 20
Oleic acid	113,153	L1 Tx 100		97,909	L1 Lubrol		114,989	L1 Tween 20
Oleic acid	118,330	L1 Tx 100		100,465	L1 Lubrol		102,648	L1 Tween 20
Oleic acid	111,275	L1 Tx 100		111,796	L1 Lubrol		250,103	L1 Tween 20
Oleic acid	118,825	L1 Tx 100		111,783	L1 Lubrol		248,664	L1 Tween 20
Oleic acid	136,346	L1 Tx 100		241,158	L1 Lubrol		115,549	L1 Tween 20
Oleic acid	136,973	L1 Tx 100		245,743	L1 Lubrol		117,392	L1 Tween 20
Oleic acid	105,633	L2 Tx 100		113,088	L2 Lubrol		80,767	L2 Tween 20
Oleic acid	106,784	L2 Tx 100		114,462	L2 Lubrol		79,682	L2 Tween 20
Oleic acid	110,098	L2 Tx 100		109,302	L2 Lubrol		123,518	L2 Tween 20
Oleic acid	112,067	L2 Tx 100		113,510	L2 Lubrol		114,661	L2 Tween 20
Oleic acid	228,253	L2 Tx 100		107,680	L2 Lubrol		116,798	L2 Tween 20
Oleic acid	228,488	L2 Tx 100		103,652	L2 Lubrol		118,683	L2 Tween 20
Oleic acid	156,786	L2 Tx 100		118,278	L2 Lubrol		109,829	L2 Tween 20
Oleic acid	155,439	L2 Tx 100		114,256	L2 Lubrol		115,801	L2 Tween 20
Cholesterol	86,655	K1 Tx 100		226,310	K1 Lubrol		88,854	K1 Tween 20
Cholesterol	86,201	K1 Tx 100		230,899	K1 Lubrol		247,745	K1 Tween 20
Cholesterol	222,503	K1 Tx 100		198,973	K1 Lubrol		62,894	K1 Tween 20
Cholesterol	226,110	K1 Tx 100		196,329	K1 Lubrol		62,966	K1 Tween 20
Cholesterol	204,291	K1 Tx 100		187,986	K1 Lubrol		206,307	K1 Tween 20
Cholesterol	203,822	K1 Tx 100		192,244	K1 Lubrol		219,873	K1 Tween 20

Cholesterol	176,169	K1 Tx 100		188,381	K1 Lubrol		215,836	K1 Tween 20
Cholesterol	178,715	K1 Tx 100		187,087	K1 Lubrol		219,118	K1 Tween 20
Cholesterol	156,140	L1 Tx 100		211,696	L1 Lubrol		157,472	L1 Tween 20
Cholesterol	161,169	L1 Tx 100		223,662	L1 Lubrol		159,725	L1 Tween 20
Cholesterol	152,134	L1 Tx 100		227,452	L1 Lubrol		171,362	L1 Tween 20
Cholesterol	153,436	L1 Tx 100		252,004	L1 Lubrol		173,003	L1 Tween 20
Cholesterol	155,901	L1 Tx 100		182,225	L1 Lubrol		256,731	L1 Tween 20
Cholesterol	181,755	L1 Tx 100		186,078	L1 Lubrol		273,923	L1 Tween 20
Cholesterol	170,664	L1 Tx 100		223,158	L1 Lubrol		186,064	L1 Tween 20
Cholesterol	173,416	L1 Tx 100		228,179	L1 Lubrol		195,335	L1 Tween 20
Cholesterol	188,057	L2 Tx 100		203,129	L2 Lubrol		72,078	L2 Tween 20
Cholesterol	190,566	L2 Tx 100		201,103	L2 Lubrol		76,271	L2 Tween 20
Cholesterol	170,827	L2 Tx 100		176,201	L2 Lubrol		165,723	L2 Tween 20
Cholesterol	174,017	L2 Tx 100		171,020	L2 Lubrol		163,140	L2 Tween 20
Cholesterol	264,694	L2 Tx 100		168,780	L2 Lubrol		173,615	L2 Tween 20
Cholesterol	255,725	L2 Tx 100		164,613	L2 Lubrol		172,658	L2 Tween 20
Cholesterol	200,067	L2 Tx 100		160,507	L2 Lubrol		147,756	L2 Tween 20
Cholesterol	203,318	L2 Tx 100		165,486	L2 Lubrol		156,543	L2 Tween 20
Monoacylglycerol	70,791	K1 Tx 100		100,204	K1 Lubrol		80,572	K1 Tween 20
Monoacylglycerol	75,343	K1 Tx 100		99,506	K1 Lubrol		110,857	K1 Tween 20
Monoacylglycerol	103,846	K1 Tx 100		91,881	K1 Lubrol		73,829	K1 Tween 20
Monoacylglycerol	110,754	K1 Tx 100		91,222	K1 Lubrol		77,819	K1 Tween 20
Monoacylglycerol	97,884	K1 Tx 100		80,274	K1 Lubrol		102,871	K1 Tween 20
Monoacylglycerol	95,525	K1 Tx 100		83,985	K1 Lubrol		101,776	K1 Tween 20
Monoacylglycerol	100,593	K1 Tx 100		80,055	K1 Lubrol		110,617	K1 Tween 20
Monoacylglycerol	100,160	K1 Tx 100		82,598	K1 Lubrol		110,544	K1 Tween 20
Monoacylglycerol	0,000	L1 Tx 100		74,872	L1 Lubrol		80,191	L1 Tween 20
Monoacylglycerol	0,000	L1 Tx 100		80,982	L1 Lubrol		87,489	L1 Tween 20
Monoacylglycerol	0,000	L1 Tx 100		92,356	L1 Lubrol		89,966	L1 Tween 20
Monoacylglycerol	0,000	L1 Tx 100		93,826	L1 Lubrol		91,466	L1 Tween 20
Monoacylglycerol	0,000	L1 Tx 100		0,000	L1 Lubrol		93,268	L1 Tween 20
Monoacylglycerol	0,000	L1 Tx 100		0,000	L1 Lubrol		101,251	L1 Tween 20
Monoacylglycerol	86,428	L1 Tx 100		73,472	L1 Lubrol		72,931	L1 Tween 20
Monoacylglycerol	81,985	L1 Tx 100		80,742	L1 Lubrol		77,850	L1 Tween 20
Monoacylglycerol	0,000	L2 Tx 100		100,473	L2 Lubrol		84,151	L2 Tween 20
Monoacylglycerol	0,000	L2 Tx 100		99,021	L2 Lubrol		79,837	L2 Tween 20
Monoacylglycerol	0,000	L2 Tx 100		96,823	L2 Lubrol		95,431	L2 Tween 20
Monoacylglycerol	0,000	L2 Tx 100		94,316	L2 Lubrol		87,840	L2 Tween 20
Monoacylglycerol	93,899	L2 Tx 100		66,001	L2 Lubrol		68,448	L2 Tween 20
Monoacylglycerol	84,153	L2 Tx 100		64,032	L2 Lubrol		67,052	L2 Tween 20
Monoacylglycerol	0,000	L2 Tx 100		57,849	L2 Lubrol		68,590	L2 Tween 20
Monoacylglycerol	0,000	L2 Tx 100		57,841	L2 Lubrol		69,499	L2 Tween 20
Galactosyl cerebroside	0,000	K1 Tx 100		0,000	K1 Lubrol		0,000	K1 Tween 20
Galactosyl cerebroside	0,000	K1 Tx 100		0,000	K1 Lubrol		117,797	K1 Tween 20
Galactosyl cerebroside	0,000	K1 Tx 100		0,000	K1 Lubrol		0,000	K1 Tween 20
Galactosyl cerebroside	0,000	K1 Tx 100		0,000	K1 Lubrol		0,000	K1 Tween 20
Galactosyl cerebroside	0,000	K1 Tx 100		0,000	K1 Lubrol		110,433	K1 Tween 20
Galactosyl cerebroside	0,000	K1 Tx 100		0,000	K1 Lubrol		104,568	K1 Tween 20
Galactosyl cerebroside	0,000	K1 Tx 100		0,000	K1 Lubrol		106,794	K1 Tween 20
Galactosyl cerebroside	0,000	K1 Tx 100		0,000	K1 Lubrol		114,867	K1 Tween 20
Galactosyl cerebroside	0,000	L1 Tx 100		0,000	L1 Lubrol		0,000	L1 Tween 20

Galactosyl cerebroside	0,000	L1 Tx 100		0,000	L1 Lubrol	0,000	L1 Tween 20
Galactosyl cerebroside	0,000	L1 Tx 100		0,000	L1 Lubrol	0,000	L1 Tween 20
Galactosyl cerebroside	0,000	L1 Tx 100		0,000	L1 Lubrol	0,000	L1 Tween 20
Galactosyl cerebroside	0,000	L1 Tx 100		0,000	L1 Lubrol	99,922	L1 Tween 20
Galactosyl cerebroside	0,000	L1 Tx 100		0,000	L1 Lubrol	112,476	L1 Tween 20
Galactosyl cerebroside	0,000	L1 Tx 100		88,689	L1 Lubrol	0,000	L1 Tween 20
Galactosyl cerebroside	0,000	L1 Tx 100		98,982	L1 Lubrol	0,000	L1 Tween 20
Galactosyl cerebroside	0,000	L2 Tx 100		0,000	L2 Lubrol	0,000	L2 Tween 20
Galactosyl cerebroside	0,000	L2 Tx 100		0,000	L2 Lubrol	0,000	L2 Tween 20
Galactosyl cerebroside	0,000	L2 Tx 100		0,000	L2 Lubrol	0,000	L2 Tween 20
Galactosyl cerebroside	0,000	L2 Tx 100		0,000	L2 Lubrol	0,000	L2 Tween 20
Galactosyl cerebroside	135,773	L2 Tx 100		0,000	L2 Lubrol	0,000	L2 Tween 20
Galactosyl cerebroside	124,963	L2 Tx 100		0,000	L2 Lubrol	0,000	L2 Tween 20
Galactosyl cerebroside	0,000	L2 Tx 100		0,000	L2 Lubrol	0,000	L2 Tween 20
Galactosyl cerebroside	0,000	L2 Tx 100		0,000	L2 Lubrol	0,000	L2 Tween 20
Ethanolamine	0,000	K1 Tx 100		328,843	K1 Lubrol	0,000	K1 Tween 20
Ethanolamine	0,000	K1 Tx 100		347,687	K1 Lubrol	231,949	K1 Tween 20
Ethanolamine	150,327	K1 Tx 100		318,393	K1 Lubrol	0,000	K1 Tween 20
Ethanolamine	162,451	K1 Tx 100		313,037	K1 Lubrol	0,000	K1 Tween 20
Ethanolamine	145,550	K1 Tx 100		281,305	K1 Lubrol	192,391	K1 Tween 20
Ethanolamine	141,359	K1 Tx 100		317,746	K1 Lubrol	196,586	K1 Tween 20
Ethanolamine	277,219	K1 Tx 100		293,975	K1 Lubrol	169,849	K1 Tween 20
Ethanolamine	257,731	K1 Tx 100		303,023	K1 Lubrol	168,166	K1 Tween 20
Ethanolamine	92,686	L1 Tx 100		340,600	L1 Lubrol	335,124	L1 Tween 20
Ethanolamine	103,090	L1 Tx 100		410,792	L1 Lubrol	344,100	L1 Tween 20
Ethanolamine	104,079	L1 Tx 100		407,485	L1 Lubrol	380,947	L1 Tween 20
Ethanolamine	106,542	L1 Tx 100		488,588	L1 Lubrol	382,743	L1 Tween 20
Ethanolamine	0,000	L1 Tx 100		410,848	L1 Lubrol	144,737	L1 Tween 20
Ethanolamine	0,000	L1 Tx 100		422,385	L1 Lubrol	194,397	L1 Tween 20
Ethanolamine	0,000	L1 Tx 100		335,835	L1 Lubrol	226,582	L1 Tween 20
Ethanolamine	0,000	L1 Tx 100		382,623	L1 Lubrol	234,382	L1 Tween 20
Ethanolamine	153,352	L2 Tx 100		401,212	L2 Lubrol	0,000	L2 Tween 20
Ethanolamine	149,406	L2 Tx 100		388,534	L2 Lubrol	0,000	L2 Tween 20
Ethanolamine	130,396	L2 Tx 100		309,340	L2 Lubrol	352,152	L2 Tween 20
Ethanolamine	142,176	L2 Tx 100		325,340	L2 Lubrol	333,578	L2 Tween 20
Ethanolamine	96,817	L2 Tx 100		307,605	L2 Lubrol	171,531	L2 Tween 20
Ethanolamine	98,123	L2 Tx 100		322,131	L2 Lubrol	161,261	L2 Tween 20
Ethanolamine	95,120	L2 Tx 100		206,807	L2 Lubrol	103,584	L2 Tween 20
Ethanolamine	103,159	L2 Tx 100		211,777	L2 Lubrol	114,749	L2 Tween 20
Cardiolipin	0,000	K1 Tx 100		78,010	K1 Lubrol	0,000	K1 Tween 20
Cardiolipin	0,000	K1 Tx 100		83,996	K1 Lubrol	45,894	K1 Tween 20
Cardiolipin	39,489	K1 Tx 100		72,295	K1 Lubrol	0,000	K1 Tween 20
Cardiolipin	40,847	K1 Tx 100		76,079	K1 Lubrol	0,000	K1 Tween 20
Cardiolipin	37,106	K1 Tx 100		62,251	K1 Lubrol	37,149	K1 Tween 20
Cardiolipin	36,700	K1 Tx 100		70,847	K1 Lubrol	42,450	K1 Tween 20
Cardiolipin	40,862	K1 Tx 100		65,502	K1 Lubrol	41,624	K1 Tween 20
Cardiolipin	41,600	K1 Tx 100		66,735	K1 Lubrol	42,961	K1 Tween 20
Cardiolipin	30,181	L1 Tx 100		52,852	L1 Lubrol	111,362	L1 Tween 20
Cardiolipin	37,258	L1 Tx 100		69,968	L1 Lubrol	114,716	L1 Tween 20
Cardiolipin	32,640	L1 Tx 100		77,945	L1 Lubrol	124,814	L1 Tween 20
Cardiolipin	33,613	L1 Tx 100		93,505	L1 Lubrol	124,881	L1 Tween 20

Cardiolipin	0,000	L1 Tx 100		69,871	L1 Lubrol	30,292	L1 Tween 20
Cardiolipin	0,000	L1 Tx 100		75,072	L1 Lubrol	35,524	L1 Tween 20
Cardiolipin	0,000	L1 Tx 100		60,936	L1 Lubrol	31,461	L1 Tween 20
Cardiolipin	0,000	L1 Tx 100		68,127	L1 Lubrol	32,042	L1 Tween 20
Cardiolipin	34,122	L2 Tx 100		68,354	L2 Lubrol	0,000	L2 Tween 20
Cardiolipin	32,922	L2 Tx 100		65,723	L2 Lubrol	0,000	L2 Tween 20
Cardiolipin	35,144	L2 Tx 100		53,546	L2 Lubrol	117,888	L2 Tween 20
Cardiolipin	37,559	L2 Tx 100		60,239	L2 Lubrol	121,418	L2 Tween 20
Cardiolipin	38,778	L2 Tx 100		58,940	L2 Lubrol	35,560	L2 Tween 20
Cardiolipin	37,993	L2 Tx 100		61,346	L2 Lubrol	31,581	L2 Tween 20
Cardiolipin	39,966	L2 Tx 100		40,448	L2 Lubrol	30,797	L2 Tween 20
Cardiolipin	41,800	L2 Tx 100		42,005	L2 Lubrol	34,466	L2 Tween 20
Serine	0,000	K1 Tx 100		172,012	K1 Lubrol	0,000	K1 Tween 20
Serine	0,000	K1 Tx 100		186,117	K1 Lubrol	81,194	K1 Tween 20
Serine	63,268	K1 Tx 100		152,382	K1 Lubrol	0,000	K1 Tween 20
Serine	65,096	K1 Tx 100		157,062	K1 Lubrol	0,000	K1 Tween 20
Serine	59,408	K1 Tx 100		112,638	K1 Lubrol	77,215	K1 Tween 20
Serine	60,961	K1 Tx 100		127,294	K1 Lubrol	78,391	K1 Tween 20
Serine	77,234	K1 Tx 100		119,109	K1 Lubrol	75,243	K1 Tween 20
Serine	79,380	K1 Tx 100		118,261	K1 Lubrol	75,326	K1 Tween 20
Serine	43,779	L1 Tx 100		91,550	L1 Lubrol	94,718	L1 Tween 20
Serine	47,643	L1 Tx 100		120,852	L1 Lubrol	96,137	L1 Tween 20
Serine	46,497	L1 Tx 100		132,212	L1 Lubrol	106,907	L1 Tween 20
Serine	47,668	L1 Tx 100		175,045	L1 Lubrol	106,681	L1 Tween 20
Serine	0,000	L1 Tx 100		118,418	L1 Lubrol	55,966	L1 Tween 20
Serine	0,000	L1 Tx 100		121,211	L1 Lubrol	74,120	L1 Tween 20
Serine	0,000	L1 Tx 100		96,504	L1 Lubrol	68,380	L1 Tween 20
Serine	0,000	L1 Tx 100		105,651	L1 Lubrol	72,095	L1 Tween 20
Serine	48,574	L2 Tx 100		134,066	L2 Lubrol	0,000	L2 Tween 20
Serine	50,166	L2 Tx 100		135,746	L2 Lubrol	0,000	L2 Tween 20
Serine	50,966	L2 Tx 100		109,284	L2 Lubrol	100,451	L2 Tween 20
Serine	56,611	L2 Tx 100		117,078	L2 Lubrol	103,888	L2 Tween 20
Serine	50,907	L2 Tx 100		93,727	L2 Lubrol	66,925	L2 Tween 20
Serine	52,787	L2 Tx 100		94,324	L2 Lubrol	60,824	L2 Tween 20
Serine	55,335	L2 Tx 100		62,934	L2 Lubrol	54,610	L2 Tween 20
Serine	62,811	L2 Tx 100		67,560	L2 Lubrol	58,845	L2 Tween 20
Choline	29,299	K1 Tx 100		165,135	K1 Lubrol	29,629	K1 Tween 20
Choline	31,454	K1 Tx 100		165,628	K1 Lubrol	138,345	K1 Tween 20
Choline	79,925	K1 Tx 100		162,709	K1 Lubrol	27,240	K1 Tween 20
Choline	83,315	K1 Tx 100		170,872	K1 Lubrol	28,460	K1 Tween 20
Choline	79,021	K1 Tx 100		122,117	K1 Lubrol	129,524	K1 Tween 20
Choline	75,899	K1 Tx 100		138,001	K1 Lubrol	130,144	K1 Tween 20
Choline	145,532	K1 Tx 100		128,268	K1 Lubrol	128,748	K1 Tween 20
Choline	149,664	K1 Tx 100		127,596	K1 Lubrol	125,848	K1 Tween 20
Choline	63,111	L1 Tx 100		134,093	L1 Lubrol	187,126	L1 Tween 20
Choline	66,936	L1 Tx 100		158,419	L1 Lubrol	191,830	L1 Tween 20
Choline	60,059	L1 Tx 100		163,488	L1 Lubrol	209,660	L1 Tween 20
Choline	60,618	L1 Tx 100		189,874	L1 Lubrol	206,551	L1 Tween 20
Choline	34,136	L1 Tx 100		150,146	L1 Lubrol	119,661	L1 Tween 20
Choline	38,319	L1 Tx 100		153,694	L1 Lubrol	163,461	L1 Tween 20
Choline	36,876	L1 Tx 100		115,999	L1 Lubrol	157,336	L1 Tween 20

Choline	36,525	L1 Tx 100		131,107	L1 Lubrol	161,701	L1 Tween 20
Choline	87,876	L2 Tx 100		150,824	L2 Lubrol	0,000	L2 Tween 20
Choline	88,814	L2 Tx 100		149,106	L2 Lubrol	0,000	L2 Tween 20
Choline	80,009	L2 Tx 100		126,567	L2 Lubrol	188,432	L2 Tween 20
Choline	83,953	L2 Tx 100		129,445	L2 Lubrol	177,420	L2 Tween 20
Choline	86,320	L2 Tx 100		111,630	L2 Lubrol	123,085	L2 Tween 20
Choline	82,046	L2 Tx 100		115,935	L2 Lubrol	122,499	L2 Tween 20
Choline	84,424	L2 Tx 100		79,122	L2 Lubrol	84,617	L2 Tween 20
Choline	81,941	L2 Tx 100		83,036	L2 Lubrol	88,777	L2 Tween 20
Sphingomyelin	22,796	K1 Tx 100		144,624	K1 Lubrol	21,867	K1 Tween 20
Sphingomyelin	24,332	K1 Tx 100		155,203	K1 Lubrol	161,053	K1 Tween 20
Sphingomyelin	113,584	K1 Tx 100		127,162	K1 Lubrol	0,000	K1 Tween 20
Sphingomyelin	125,748	K1 Tx 100		137,888	K1 Lubrol	0,000	K1 Tween 20
Sphingomyelin	108,431	K1 Tx 100		108,911	K1 Lubrol	71,521	K1 Tween 20
Sphingomyelin	77,339	K1 Tx 100		121,056	K1 Lubrol	72,829	K1 Tween 20
Sphingomyelin	144,904	K1 Tx 100		113,357	K1 Lubrol	72,635	K1 Tween 20
Sphingomyelin	148,204	K1 Tx 100		116,274	K1 Lubrol	69,768	K1 Tween 20
Sphingomyelin	65,975	L1 Tx 100		92,170	L1 Lubrol	78,707	L1 Tween 20
Sphingomyelin	68,907	L1 Tx 100		113,203	L1 Lubrol	80,442	L1 Tween 20
Sphingomyelin	61,547	L1 Tx 100		105,041	L1 Lubrol	94,865	L1 Tween 20
Sphingomyelin	65,214	L1 Tx 100		123,694	L1 Lubrol	93,006	L1 Tween 20
Sphingomyelin	28,485	L1 Tx 100		101,623	L1 Lubrol	52,053	L1 Tween 20
Sphingomyelin	37,878	L1 Tx 100		102,105	L1 Lubrol	77,210	L1 Tween 20
Sphingomyelin	29,349	L1 Tx 100		80,535	L1 Lubrol	69,811	L1 Tween 20
Sphingomyelin	30,088	L1 Tx 100		90,565	L1 Lubrol	74,271	L1 Tween 20
Sphingomyelin	107,687	L2 Tx 100		91,108	L2 Lubrol	0,000	L2 Tween 20
Sphingomyelin	108,734	L2 Tx 100		89,115	L2 Lubrol	0,000	L2 Tween 20
Sphingomyelin	87,050	L2 Tx 100		72,445	L2 Lubrol	82,351	L2 Tween 20
Sphingomyelin	94,106	L2 Tx 100		80,723	L2 Lubrol	78,527	L2 Tween 20
Sphingomyelin	102,929	L2 Tx 100		86,059	L2 Lubrol	55,368	L2 Tween 20
Sphingomyelin	95,924	L2 Tx 100		92,450	L2 Lubrol	60,025	L2 Tween 20
Sphingomyelin	88,451	L2 Tx 100		64,128	L2 Lubrol	42,979	L2 Tween 20
Sphingomyelin	90,237	L2 Tx 100		66,283	L2 Lubrol	45,527	L2 Tween 20
L-Choline	0,000	K1 Tx 100		0,000	K1 Lubrol	0,000	K1 Tween 20
L-Choline	0,000	K1 Tx 100		0,000	K1 Lubrol	0,000	K1 Tween 20
L-Choline	0,000	K1 Tx 100		0,000	K1 Lubrol	0,000	K1 Tween 20
L-Choline	0,000	K1 Tx 100		0,000	K1 Lubrol	0,000	K1 Tween 20
L-Choline	0,000	K1 Tx 100		0,000	K1 Lubrol	0,000	K1 Tween 20
L-Choline	0,000	K1 Tx 100		0,000	K1 Lubrol	0,000	K1 Tween 20
L-Choline	0,000	K1 Tx 100		0,000	K1 Lubrol	0,000	K1 Tween 20
L-Choline	0,000	K1 Tx 100		0,000	K1 Lubrol	0,000	K1 Tween 20
L-Choline	0,000	L1 Tx 100		51,725	L1 Lubrol	58,765	L1 Tween 20
L-Choline	0,000	L1 Tx 100		56,598	L1 Lubrol	62,021	L1 Tween 20
L-Choline	0,000	L1 Tx 100		72,819	L1 Lubrol	83,200	L1 Tween 20
L-Choline	0,000	L1 Tx 100		48,650	L1 Lubrol	75,488	L1 Tween 20
L-Choline	0,000	L1 Tx 100		0,000	L1 Lubrol	0,000	L1 Tween 20
L-Choline	0,000	L1 Tx 100		0,000	L1 Lubrol	0,000	L1 Tween 20
L-Choline	0,000	L1 Tx 100		0,000	L1 Lubrol	0,000	L1 Tween 20
L-Choline	0,000	L1 Tx 100		0,000	L1 Lubrol	0,000	L1 Tween 20
L-Choline	0,000	L2 Tx 100		60,444	L2 Lubrol	0,000	L2 Tween 20
L-Choline	0,000	L2 Tx 100		57,537	L2 Lubrol	0,000	L2 Tween 20

L-Choline	0,000	L2 Tx 100	57,782	L2 Lubrol	73,833	L2 Tween 20
L-Choline	0,000	L2 Tx 100	58,826	L2 Lubrol	74,877	L2 Tween 20
L-Choline	0,000	L2 Tx 100	0,000	L2 Lubrol	0,000	L2 Tween 20
L-Choline	0,000	L2 Tx 100	0,000	L2 Lubrol	0,000	L2 Tween 20
L-Choline	0,000	L2 Tx 100	0,000	L2 Lubrol	0,000	L2 Tween 20
L-Choline	0,000	L2 Tx 100	0,000	L2 Lubrol	0,000	L2 Tween 20

6.6 Results of the Mann-Whitney U test

For the analysis of lipid components the Mann-Whitney U test was used. It was tested for significant differences in the amount of lipid components between CHO K1 (0) and Lec1 (1) or between CHO K1 (0) and Lec2 (2). The tables show the data conducted by using the program SPSS (version 18, PSAW).

For Triton X-100 extraction:

Cholesterol ester:

Ränge

	cell line	N	Mittlerer Rang	Rangsumme
microgram	0	8	7,50	60,00
	1	8	9,50	76,00
	Gesamt	16		

Statistik für Test[b]

	microgram
Mann-Whitney-U	24,000
Wilcoxon-W	60,000
Z	-,840
Asymptotische Signifikanz (2-seitig)	,401
Exakte Signifikanz [2*(1-seitig Sig.)]	,442[a]

a. Nicht für Bindungen korrigiert.

b. Gruppenvariable: cell line

Ränge

	cell line	N	Mittlerer Rang	Rangsumme
microgram	0	8	8,75	70,00
	2	8	8,25	66,00
	Gesamt	16		

Statistik für Test[b]

	microgram
Mann-Whitney-U	30,000
Wilcoxon-W	66,000
Z	-,210
Asymptotische Signifikanz (2-seitig)	,834
Exakte Signifikanz [2*(1-seitig Sig.)]	,878[a]

a. Nicht für Bindungen korrigiert.

b. Gruppenvariable: cell line

Triglycerides:

Ränge

	cell line	N	Mittlerer Rang	Rangsumme
microgram	0	8	6,50	52,00
	1	8	10,50	84,00
	Gesamt	16		

Statistik für Test[b]

	microgram
Mann-Whitney-U	16,000
Wilcoxon-W	52,000
Z	-1,682
Asymptotische Signifikanz (2-seitig)	,093
Exakte Signifikanz [2*(1-seitig Sig.)]	,105[a]

a. Nicht für Bindungen korrigiert.

b. Gruppenvariable: cell line

Ränge

	cell line	N	Mittlerer Rang	Rangsumme
microgram	0	8	8,50	68,00
	2	8	8,50	68,00
	Gesamt	16		

Statistik für Test[b]

	microgram
Mann-Whitney-U	32,000
Wilcoxon-W	68,000
Z	,000
Asymptotische Signifikanz (2-seitig)	1,000
Exakte Signifikanz [2*(1-seitig Sig.)]	1,000[a]

a. Nicht für Bindungen korrigiert.

b. Gruppenvariable: cell line

Oleic acid:

Ränge

	cell line	N	Mittlerer Rang	Rangsumme
Microgram	0	8	5,00	40,00
	1	8	12,00	96,00
	Gesamt	16		

Statistik für Test[b]

	microgram
Mann-Whitney-U	4,000
Wilcoxon-W	40,000
Z	-2,941
Asymptotische Signifikanz (2-seitig)	,003
Exakte Signifikanz [2*(1-seitig Sig.)]	,002[a]

a. Nicht für Bindungen korrigiert.

b. Gruppenvariable: cell line

Ränge

	cell line	N	Mittlerer Rang	Rangsumme
Microgram	0	8	4,88	39,00
	2	8	12,13	97,00
	Gesamt	16		

Statistik für Test[b]

	microgram
Mann-Whitney-U	3,000
Wilcoxon-W	39,000
Z	-3,046
Asymptotische Signifikanz (2-seitig)	,002
Exakte Signifikanz [2*(1-seitig Sig.)]	,001[a]

a. Nicht für Bindungen korrigiert.

b. Gruppenvariable: cell line

Cholesterol:

Ränge

	cell line	N	Mittlerer Rang	Rangsumme
microgram	0	8	10,25	82,00
	1	8	6,75	54,00
	Gesamt	16		

Statistik für Test[b]

	microgram
Mann-Whitney-U	18,000
Wilcoxon-W	54,000
Z	-1,470
Asymptotische Signifikanz (2-seitig)	,141
Exakte Signifikanz [2*(1-seitig Sig.)]	,161[a]

a. Nicht für Bindungen korrigiert.

b. Gruppenvariable: cell line

Ränge

	cell line	N	Mittlerer Rang	Rangsumme
microgram	0	8	8,00	64,00
	2	8	9,00	72,00
	Gesamt	16		

Statistik für Test[b]

	microgram
Mann-Whitney-U	28,000
Wilcoxon-W	64,000
Z	-,420
Asymptotische Signifikanz (2-seitig)	,674
Exakte Signifikanz [2*(1-seitig Sig.)]	,721[a]

a. Nicht für Bindungen korrigiert.

b. Gruppenvariable: cell line

Monoacylglycerol:

Ränge

	cell line	N	Mittlerer Rang	Rangsumme
microgram	0	8	12,00	96,00
	1	8	5,00	40,00
	Gesamt	16		

Statistik für Test[b]

	microgram
Mann-Whitney-U	4,000
Wilcoxon-W	40,000
Z	-3,019
Asymptotische Signifikanz (2-seitig)	,003
Exakte Signifikanz [2*(1-seitig Sig.)]	,002[a]

a. Nicht für Bindungen korrigiert.

b. Gruppenvariable: cell line

Ränge

	cell line	N	Mittlerer Rang	Rangsumme
microgram	0	8	12,00	96,00
	2	8	5,00	40,00
	Gesamt	16		

Statistik für Test[b]

	microgram
Mann-Whitney-U	4,000
Wilcoxon-W	40,000
Z	-3,019
Asymptotische Signifikanz (2-seitig)	,003
Exakte Signifikanz [2*(1-seitig Sig.)]	,002[a]

a. Nicht für Bindungen korrigiert.

b. Gruppenvariable: cell line

Galactosyl cerebroside:

Ränge

	cell line	N	Mittlerer Rang	Rangsumme
microgram	0	8	8,50	68,00
	1	8	8,50	68,00
	Gesamt	16		

Statistik für Test[b]

	microgram
Mann-Whitney-U	32,000
Wilcoxon-W	68,000
Z	,000
Asymptotische Signifikanz (2-seitig)	1,000
Exakte Signifikanz [2*(1-seitig Sig.)]	1,000[a]

a. Nicht für Bindungen korrigiert.

b. Gruppenvariable: cell line

Ränge

	cell line	N	Mittlerer Rang	Rangsumme
microgram	0	8	7,50	60,00
	2	8	9,50	76,00
	Gesamt	16		

Statistik für Test[b]

	microgram
Mann-Whitney-U	24,000
Wilcoxon-W	60,000
Z	-1,461
Asymptotische Signifikanz (2-seitig)	,144
Exakte Signifikanz [2*(1-seitig Sig.)]	,442[a]

a. Nicht für Bindungen korrigiert.

b. Gruppenvariable: cell line

Ethanolamine:

Ränge

	cell line	N	Mittlerer Rang	Rangsumme
microgram	0	8	11,00	88,00
	1	8	6,00	48,00
	Gesamt	16		

Statistik für Test[b]

	microgram
Mann-Whitney-U	12,000
Wilcoxon-W	48,000
Z	-2,157
Asymptotische Signifikanz (2-seitig)	,031
Exakte Signifikanz [2*(1-seitig Sig.)]	,038[a]

a. Nicht für Bindungen korrigiert.

b. Gruppenvariable: cell line

Ränge

	cell line	N	Mittlerer Rang	Rangsumme
microgram	0	8	9,75	78,00
	2	8	7,25	58,00
	Gesamt	16		

Statistik für Test[b]

	microgram
Mann-Whitney-U	22,000
Wilcoxon-W	58,000
Z	-1,051
Asymptotische Signifikanz (2-seitig)	,293
Exakte Signifikanz [2*(1-seitig Sig.)]	,328[a]

a. Nicht für Bindungen korrigiert.

b. Gruppenvariable: cell line

Cardiolipin:

Ränge

	cell line	N	Mittlerer Rang	Rangsumme
microgram	0	8	10,75	86,00
	1	8	6,25	50,00
	Gesamt	16		

Statistik für Test[b]

	microgram
Mann-Whitney-U	14,000
Wilcoxon-W	50,000
Z	-1,941
Asymptotische Signifikanz (2-seitig)	,052
Exakte Signifikanz [2*(1-seitig Sig.)]	,065[a]

a. Nicht für Bindungen korrigiert.

b. Gruppenvariable: cell line

Ränge

	cell line	N	Mittlerer Rang	Rangsumme
microgram	0	8	8,63	69,00
	2	8	8,38	67,00
	Gesamt	16		

Statistik für Test[b]

	microgram
Mann-Whitney-U	31,000
Wilcoxon-W	67,000
Z	-,105
Asymptotische Signifikanz (2-seitig)	,916
Exakte Signifikanz [2*(1-seitig Sig.)]	,959[a]

a. Nicht für Bindungen korrigiert.

b. Gruppenvariable: cell line

Serine:

Ränge

	cell line	N	Mittlerer Rang	Rangsumme
microgram	0	8	11,00	88,00
	1	8	6,00	48,00
	Gesamt	16		

Statistik für Test[b]

	microgram
Mann-Whitney-U	12,000
Wilcoxon-W	48,000
Z	-2,157
Asymptotische Signifikanz (2-seitig)	,031
Exakte Signifikanz [2*(1-seitig Sig.)]	,038[a]

a. Nicht für Bindungen korrigiert.

b. Gruppenvariable: cell line

Ränge

	cell line	N	Mittlerer Rang	Rangsumme
microgram	0	8	10,25	82,00
	2	8	6,75	54,00
	Gesamt	16		

Statistik für Test[b]

	microgram
Mann-Whitney-U	18,000
Wilcoxon-W	54,000
Z	-1,471
Asymptotische Signifikanz (2-seitig)	,141
Exakte Signifikanz [2*(1-seitig Sig.)]	,161[a]

a. Nicht für Bindungen korrigiert.

b. Gruppenvariable: cell line

Choline:

Ränge

	cell line	N	Mittlerer Rang	Rangsumme
microgram	0	8	10,50	84,00
	1	8	6,50	52,00
	Gesamt	16		

Statistik für Test[b]

	microgram
Mann-Whitney-U	16,000
Wilcoxon-W	52,000
Z	-1,680
Asymptotische Signifikanz (2-seitig)	,093
Exakte Signifikanz [2*(1-seitig Sig.)]	,105[a]

a. Nicht für Bindungen korrigiert.

b. Gruppenvariable: cell line

Ränge

	cell line	N	Mittlerer Rang	Rangsumme
microgram	0	8	6,88	55,00
	2	8	10,13	81,00
	Gesamt	16		

Statistik für Test[b]

	microgram
Mann-Whitney-U	19,000
Wilcoxon-W	55,000
Z	-1,365
Asymptotische Signifikanz (2-seitig)	,172
Exakte Signifikanz [2*(1-seitig Sig.)]	,195[a]

a. Nicht für Bindungen korrigiert.

b. Gruppenvariable: cell line

Sphingomyelin:

Ränge

	cell line	N	Mittlerer Rang	Rangsumme
microgram	0	8	10,50	84,00
	1	8	6,50	52,00
	Gesamt	16		

Statistik für Test[b]

	microgram
Mann-Whitney-U	16,000
Wilcoxon-W	52,000
Z	-1,680
Asymptotische Signifikanz (2-seitig)	,093
Exakte Signifikanz [2*(1-seitig Sig.)]	,105[a]

a. Nicht für Bindungen korrigiert.

b. Gruppenvariable: cell line

Ränge

	cell line	N	Mittlerer Rang	Rangsumme
microgram	0	8	9,38	75,00
	2	8	7,63	61,00
	Gesamt	16		

Statistik für Test[b]

	microgram
Mann-Whitney-U	25,000
Wilcoxon-W	61,000
Z	-,735
Asymptotische Signifikanz (2-seitig)	,462
Exakte Signifikanz [2*(1-seitig Sig.)]	,505[a]

a. Nicht für Bindungen korrigiert.

b. Gruppenvariable: cell line

L-choline:

Ränge

	cell line	N	Mittlerer Rang	Rangsumme
Microgram	0	8	8,50	68,00
	1	8	8,50	68,00
	Gesamt	16		

Statistik für Test[b]

	microgram
Mann-Whitney-U	32,000
Wilcoxon-W	68,000
Z	,000
Asymptotische Signifikanz (2-seitig)	1,000
Exakte Signifikanz [2*(1-seitig Sig.)]	1,000[a]

a. Nicht für Bindungen korrigiert.

b. Gruppenvariable: cell line

Ränge

	cell line	N	Mittlerer Rang	Rangsumme
Microgram	0	8	8,50	68,00
	2	8	8,50	68,00
	Gesamt	16		

Statistik für Test[b]

	microgram
Mann-Whitney-U	32,000
Wilcoxon-W	68,000
Z	,000
Asymptotische Signifikanz (2-seitig)	1,000
Exakte Signifikanz [2*(1-seitig Sig.)]	1,000[a]

a. Nicht für Bindungen korrigiert.

b. Gruppenvariable: cell line

For Lubrol WX extraction:

Cholesterol ester:

Ränge

	cell line	N	Mittlerer Rang	Rangsumme
microgram	0	8	7,75	62,00
	1	8	9,25	74,00
	Gesamt	16		

Statistik für Test[b]

	microgram
Mann-Whitney-U	26,000
Wilcoxon-W	62,000
Z	-,630
Asymptotische Signifikanz (2-seitig)	,529
Exakte Signifikanz [2*(1-seitig Sig.)]	,574[a]

a. Nicht für Bindungen korrigiert.

b. Gruppenvariable: cell line

Ränge

	cell line	N	Mittlerer Rang	Rangsumme
microgram	0	8	10,50	84,00
	2	8	6,50	52,00
	Gesamt	16		

Statistik für Test[b]

	microgram
Mann-Whitney-U	16,000
Wilcoxon-W	52,000
Z	-1,680
Asymptotische Signifikanz (2-seitig)	,093
Exakte Signifikanz [2*(1-seitig Sig.)]	,105[a]

a. Nicht für Bindungen korrigiert.

b. Gruppenvariable: cell line

Triglycerides:

Ränge

	cell line	N	Mittlerer Rang	Rangsumme
microgram	0	8	9,00	72,00
	1	8	8,00	64,00
	Gesamt	16		

Statistik für Test[b]

	microgram
Mann-Whitney-U	28,000
Wilcoxon-W	64,000
Z	-,420
Asymptotische Signifikanz (2-seitig)	,674
Exakte Signifikanz [2*(1-seitig Sig.)]	,721[a]

a. Nicht für Bindungen korrigiert.

b. Gruppenvariable: cell line

Ränge

	cell line	N	Mittlerer Rang	Rangsumme
microgram	0	8	9,75	78,00
	2	8	7,25	58,00
	Gesamt	16		

Statistik für Test[b]

	microgram
Mann-Whitney-U	22,000
Wilcoxon-W	58,000
Z	-1,050
Asymptotische Signifikanz (2-seitig)	,294
Exakte Signifikanz [2*(1-seitig Sig.)]	,328[a]

a. Nicht für Bindungen korrigiert.

b. Gruppenvariable: cell line

Oleic acid:

Ränge

	cell line	N	Mittlerer Rang	Rangsumme
microgram	0	8	9,75	78,00
	1	8	7,25	58,00
	Gesamt	16		

Statistik für Test[b]

	microgram
Mann-Whitney-U	22,000
Wilcoxon-W	58,000
Z	-1,050
Asymptotische Signifikanz (2-seitig)	,294
Exakte Signifikanz [2*(1-seitig Sig.)]	,328[a]

a. Nicht für Bindungen korrigiert.

b. Gruppenvariable: cell line

Ränge

	cell line	N	Mittlerer Rang	Rangsumme
microgram	0	8	10,50	84,00
	2	8	6,50	52,00
	Gesamt	16		

Statistik für Test[b]

	microgram
Mann-Whitney-U	16,000
Wilcoxon-W	52,000
Z	-1,680
Asymptotische Signifikanz (2-seitig)	,093
Exakte Signifikanz [2*(1-seitig Sig.)]	,105[a]

a. Nicht für Bindungen korrigiert.

b. Gruppenvariable: cell line

Cholesterol:

Ränge

	cell line	N	Mittlerer Rang	Rangsumme
microgram	0	8	7,50	60,00
	1	8	9,50	76,00
	Gesamt	16		

Statistik für Test[b]

	microgram
Mann-Whitney-U	24,000
Wilcoxon-W	60,000
Z	-,840
Asymptotische Signifikanz (2-seitig)	,401
Exakte Signifikanz [2*(1-seitig Sig.)]	,442[a]

a. Nicht für Bindungen korrigiert.

b. Gruppenvariable: cell line

Ränge

	cell line	N	Mittlerer Rang	Rangsumme
microgram	0	8	11,00	88,00
	2	8	6,00	48,00
	Gesamt	16		

Statistik für Test[b]

	microgram
Mann-Whitney-U	12,000
Wilcoxon-W	48,000
Z	-2,100
Asymptotische Signifikanz (2-seitig)	,036
Exakte Signifikanz [2*(1-seitig Sig.)]	,038[a]

a. Nicht für Bindungen korrigiert.

b. Gruppenvariable: cell line

Monoacylglycerol:

Ränge

	cell line	N	Mittlerer Rang	Rangsumme
microgram	0	8	10,50	84,00
	1	8	6,50	52,00
	Gesamt	16		

Statistik für Test[b]

	microgram
Mann-Whitney-U	16,000
Wilcoxon-W	52,000
Z	-1,682
Asymptotische Signifikanz (2-seitig)	,093
Exakte Signifikanz [2*(1-seitig Sig.)]	,105[a]

a. Nicht für Bindungen korrigiert.

b. Gruppenvariable: cell line

Ränge

	cell line	N	Mittlerer Rang	Rangsumme
microgram	0	8	9,25	74,00
	2	8	7,75	62,00
	Gesamt	16		

Statistik für Test[b]

	microgram
Mann-Whitney-U	26,000
Wilcoxon-W	62,000
Z	-,630
Asymptotische Signifikanz (2-seitig)	,529
Exakte Signifikanz [2*(1-seitig Sig.)]	,574[a]

a. Nicht für Bindungen korrigiert.

b. Gruppenvariable: cell line

Galactosyl cerebroside:

Ränge

	cell line	N	Mittlerer Rang	Rangsumme
microgram	0	8	7,50	60,00
	1	8	9,50	76,00
	Gesamt	16		

Statistik für Test[b]

	microgram
Mann-Whitney-U	24,000
Wilcoxon-W	60,000
Z	-1,461
Asymptotische Signifikanz (2-seitig)	,144
Exakte Signifikanz [2*(1-seitig Sig.)]	,442[a]

a. Nicht für Bindungen korrigiert.

b. Gruppenvariable: cell line

Ränge

	cell line	N	Mittlerer Rang	Rangsumme
microgram	0	8	8,50	68,00
	2	8	8,50	68,00
	Gesamt	16		

Statistik für Test[b]

	microgram
Mann-Whitney-U	32,000
Wilcoxon-W	68,000
Z	,000
Asymptotische Signifikanz (2-seitig)	1,000
Exakte Signifikanz [2*(1-seitig Sig.)]	1,000[a]

a. Nicht für Bindungen korrigiert.

b. Gruppenvariable: cell line

Ethanolamine:

Ränge

	Cell line	N	Mittlerer Rang	Rangsumme
microgram	0	8	4,75	38,00
	1	8	12,25	98,00
	Gesamt	16		

Statistik für Test[b]

	microgram
Mann-Whitney-U	2,000
Wilcoxon-W	38,000
Z	-3,151
Asymptotische Signifikanz (2-seitig)	,002
Exakte Signifikanz [2*(1-seitig Sig.)]	,001[a]

a. Nicht für Bindungen korrigiert.

b. Gruppenvariable: cell line

Ränge

	Cell line	N	Mittlerer Rang	Rangsumme
microgram	0	8	8,25	66,00
	2	8	8,75	70,00
	Gesamt	16		

Statistik für Test[b]

	microgram
Mann-Whitney-U	30,000
Wilcoxon-W	66,000
Z	-,210
Asymptotische Signifikanz (2-seitig)	,834
Exakte Signifikanz [2*(1-seitig Sig.)]	,878[a]

a. Nicht für Bindungen korrigiert.

b. Gruppenvariable: cell line

Cardiolipin:

Ränge

	Cell line	N	Mittlerer Rang	Rangsumme
microgram	0	8	9,00	72,00
	1	8	8,00	64,00
	Gesamt	16		

Statistik für Test[b]

	microgram
Mann-Whitney-U	28,000
Wilcoxon-W	64,000
Z	-,420
Asymptotische Signifikanz (2-seitig)	,674
Exakte Signifikanz [2*(1-seitig Sig.)]	,721[a]

a. Nicht für Bindungen korrigiert.

b. Gruppenvariable: cell line

Ränge

	Cell line	N	Mittlerer Rang	Rangsumme
microgram	0	8	11,88	95,00
	2	8	5,13	41,00
	Gesamt	16		

Statistik für Test[b]

	microgram
Mann-Whitney-U	5,000
Wilcoxon-W	41,000
Z	-2,836
Asymptotische Signifikanz (2-seitig)	,005
Exakte Signifikanz [2*(1-seitig Sig.)]	,003[a]

a. Nicht für Bindungen korrigiert.

b. Gruppenvariable: cell line

Serine:

Ränge

	Cell line	N	Mittlerer Rang	Rangsumme
microgram	0	8	10,13	81,00
	1	8	6,88	55,00
	Gesamt	16		

Statistik für Test[b]

	microgram
Mann-Whitney-U	19,000
Wilcoxon-W	55,000
Z	-1,365
Asymptotische Signifikanz (2-seitig)	,172
Exakte Signifikanz [2*(1-seitig Sig.)]	,195[a]

a. Nicht für Bindungen korrigiert.

b. Gruppenvariable: cell line

Ränge

	Cell line	N	Mittlerer Rang	Rangsumme
microgram	0	8	11,38	91,00
	2	8	5,63	45,00
	Gesamt	16		

Statistik für Test[b]

	microgram
Mann-Whitney-U	9,000
Wilcoxon-W	45,000
Z	-2,415
Asymptotische Signifikanz (2-seitig)	,016
Exakte Signifikanz [2*(1-seitig Sig.)]	,015[a]

a. Nicht für Bindungen korrigiert.

b. Gruppenvariable: cell line

Choline:

Ränge

	Cell line	N	Mittlerer Rang	Rangsumme
microgram	0	8	8,63	69,00
	1	8	8,38	67,00
	Gesamt	16		

Statistik für Test[b]

	microgram
Mann-Whitney-U	31,000
Wilcoxon-W	67,000
Z	-,105
Asymptotische Signifikanz (2-seitig)	,916
Exakte Signifikanz [2*(1-seitig Sig.)]	,959[a]

a. Nicht für Bindungen korrigiert.

b. Gruppenvariable: cell line

Ränge

	Cell line	N	Mittlerer Rang	Rangsumme
microgram	0	8	11,00	88,00
	2	8	6,00	48,00
	Gesamt	16		

Statistik für Test[b]

	microgram
Mann-Whitney-U	12,000
Wilcoxon-W	48,000
Z	-2,100
Asymptotische Signifikanz (2-seitig)	,036
Exakte Signifikanz [2*(1-seitig Sig.)]	,038[a]

a. Nicht für Bindungen korrigiert.

b. Gruppenvariable: cell line

Sphingomyelin:

Ränge

	cell line	N	Mittlerer Rang	Rangsumme
microgram	0	8	11,88	95,00
	1	8	5,13	41,00
	Gesamt	16		

Statistik für Test[b]

	microgram
Mann-Whitney-U	5,000
Wilcoxon-W	41,000
Z	-2,836
Asymptotische Signifikanz (2-seitig)	,005
Exakte Signifikanz [2*(1-seitig Sig.)]	,003[a]

a. Nicht für Bindungen korrigiert.

b. Gruppenvariable: cell line

Ränge

	Cell line	N	Mittlerer Rang	Rangsumme
microgram	0	8	12,50	100,00
	2	8	4,50	36,00
	Gesamt	16		

Statistik für Test[b]

	microgram
Mann-Whitney-U	,000
Wilcoxon-W	36,000
Z	-3,361
Asymptotische Signifikanz (2-seitig)	,001
Exakte Signifikanz [2*(1-seitig Sig.)]	,000[a]

a. Nicht für Bindungen korrigiert.

b. Gruppenvariable: cell line

L-Choline:

Ränge

	Cell line	N	Mittlerer Rang	Rangsumme
microgram	0	8	6,50	52,00
	1	8	10,50	84,00
	Gesamt	16		

Statistik für Test[b]

	microgram
Mann-Whitney-U	16,000
Wilcoxon-W	52,000
Z	-2,208
Asymptotische Signifikanz (2-seitig)	,027
Exakte Signifikanz [2*(1-seitig Sig.)]	,105[a]

a. Nicht für Bindungen korrigiert.

b. Gruppenvariable: cell line

Ränge

	Cell line	N	Mittlerer Rang	Rangsumme
microgram	0	8	6,50	52,00
	2	8	10,50	84,00
	Gesamt	16		

Statistik für Test[b]

	microgram
Mann-Whitney-U	16,000
Wilcoxon-W	52,000
Z	-2,208
Asymptotische Signifikanz (2-seitig)	,027
Exakte Signifikanz [2*(1-seitig Sig.)]	,105[a]

a. Nicht für Bindungen korrigiert.

b. Gruppenvariable: cell line

For Tween 20 extraction:

Cholesterol ester:

Ränge

	Cell line	N	Mittlerer Rang	Rangsumme
microgram	0	8	7,50	60,00
	1	8	9,50	76,00
	Gesamt	16		

Statistik für Test[b]

	microgram
Mann-Whitney-U	24,000
Wilcoxon-W	60,000
Z	-,840
Asymptotische Signifikanz (2-seitig)	,401
Exakte Signifikanz [2*(1-seitig Sig.)]	,442[a]

a. Nicht für Bindungen korrigiert.

b. Gruppenvariable: cell line

Ränge

	Cell line	N	Mittlerer Rang	Rangsumme
microgram	0	8	8,75	70,00
	2	8	8,25	66,00
	Gesamt	16		

Statistik für Test[b]

	microgram
Mann-Whitney-U	30,000
Wilcoxon-W	66,000
Z	-,210
Asymptotische Signifikanz (2-seitig)	,834
Exakte Signifikanz [2*(1-seitig Sig.)]	,878[a]

a. Nicht für Bindungen korrigiert.

b. Gruppenvariable: cell line

Triglycerides:

Ränge

	Cell line	N	Mittlerer Rang	Rangsumme
microgram	0	8	8,50	68,00
	1	8	8,50	68,00
	Gesamt	16		

Statistik für Test[b]

	microgram
Mann-Whitney-U	32,000
Wilcoxon-W	68,000
Z	,000
Asymptotische Signifikanz (2-seitig)	1,000
Exakte Signifikanz [2*(1-seitig Sig.)]	1,000[a]

a. Nicht für Bindungen korrigiert.

b. Gruppenvariable: cell line

Ränge

	Cell line	N	Mittlerer Rang	Rangsumme
microgram	0	8	9,75	78,00
	2	8	7,25	58,00
	Gesamt	16		

Statistik für Test[b]

	microgram
Mann-Whitney-U	22,000
Wilcoxon-W	58,000
Z	-1,050
Asymptotische Signifikanz (2-seitig)	,294
Exakte Signifikanz [2*(1-seitig Sig.)]	,328[a]

a. Nicht für Bindungen korrigiert.

b. Gruppenvariable: cell line

Oleic acid:

Ränge

	Cell line	N	Mittlerer Rang	Rangsumme
microgram	0	8	7,50	60,00
	1	8	9,50	76,00
	Gesamt	16		

Statistik für Test[b]

	microgram
Mann-Whitney-U	24,000
Wilcoxon-W	60,000
Z	-,840
Asymptotische Signifikanz (2-seitig)	,401
Exakte Signifikanz [2*(1-seitig Sig.)]	,442[a]

a. Nicht für Bindungen korrigiert.

b. Gruppenvariable: cell line

Ränge

	Cell line	N	Mittlerer Rang	Rangsumme
microgram	0	8	9,00	72,00
	2	8	8,00	64,00
	Gesamt	16		

Statistik für Test[b]

	microgram
Mann-Whitney-U	28,000
Wilcoxon-W	64,000
Z	-,420
Asymptotische Signifikanz (2-seitig)	,674
Exakte Signifikanz [2*(1-seitig Sig.)]	,721[a]

a. Nicht für Bindungen korrigiert.

b. Gruppenvariable: cell line

Cholesterol:

Ränge

	Cell line	N	Mittlerer Rang	Rangsumme
microgram	0	8	8,25	66,00
	1	8	8,75	70,00
	Gesamt	16		

Statistik für Test[b]

	microgram
Mann-Whitney-U	30,000
Wilcoxon-W	66,000
Z	-,210
Asymptotische Signifikanz (2-seitig)	,834
Exakte Signifikanz [2*(1-seitig Sig.)]	,878[a]

a. Nicht für Bindungen korrigiert.

b. Gruppenvariable: cell line

Ränge

	cell line	N	Mittlerer Rang	Rangsumme
microgram	0	8	9,75	78,00
	2	8	7,25	58,00
	Gesamt	16		

Statistik für Test[b]

	microgram
Mann-Whitney-U	22,000
Wilcoxon-W	58,000
Z	-1,050
Asymptotische Signifikanz (2-seitig)	,294
Exakte Signifikanz [2*(1-seitig Sig.)]	,328[a]

a. Nicht für Bindungen korrigiert.

b. Gruppenvariable: cell line

Monoacylglycerol:

Ränge

	Cell line	N	Mittlerer Rang	Rangsumme
microgram	0	8	10,13	81,00
	1	8	6,88	55,00
	Gesamt	16		

Statistik für Test[b]

	microgram
Mann-Whitney-U	19,000
Wilcoxon-W	55,000
Z	-1,365
Asymptotische Signifikanz (2-seitig)	,172
Exakte Signifikanz [2*(1-seitig Sig.)]	,195[a]

a. Nicht für Bindungen korrigiert.

b. Gruppenvariable: cell line

Ränge

	Cell line	N	Mittlerer Rang	Rangsumme
microgram	0	8	11,13	89,00
	2	8	5,88	47,00
	Gesamt	16		

Statistik für Test[b]

	microgram
Mann-Whitney-U	11,000
Wilcoxon-W	47,000
Z	-2,205
Asymptotische Signifikanz (2-seitig)	,027
Exakte Signifikanz [2*(1-seitig Sig.)]	,028[a]

a. Nicht für Bindungen korrigiert.

b. Gruppenvariable: cell line

Galactosyl cerebroside:

Ränge

	Cell line	N	Mittlerer Rang	Rangsumme
microgram	0	8	10,25	82,00
	1	8	6,75	54,00
	Gesamt	16		

Statistik für Test[b]

	microgram
Mann-Whitney-U	18,000
Wilcoxon-W	54,000
Z	-1,620
Asymptotische Signifikanz (2-seitig)	,105
Exakte Signifikanz [2*(1-seitig Sig.)]	,161[a]

a. Nicht für Bindungen korrigiert.

b. Gruppenvariable: cell line

Ränge

	Cell line	N	Mittlerer Rang	Rangsumme
microgram	0	8	11,00	88,00
	2	8	6,00	48,00
	Gesamt	16		

Statistik für Test[b]

	microgram
Mann-Whitney-U	12,000
Wilcoxon-W	48,000
Z	-2,554
Asymptotische Signifikanz (2-seitig)	,011
Exakte Signifikanz [2*(1-seitig Sig.)]	,038[a]

a. Nicht für Bindungen korrigiert.

b. Gruppenvariable: cell line

Ethanolamine:

Ränge

	Cell line	N	Mittlerer Rang	Rangsumme
microgram	0	8	5,50	44,00
	1	8	11,50	92,00
	Gesamt	16		

Statistik für Test[b]

	microgram
Mann-Whitney-U	8,000
Wilcoxon-W	44,000
Z	-2,528
Asymptotische Signifikanz (2-seitig)	,011
Exakte Signifikanz [2*(1-seitig Sig.)]	,010[a]

a. Nicht für Bindungen korrigiert.

b. Gruppenvariable: cell line

Ränge

	Cell line	N	Mittlerer Rang	Rangsumme
microgram	0	8	8,38	67,00
	2	8	8,63	69,00
	Gesamt	16		

Statistik für Test[b]

	microgram
Mann-Whitney-U	31,000
Wilcoxon-W	67,000
Z	-,107
Asymptotische Signifikanz (2-seitig)	,915
Exakte Signifikanz [2*(1-seitig Sig.)]	,959[a]

a. Nicht für Bindungen korrigiert.

b. Gruppenvariable: cell line

Cardiolipin:

Ränge

	Cell line	N	Mittlerer Rang	Rangsumme
microgram	0	8	7,00	56,00
	1	8	10,00	80,00
	Gesamt	16		

Statistik für Test[b]

	microgram
Mann-Whitney-U	20,000
Wilcoxon-W	56,000
Z	-1,264
Asymptotische Signifikanz (2-seitig)	,206
Exakte Signifikanz [2*(1-seitig Sig.)]	,234[a]

a. Nicht für Bindungen korrigiert.

b. Gruppenvariable: cell line

Ränge

	Cell line	N	Mittlerer Rang	Rangsumme
microgram	0	8	8,63	69,00
	2	8	8,38	67,00
	Gesamt	16		

Statistik für Test[b]

	microgram
Mann-Whitney-U	31,000
Wilcoxon-W	67,000
Z	-,107
Asymptotische Signifikanz (2-seitig)	,915
Exakte Signifikanz [2*(1-seitig Sig.)]	,959[a]

a. Nicht für Bindungen korrigiert.

b. Gruppenvariable: cell line

Serine:

Ränge

	Cell line	N	Mittlerer Rang	Rangsumme
microgram	0	8	7,00	56,00
	1	8	10,00	80,00
	Gesamt	16		

Statistik für Test[b]

	microgram
Mann-Whitney-U	20,000
Wilcoxon-W	56,000
Z	-1,264
Asymptotische Signifikanz (2-seitig)	,206
Exakte Signifikanz [2*(1-seitig Sig.)]	,234[a]

a. Nicht für Bindungen korrigiert.

b. Gruppenvariable: cell line

Ränge

	Cell line	N	Mittlerer Rang	Rangsumme
microgram	0	8	8,63	69,00
	2	8	8,38	67,00
	Gesamt	16		

Statistik für Test[b]

	microgram
Mann-Whitney-U	31,000
Wilcoxon-W	67,000
Z	-,107
Asymptotische Signifikanz (2-seitig)	,915
Exakte Signifikanz [2*(1-seitig Sig.)]	,959[a]

a. Nicht für Bindungen korrigiert.

b. Gruppenvariable: cell line

Choline:

Ränge

	Cell line	N	Mittlerer Rang	Rangsumme
microgram	0	8	5,13	41,00
	1	8	11,88	95,00
	Gesamt	16		

Statistik für Test[b]

	microgram
Mann-Whitney-U	5,000
Wilcoxon-W	41,000
Z	-2,836
Asymptotische Signifikanz (2-seitig)	,005
Exakte Signifikanz [2*(1-seitig Sig.)]	,003[a]

a. Nicht für Bindungen korrigiert.

b. Gruppenvariable: cell line

Ränge

	Cell line	N	Mittlerer Rang	Rangsumme
microgram	0	8	9,00	72,00
	2	8	8,00	64,00
	Gesamt	16		

Statistik für Test[b]

	microgram
Mann-Whitney-U	28,000
Wilcoxon-W	64,000
Z	-,420
Asymptotische Signifikanz (2-seitig)	,674
Exakte Signifikanz [2*(1-seitig Sig.)]	,721[a]

a. Nicht für Bindungen korrigiert.

b. Gruppenvariable: cell line

Sphingomyelin:

Ränge

	Cell line	N	Mittlerer Rang	Rangsumme
microgram	0	8	6,38	51,00
	1	8	10,63	85,00
	Gesamt	16		

Statistik für Test[b]

	microgram
Mann-Whitney-U	15,000
Wilcoxon-W	51,000
Z	-1,787
Asymptotische Signifikanz (2-seitig)	,074
Exakte Signifikanz [2*(1-seitig Sig.)]	,083[a]

a. Nicht für Bindungen korrigiert.

b. Gruppenvariable: cell line

Ränge

	cell line	N	Mittlerer Rang	Rangsumme
microgram	0	8	9,00	72,00
	2	8	8,00	64,00
	Gesamt	16		

Statistik für Test[b]

	microgram
Mann-Whitney-U	28,000
Wilcoxon-W	64,000
Z	-,423
Asymptotische Signifikanz (2-seitig)	,672
Exakte Signifikanz [2*(1-seitig Sig.)]	,721[a]

a. Nicht für Bindungen korrigiert.

b. Gruppenvariable: cell line

L-Choline:

Ränge

	cell line	N	Mittlerer Rang	Rangsumme
microgram	0	8	6,50	52,00
	1	8	10,50	84,00
	Gesamt	16		

Statistik für Test[b]

	microgram
Mann-Whitney-U	16,000
Wilcoxon-W	52,000
Z	-2,208
Asymptotische Signifikanz (2-seitig)	,027
Exakte Signifikanz [2*(1-seitig Sig.)]	,105[a]

a. Nicht für Bindungen korrigiert.

b. Gruppenvariable: cell line

Ränge

	cell line	N	Mittlerer Rang	Rangsumme
microgram	0	8	7,50	60,00
	2	8	9,50	76,00
	Gesamt	16		

Statistik für Test[b]

	microgram
Mann-Whitney-U	24,000
Wilcoxon-W	60,000
Z	-1,461
Asymptotische Signifikanz (2-seitig)	,144
Exakte Signifikanz [2*(1-seitig Sig.)]	,442[a]

a. Nicht für Bindungen korrigiert.

b. Gruppenvariable: cell line